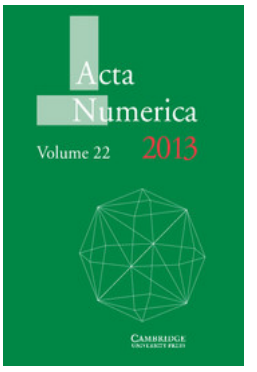

Atomistic-to-continuum coupling

Mitchell Luskin and Christoph Ortner

Acta Numerica / Volume 22 / May 2013, pp 397 - 508
DOI: 10.1017/S0962492913000068, Published online: 02 April 2013

Acta Numerica (2013), pp. 397–508
doi:10.1017/S0962492913000068

Atomistic-to-continuum coupling

Mitchell Luskin
School of Mathematics,
University of Minnesota,
MN 55455, USA
E-mail: luskin@umn.edu

Christoph Ortner
Mathematics Institute,
University of Warwick,
Coventry CV4 7AL, UK
E-mail: c.ortner@warwick.ac.uk

Atomistic-to-continuum (a/c) coupling methods are a class of computational multiscale schemes that combine the accuracy of atomistic models with the efficiency of continuum elasticity. They are increasingly being utilized in materials science to study the fundamental mechanisms of material failure such as crack propagation and plasticity, which are governed by the interaction between crystal defects and long-range elastic fields.

In the construction of a/c coupling methods, various approximation errors are committed. A rigorous numerical analysis approach that classifies and quantifies these errors can give confidence in the simulation results, as well as enable optimization of the numerical methods for accuracy and computational cost. In this article, we present such a numerical analysis framework, which is inspired by recent research activity.

CONTENTS

1. Introduction

Crystal defects such as grain boundaries, cracks, or dislocations play a central role in determining material behaviour, and their study represents a substantial component of materials science research. Molecular simulation provides a unique way to study complex material behaviour at the nanoscale, in particular how defects affect macroscopic processes such as elasticity, plasticity, and fracture.

The key difficulty in atomistic simulation is that crystal defects affect elastic fields far beyond their immediate atomic neighbourhood; that is, they give rise to *strongly coupled multiscale problems*. Computational materials scientists therefore face a compromise between inaccurate atomistic models and inaccurate representations of the crystal environment.

Since defects occupy only a small proportion of bulk crystals, one may attempt to model the elastic fields using more efficient models of continuum elasticity. This idea naturally leads to the construction of concurrent couplings between atomistic descriptions of defect cores and continuum elasticity descriptions of the elastic fields. We henceforth refer to techniques of this kind as atomistic-to-continuum coupling methods, or simply a/c methods. By employing coarse discretizations (*e.g.*, finite elements) of the continuum elasticity model they achieve a considerable reduction in computational cost compared to full atomistic descriptions, and potentially circumvent the compromise between model accuracy and system size.

The present review article develops a numerical analysis framework within which to assess and control the approximation errors committed when replacing the fully atomistic model of a crystal (the 'exact' model) with an

a/c coupling scheme, and to evaluate the relative accuracy and efficiency of different types of a/c coupling. Our aim is to provide a reference that will motivate further work by applied mathematicians in general and numerical analysts in particular, and a transfer of modern numerical analysis methodologies.

During the past century, physicists and engineers have developed the subject of micromechanics to give a fundamental understanding to the mechanism of material failure. The building blocks of micromechanics are the nucleation and movement of point, line, and surface defects and their long-range elastic interactions. These mechanisms were first verified against macroscopic experiments and then more recently against experiments at the nanoscale. Computational micromechanics has begun to extend the predictive scope of theoretical micromechanics, but mathematical theory able to assess the accuracy and efficiency of multiscale methods is needed for computational micromechanics to reach its full potential. We hope that this article will help to nucleate a much wider research effort to establish rigorous mathematical underpinnings for (computational) micromechanics.

1.1. Brief history

Remarkably, the history of atomistic-to-continuum multiscale methods begins at a time when the existence of atoms had not even been confirmed: Cauchy (1882), in a search for simplified stress–strain relations for continuum elasticity, postulated a pair interaction law between atoms arranged in a crystalline structure and derived symmetry relations for the elastic constants known as *Cauchy relations*. Various similar connections between atomistic and continuum descriptions of matter were used in solid state physics throughout the twentieth century: see Born and Huang (1954) for a standard reference.

As the critical role of crystal defects became more widely understood, the first ideas of a/c coupling emerged. Numerous authors in the 1950s and 1960s employed continuum linear elasticity to obtain boundary conditions for an atomistic simulation of a defect core; see Kanzaki (1957) for an early example. Eventually, it was recognized that, conversely, the defect core also provides boundary conditions for the elastic field and hence the two descriptions were coupled to interact concurrently. The first instance of such a method that we are aware of was developed by Sinclair (1971), and we may consider this as the first a/c coupling scheme.

The first occurrences of a/c couplings employing finite element methodology to discretize the continuum model can be found in the works of Baskes, Melius and Wilson (1981), Mullins and Dokainish (1982), Fischmeister *et al.* (1989) and Kohlhoff, Gumbsch and Fischmeister (1991). Another critical step was the introduction of the variational framework and the introduction

of the Cauchy–Born model by Tadmor, Ortiz and Phillips (1996). The latter reference coined the popular term 'quasicontinuum method'.

By this point, it had became widely understood that the interface (or handshake region) treatment was critical in the construction of accurate and reliable a/c couplings. Various new ideas were put forward, most prominently, the iterative ghost force correction method (Shenoy *et al.* 1999), force-based a/c coupling (Curtin and Miller 2003), blending schemes (Xiao and Belytschko 2004), and the quasi-nonlocal coupling (Shimokawa, Mortensen, Schiøtz and Jacobsen 2004).

The first numerical analysis contributions to the field of a/c coupling are the works of Lin (2003) and Blanc, Le Bris and Legoll (2005). The first analyses that focused on the effect of different a/c interface treatments on the global error can be found in Dobson and Luskin (2009*a*, 2009*b*) and Ming and Yang (2009). The nonlinear analysis framework that we use in this article was introduced in Ortner and Süli (2008) and Ortner (2011). From here on, the numerical analysis of a/c coupling has turned into a rapidly developing field. We will introduce some of the key ideas and survey the various contributions throughout the remainder of this paper.

1.2. Outline and reading guide

This article is essentially divided into two parts, which can be read independently. The first part, which comprises only Section 2, gives a rapid formal introduction to the main ideas in the simplest possible non-trivial setting of second neighbour Lennard-Jones interaction in one dimension. Already in this simple setting, many interesting aspect of a/c coupling can be discussed. Section 2 is intended to provide a first glimpse of the subject, or as the basis of a short series of lectures, or simply for readers who prefer explicit computations in a relatively simple setting over general mathematical structure and rigorous proofs. We summarize the main conclusions of Section 2 in Table 2.1.

In the remainder of the article we develop a complete theory of a/c coupling for static defect computations in 1D. Although a theory of a/c coupling in 2D/3D is now beginning to emerge, there are too many gaps and open questions to present a unified picture. Instead, we have chosen to present the 1D theory in a way that allows us to discuss existing generalizations to 2D/3D, as well as point out gaps. Moreover, with the exception of the reflection method introduced in Section 4.5, we only analyse a/c couplings whose formulations translate verbatim to 2D/3D.

We begin by presenting a rigorous formulation of an atomistic model problem for an infinite chain. This infinite-dimensional problem allows us to discuss the *rates of convergence* of various approximation schemes.

Atomistic-to-continuum couplings can simply be considered as an approximation scheme for this atomistic model. To analyse the errors committed, we employ the two fundamental concepts of numerical analysis: *consistency and stability* (see Section 4.7 for a formal outline of the approximation error analysis). The two central sections in this article are Section 6, where we establish the *consistency* of a/c couplings, and Section 7, where we establish their *stability*. These results are then combined and further refined in Section 8 into *a priori error estimates in terms of computational cost*.

The consistency error estimates and the *a priori* error estimates are summarized, respectively, in Tables 6.1 and 8.1.

Throughout the article, we discuss relevant background literature, existing extensions of our presentation to 2D/3D, and open problems. In addition, in Section 9 we give brief summaries of various extensions of the presentation in this article and a discussion of pressing open problems.

1.3. Omissions

No review article on a field of research as rich as a/c coupling can be complete. Our choice of topics reflects our personal view on the most important generic ideas in a/c coupling: the Cauchy–Born approximation, ghost forces at local/nonlocal model interfaces, ghost force reduction via blending, ghost force removal by conservative interface corrections, and force-based (non-conservative) a/c coupling.

We exclude many variants of how to combine these ingredients into practical a/c coupling schemes, as well as other classes of a/c multiscale methods. The analytical tools developed in this article for a/c coupling can potentially provide a framework for analysing these omitted methods, and we would consider the writing of this article a success if it motivates new research in this direction. The reader should refer to Section 9 for further discussions.

1.4. Notation

Notation is introduced throughout the manuscript where it is natural to do so. We have included a table of symbols in Appendix C.

Here, we merely mention that our notation for ℓ^p and L^p norms is standard. For a function v with discrete domain $\mathcal{X}$ and $\mathcal{A} \subset \mathcal{X}$, we define

$$\|v\|_{\ell^p(\mathcal{A})} := \begin{cases} (\sum_{\xi\in\mathcal{A}} |v(\xi)|^p)^{1/p}, & 1 \le p < \infty, \\ \sup_{\xi\in\mathcal{A}} |v(\xi)|, & p = \infty. \end{cases}$$

If we omit the domain in $\|v\|_{\ell^p}$, then the norm is computed on the entire domain of definition $\mathcal{X}$.

Analogously, for a Lebesgue-measurable function $v : X \to \mathbb{R}$, where $X \subset \mathbb{R}$ is measurable, and for $A \subset X$, we define

$$\|v\|_{L^p(A)} := \begin{cases} (\int_A |v(x)|^p \,\mathrm{d}x)^{1/p}, & 1 \le p < \infty, \\ \operatorname{ess\,sup}_{x\in A} |v(x)|, & p = \infty. \end{cases}$$

If we omit the domain in $\|v\|_{L^p}$, then the norm is computed on the entire domain of definition X.

When we write $f \lesssim g$, we mean that there exists a constant $C > 0$, independent of the solution and approximation parameters, such that $f \le Cg$.

2. Atomistic-to-continuum Lennard-Jones next-nearest neighbour models

In this section, we offer a brief introduction in the simplest non-trivial setting, the Lennard-Jones next-nearest neighbour model. For the sake of simplicity of presentation, we keep this section entirely formal. Except where stated otherwise, all statements can be made rigorous. In fact, we present rigorous proofs for most of the statements in greater generality in subsequent sections.

We emphasize from the outset that the 1D Lennard-Jones model hides many fundamental issues one has to face when dealing with general many-body and 2D/3D situations, which are not merely of a technical nature. We will occasionally comment on such discrepancies.

2.1. The atomistic Lennard-Jones next-nearest neighbour model

We consider an infinite atomistic chain, indexed by $\mathbb{Z}$. A displacement of the chain is a map $u : \mathbb{Z} \to \mathbb{R}$, where we will assume that $u(\xi) \to 0$ as $|\xi| \to \infty$. The reference lattice is $\mathsf{A}\mathbb{Z}$, where $\mathsf{A} > 0$ is a macroscopic stretch, so the corresponding deformation of the atomistic chain is given by the mapping $\xi \in \mathbb{Z}$ to $y(\xi) := \mathsf{A}\xi + u(\xi)$. We normally assume that y is strictly increasing, that is, $y(\xi) - y(\xi - 1) > 0$, and hence $u(\xi) - u(\xi - 1) > -1$ for all ξ.

We assume in this introductory section that first and second neighbours interact via the Lennard-Jones potential $\phi(r) = r^{-12} - 2r^{-6}$ (or a similar pair potential): see Figure 2.1. The energy of a displacement u can then be written as

$$\begin{aligned} \mathcal{E}^{\mathrm{a}}(u) &:= \sum_{\xi\in\mathbb{Z}} \big\{\phi\big(y(\xi) - y(\xi-1)\big) + \phi\big(y(\xi+1) - y(\xi-1)\big)\big\} \\ &= \sum_{\xi\in\mathbb{Z}} \big\{\phi(\mathsf{A} + u'_\xi) + \phi(2\mathsf{A} + u'_\xi + u'_{\xi+1})\big\} \\ &= \sum_{\xi\in\mathbb{Z}} \big\{\phi_1(u'_\xi) + \phi_2(u'_\xi + u'_{\xi+1})\big\}, \end{aligned} \tag{2.1}$$

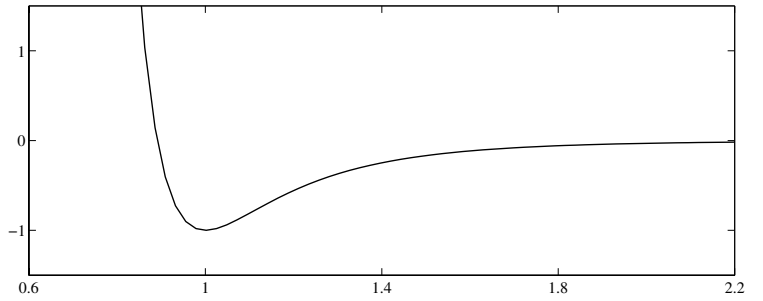

Figure 2.1. The Lennard-Jones potential.

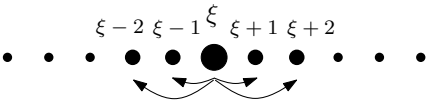

Figure 2.2. Interactions in a 1D second-neighbour model.

where

$$\phi_i(s) := \phi(i\mathsf{A} + s) \quad \text{and} \quad u'_\xi := u(\xi) - u(\xi - 1)$$

(and hence $u'_\xi + u'_{\xi+1} = u(\xi + 1) - u(\xi - 1)$).

More realistic molecular interactions are usually modelled via many-body potentials (see Section 3.2). Hence, to appreciate certain design decisions in coarse-graining schemes, it is important that we sometimes write $\mathcal{E}^{\mathrm{a}}$ in a form that can be generalized:

$$\mathcal{E}^{\mathrm{a}}(u) = \sum_{\xi\in\mathbb{Z}} \Phi^{\mathrm{a}}_\xi(u), \quad \text{where the } \textit{atomistic site energy} \text{ is} \tag{2.2}$$

$$\Phi^{\mathrm{a}}_\xi(u) := \tfrac{1}{2}\big\{\phi_1(u'_\xi) + \phi_1(u'_{\xi+1}) + \phi_2(u'_{\xi-1} + u'_\xi) + \phi_2(u'_{\xi+1} + u'_{\xi+2})\big\}.$$

See Figure 2.2 for an illustration.

We will see in Section 3.2 that if we assume without loss of generality that $\phi_1(0) + \phi_2(0) = 0$, then $\mathcal{E}^{\mathrm{a}}$ is well-defined on a suitable function space of displacements. We will assume in this section that all displacement trial and test functions belong to this space, which we will later denote by $\mathcal{U}$.

For simplicity, we consider only dead load external forces throughout this article. Let $f : \mathbb{Z} \to \mathbb{R}$ with $f(\xi) \to 0$ as $|\xi| \to \infty$. Then we seek a solution of

$$u^{\mathrm{a}} \in \arg\min\big\{\mathcal{E}^{\mathrm{a}}(u) - \langle f, u\rangle_{\mathbb{Z}}\big\}, \tag{2.3}$$

where $\langle f, u\rangle_{\mathbb{Z}} := \sum_{\xi\in\mathbb{Z}} f(\xi)u(\xi)$. Solutions of (2.3) solve the Euler–Lagrange

equation

$$\langle \delta\mathcal{E}^{\mathrm{a}}(u^{\mathrm{a}}), v\rangle = \langle f, v\rangle_{\mathbb{Z}} \quad \text{for all } v, \quad \text{where} \tag{2.4}$$

$$\begin{aligned}\langle \delta\mathcal{E}^{\mathrm{a}}(u), v\rangle &= \sum_{\xi\in\mathbb{Z}} \big\{\phi_1'(u_\xi')v_\xi' + \phi_2'(u_\xi' + u_{\xi+1}')(v_\xi' + v_{\xi+1}')\big\} \\ &= \sum_{\xi\in\mathbb{Z}} \big\{\phi_1'(u_\xi') + \phi_2'(u_{\xi-1}' + u_\xi') + \phi_2'(u_\xi' + u_{\xi+1}')\big\}v_\xi' \qquad (2.5)\\ &= \sum_{\xi\in\mathbb{Z}} \mathsf{S}_\xi^{\mathrm{a}}(u)v_\xi'\end{aligned}$$

for an *atomistic stress* $\mathsf{S}_\xi^{\mathrm{a}}(u)$ defined by

$$\mathsf{S}_\xi^{\mathrm{a}}(u) := \phi_1'(u_\xi') + \phi_2'(u_{\xi-1}' + u_\xi') + \phi_2'(u_\xi' + u_{\xi+1}'). \tag{2.6}$$

Remark 2.1. We think of (2.3) as the 'thermodynamic limit' (at zero temperature) of a chain of N atoms as $N \to \infty$. The advantage over the 'scaling limit', in which one would let the atomic spacing tend to zero, is that the thermodynamic limit keeps the atomistic detail we are interested in, but removes the dependence on boundary conditions. Intuitively, we can simply think of (2.3) as an infinite chain approximation of a large but finite chain.

2.2. The Cauchy–Born approximation

To approximate the atomistic description, we wish to model the infinite chain $\mathbb{Z}$ using a continuum elasticity model with an energy functional of the form

$$\mathcal{E}^{\mathrm{c}}(u) = \int_{\mathbb{R}} W(\nabla u)\,\mathrm{d}x, \tag{2.7}$$

where $W : (-1, \infty) \to \mathbb{R}$ is a suitable strain energy function and u is now defined for $x \in \mathbb{R}$. Interpreting ∇u as a homogeneous strain applied to the infinite crystal $\mathbb{Z}$, and hence $W(\nabla u)$ as the resulting energy per unit volume corresponding to the atomistic model (2.1), we obtain the *Cauchy–Born strain energy density function*

$$W(\mathsf{F}) := \phi_1(\mathsf{F}) + \phi_2(2\mathsf{F}). \tag{2.8}$$

We note that $W(0) = 0$ since $\phi_1(0)+\phi_2(0) = 0$, and (2.7) is thus well-defined on a suitable function space of displacements that decay at infinity.

In the remainder of Section 2, we consider a finite element Cauchy–Born model, taking the atomistic chain as the set of nodes; that is, for discrete displacements $u : \mathbb{Z} \to \mathbb{R}$, we (re-)define

$$\mathcal{E}^{\mathrm{c}}(u) = \sum_{\xi\in\mathbb{Z}} W(u_\xi'),$$

which is in fact equivalent to (2.7) when $u(x) : \mathbb{R} \to \mathbb{R}$ is the continuous piecewise linear interpolant of $u : \mathbb{Z} \to \mathbb{R}$.

For this discretized Cauchy–Born model, we seek

$$u^{\mathrm{c}} \in \arg\min \big\{ \mathcal{E}^{\mathrm{c}}(u) - \langle f, u \rangle_{\mathbb{Z}} \big\}. \tag{2.9}$$

Solutions of (2.9) solve the Euler–Lagrange equation

$$\langle \delta \mathcal{E}^{\mathrm{c}}(u^{\mathrm{c}}), v \rangle = \langle f, v \rangle_{\mathbb{Z}} \quad \text{for all } v, \quad \text{where} \tag{2.10}$$

$$\langle \delta \mathcal{E}^{\mathrm{c}}(u), v \rangle = \sum_{\xi \in \mathbb{Z}} \partial_{\mathsf{F}} W(u'_\xi) v'_\xi, \tag{2.11}$$

where $\partial_{\mathsf{F}} W(u'_\xi)$ is the 1D variant of the first Piola–Kirchhoff stress tensor.

Suppose that $\mathcal{E}^{\mathrm{c}}$ is uniformly *stable* on $\{ s u^{\mathrm{a}} + (1-s) u^c \,|\, 0 \le s \le 1 \}$ in the sense that there exists $\gamma > 0$ such that

$$\gamma \|v'\|_{\ell^2}^2 \le \langle \delta^2 \mathcal{E}^{\mathrm{c}}(s u^{\mathrm{a}} + (1-s) u^c) v,\, v \rangle \quad \text{for all } v,\ 0 \le s \le 1 \tag{2.12}$$

(see (2.16) for an analysis of stability of the reference state and Section 7 for a rigorous general analysis). We then obtain

$$\begin{aligned}
\gamma \|(u^{\mathrm{a}} - u^{\mathrm{c}})'\|_{\ell^2}^2 &\le \left\langle \int_0^1 \delta^2 \mathcal{E}^{\mathrm{c}}(s u^{\mathrm{a}} + (1-s) u^c) \, \mathrm{d}s \, (u^{\mathrm{a}} - u^{\mathrm{c}}), u^{\mathrm{a}} - u^{\mathrm{c}} \right\rangle \\
&= \left\langle \int_0^1 \frac{\mathrm{d}}{\mathrm{d}s} \delta \mathcal{E}^{\mathrm{c}}(s u^{\mathrm{a}} + (1-s) u^c) \, \mathrm{d}s \, , u^{\mathrm{a}} - u^{\mathrm{c}} \right\rangle \\
&= \big\langle \delta \mathcal{E}^{\mathrm{c}}(u^{\mathrm{a}}) - \delta \mathcal{E}^{\mathrm{c}}(u^{\mathrm{c}}), u^{\mathrm{a}} - u^{\mathrm{c}} \big\rangle \\
&= \big\langle \delta \mathcal{E}^{\mathrm{c}}(u^{\mathrm{a}}) - \delta \mathcal{E}^{\mathrm{a}}(u^{\mathrm{a}}), u^{\mathrm{a}} - u^{\mathrm{c}} \big\rangle,
\end{aligned}$$

where, in the last equality, we have employed (2.4) and (2.10) (Galerkin orthogonality). Dividing through by $\gamma \|(u^{\mathrm{a}} - u^{\mathrm{c}})'\|_{\ell^2}$, we arrive at

$$\|(u^{\mathrm{a}} - u^{\mathrm{c}})'\|_{\ell^2} \le \gamma^{-1} \sup_{\|v'\|_{\ell^2} = 1} \big\langle \delta \mathcal{E}^{\mathrm{c}}(u^{\mathrm{a}}) - \delta \mathcal{E}^{\mathrm{a}}(u^{\mathrm{a}}), v \big\rangle, \tag{2.13}$$

which is reminiscent of the 'variational crimes' (or, simply, *consistency error*) studied in the finite element literature. We call the right-hand side of (2.13) the *modelling error* of the Cauchy–Born model.

Applying (2.5) and (2.11), we obtain

$$\begin{aligned}
\big\langle \delta \mathcal{E}^{\mathrm{c}}(u) - \delta \mathcal{E}^{\mathrm{a}}(u), v \big\rangle &= \sum_{\xi \in \mathbb{Z}} \big\{ \partial_{\mathsf{F}} W(u'_\xi) - \mathsf{S}^{\mathrm{a}}_\xi(u) \big\} v'_\xi \\
&= \sum_{\xi \in \mathbb{Z}} \big\{ 2\phi'_2(2u'_\xi) - \phi'_2(u'_\xi + u'_{\xi+1}) - \phi'_2(u'_{\xi-1} + u'_\xi) \big\} v'_\xi.
\end{aligned}$$

A Taylor expansion of the stress error $\partial_{\mathsf{F}} W(u'_\xi) - \mathsf{S}^{\mathrm{a}}_\xi(u)$ to second order and an application of the Cauchy–Schwarz inequality yield the modelling error

estimate

$$\left\langle \delta\mathcal{E}^{\rm c}(u) - \delta\mathcal{E}^{\rm a}(u), v\right\rangle \lesssim \left(\|u'''\|_{\ell^2} + \|u''\|_{\ell^4}^2\right)\|v'\|_{\ell^2}, \tag{2.14}$$

where $u''_\xi := u'_{\xi+1} - u'_\xi$ and $u'''_\xi := u''_\xi - u''_{\xi-1}$. Inserting this result into (2.13), we obtain the second-order error estimate

$$\|(u^{\rm a} - u^{\rm c})'\|_{\ell^2} \lesssim \|(u^{\rm a})'''\|_{\ell^2} + \|(u^{\rm a})''\|_{\ell^4}^2. \tag{2.15}$$

This error estimate states that, if $(u^{\rm a})'_\xi$ varies slowly relative to the atomic spacing, then the Cauchy–Born solution is a good approximation to the atomistic solution. A fully analogous result, valid in 2D/3D and for general many-body interactions, is given by Ortner and Theil (2013); see also E and Ming (2007) and Makridakis and Süli (2013) for related results in this direction.

Remark 2.2 (scaling). All of the formulations and results in this paper can be given from the point of view of the *scaling limit* rather than the *thermodynamic limit* as described in Remark 2.1. For example, rescaling space through $\xi \rightsquigarrow \epsilon\xi$ and $u(\xi) \rightsquigarrow \epsilon u(\xi)$, where ϵ is the atomic spacing, gives the second-order estimate

$$\|(u^{\rm a} - u^{\rm c})'\|_{\ell^2_\epsilon} \lesssim \epsilon^2\|(u^{\rm a})'''\|_{\ell^2_\epsilon} + \epsilon^2\|(u^{\rm a})''\|_{\ell^4_\epsilon}^2,$$

where $\|v\|_{\ell^p_\epsilon} := (\sum_{\xi\in\epsilon\mathbb{Z}} \epsilon|v_\xi|^p)^{1/p}$.

We prefer to use atomic units since they enable us to focus on the atomistic details, as in applications the geometry of the defect core is a quantity of interest.

Stability of atomistic and Cauchy–Born models

In the formal error analysis above, we have seen how the stability, that is, positive-definiteness of the Hessian of the approximate model, comes into play. To indicate why we would expect (2.12) to hold, we briefly analyse the atomistic and Cauchy–Born Hessians at the reference state.

The Cauchy–Born and atomistic Hessians are, respectively, given by

$$\left\langle \delta^2\mathcal{E}^{\rm c}(0)v, v\right\rangle = W''(0)\sum_{\xi\in\mathbb{Z}}|v'_\xi|^2, \tag{2.16}$$

$$\left\langle \delta^2\mathcal{E}^{\rm a}(0)v, v\right\rangle = \phi_1''(0)\sum_{\xi\in\mathbb{Z}}|v'_\xi|^2 + \phi_2''(0)\sum_{\xi\in\mathbb{Z}}\left|v'_\xi + v'_{\xi+1}\right|^2.$$

Noting that $W''(0) = \phi_1''(0) + 4\phi_2''(0)$ and applying the parallelogram identity

$$\left|v'_\xi + v'_{\xi+1}\right|^2 = 2|v'_\xi|^2 + 2|v'_{\xi+1}|^2 - |v''_\xi|^2 \tag{2.17}$$

(recall that $v''_\xi = v'_{\xi+1} - v'_\xi$), we observe that

$$\left\langle \delta^2\mathcal{E}^{\rm a}(0)v, v\right\rangle = \left\langle \delta^2\mathcal{E}^{\rm c}(0)v, v\right\rangle - \phi_2''(0)\sum_{\xi\in\mathbb{Z}}|v''_\xi|^2.$$

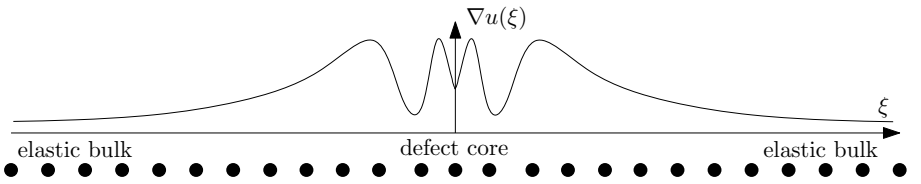

Figure 2.3. 1D analogy of a crystal defect: the deformation field varies rapidly in the defect core but is 'smooth' in the elastic bulk.

For Lennard-Jones type potentials we expect that $\phi_2''(0) < 0$, and therefore $\langle \delta^2\mathcal{E}^{\rm a}(0)v, v\rangle \geq \langle \delta^2\mathcal{E}^{\rm c}(0)v, v\rangle$. *Vice versa*, one can give general arguments that

$$\inf_{\|v'\|_{\ell^2}=1} \langle \delta^2\mathcal{E}^{\rm c}(0)v, v\rangle \geq \inf_{\|v'\|_{\ell^2}=1} \langle \delta^2\mathcal{E}^{\rm a}(0)v, v\rangle \tag{2.18}$$

(see Section 7.1; in the present case this can also be checked by a direct calculation (Dobson, Luskin and Ortner 2010*a*)). We can summarize these results (for $\phi_2''(0) < 0$) as

$$\inf_{\|v'\|_{\ell^2}=1} \langle \delta^2\mathcal{E}^{\rm a}(0)v, v\rangle = \inf_{\|v'\|_{\ell^2}=1} \langle \delta^2\mathcal{E}^{\rm c}(0)v, v\rangle. \tag{2.19}$$

Thus, we have proved that *the reference state $u = 0$ is stable in the atomistic model if and only if it is stable in the Cauchy–Born model.* We stress that, while (2.18) is a generic result, the equivalence (2.19) is specific to 1D Lennard-Jones-type interactions (Hudson and Ortner 2012, Li and Luskin 2013).

2.3. The need for atomistic-to-continuum coupling

In 2D/3D settings, crystalline solids exhibit many types of defects including, for example, impurities (an atom is replaced with an atom of a different species), vacancies (an atom is missing from a lattice site), dislocations (topological defects with high mobility that are the mechanism for crystal plasticity), or cracks. Defects themselves cannot normally be described with a continuum model. In addition, they generate elastic fields, which can be thought of as being singular at the defect core.

Due to the discrete setting, there are of course no singularities. However, in the notation of our 1D model, $(u^{\rm a})_\xi''$ will be of order $O(1)$ in a neighbourhood of the defect (see Figure 2.3), and the Cauchy–Born model therefore commits an $O(1)$ error. To obtain an accurate solution for problems with defects, a/c coupling methods decompose the reference lattice $\mathbb{Z}$ into an atomistic region $\mathcal{A}$ that contains the neighbourhood of defects where the exact atomistic model is used and a continuum region $\mathcal{C}$ where $(u^{\rm a})_\xi'$ varies slowly. See Figure 2.4 for an illustration of this decomposition.

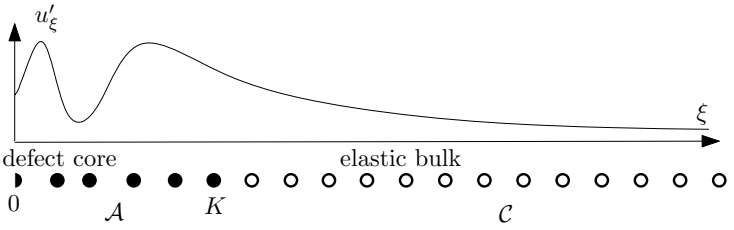

Figure 2.4. Decomposition of the atomistic chain into an atomistic region $\mathcal{A}$ and a continuum region $\mathcal{C}$, as employed in the QCE and QCF methods.

The solution of an a/c method can be expected to satisfy the error estimate

$$\|(u^{\mathrm{a}} - u^{\mathrm{ac}})'\|_{\ell^2} \lesssim \|(u^{\mathrm{a}})'''\|_{\ell^2(\mathcal{C})} + \|(u^{\mathrm{a}})''\|^2_{\ell^4(\mathcal{C})} + \text{coupling error}, \tag{2.20}$$

where u^{ac} is a minimizer of some a/c coupling functional $\mathcal{E}^{\mathrm{ac}} - \langle f, \cdot \rangle_{\mathbb{Z}}$. In this estimate, the error depends only on the 'smoothness' of u^{a} in the continuum region $\mathcal{C}$. If there is a defect in the atomistic region, that is, $(u^{\mathrm{a}}_\xi)'' = O(1)$ for some $\xi < K$, then this does not affect the error in an a/c coupling.

2.4. QCE coupling

The hybrid energy used in the energy-based quasicontinuum (QCE) coupling (Tadmor *et al.* 1996) is given by

$$\mathcal{E}^{\mathrm{qce}}(u) = \sum_{\xi \in \mathcal{A}} \Phi^{\mathrm{a}}_\xi(u) + \sum_{\xi \in \mathcal{C}} \Phi^{\mathrm{c}}_\xi(u), \tag{2.21}$$

where $\Phi^{\mathrm{a}}_\xi(u)$ is the *atomistic site energy* given in (2.2) and

$$\Phi^{\mathrm{c}}_\xi(u) := \tfrac{1}{2} W(u'_\xi) + \tfrac{1}{2} W(u'_{\xi+1})$$

is the *Cauchy–Born site energy*: see Figure 2.4. In the QCE method, we seek

$$u^{\mathrm{qce}} \in \arg\min \big\{ \mathcal{E}^{\mathrm{qce}}(u) - \langle f, u \rangle_{\mathbb{Z}} \big\}. \tag{2.22}$$

For simplicity and clarity of analysis, we will consider problems with antisymmetric forces and corresponding antisymmetric displacements

$$f_\xi = -f_{-\xi} \quad \text{and} \quad u_\xi = -u_{-\xi},$$

and a single symmetric atomistic region $\mathcal{A} := \{-K \le \xi \le K\}$. We will then define atomistic and QCE energies for $u : \mathbb{Z}_+ := \{0, \dots, \infty\} \to \mathbb{R}$ to be half

of their value when defined on $\mathbb{Z}$:

$$\begin{aligned}\mathcal{E}_+^{\rm a}(u) &:= \frac{1}{2}\Phi_0^{\rm a}(u) + \sum_{\xi=1}^{\infty} \Phi_\xi^{\rm a}(u),\\ \mathcal{E}_+^{\rm qce}(u) &:= \frac{1}{2}\Phi_0^{\rm a}(u) + \sum_{\xi=1}^{K} \Phi_\xi^{\rm a}(u) + \sum_{\xi=K+1}^{\infty} \Phi_\xi^{\rm c}(u)\end{aligned} \tag{2.23}$$

(see Figure 2.4). We then have the identity $\mathcal{E}^{\rm a}(u) = 2\mathcal{E}_+^{\rm a}(u)$ and $\mathcal{E}^{\rm qce}(u) = 2\mathcal{E}_+^{\rm qce}(u)$ for antisymmetric $u : \mathbb{Z} \to \mathbb{R}$. We note that we evaluate $\Phi_0^{\rm a}(u)$, $\Phi_1^{\rm a}(u)$, and $\Phi_0^{\rm c}(u)$ in our definition of $\mathcal{E}_+^{\rm a}(u)$ and $\mathcal{E}_+^{\rm qce}(u)$ by extending $u : \mathbb{Z}_+ \to \mathbb{R}$ to antisymmetric $u : \mathbb{Z} \to \mathbb{R}$, so $u'_0 = -u_{-1} = u_1 = u'_1$, and so forth. Since, from now on, we will analyse only the antisymmetric problem, we will drop the subscript from $\mathcal{E}_+^{\rm a}(u)$ and $\mathcal{E}_+^{\rm qce}(u)$.

The rationale behind QCE is that $\Phi_\xi^{\rm c}$ is exact under homogeneous deformation, that is, $\Phi_\xi^{\rm a}(u^{\mathsf{F}}) = \Phi_\xi^{\rm c}(u^{\mathsf{F}})$ for all $\mathsf{F} \in \mathbb{R}$ where $u_\xi^{\mathsf{F}} := \mathsf{F}\xi$. Hence, one may expect that $\mathcal{E}^{\rm qce}(u) \approx \mathcal{E}^{\rm a}(u)$ if the displacement u is 'smooth' in the continuum region $\mathcal{C}$. Indeed, if we compute the energy error, we obtain

$$\begin{aligned}\mathcal{E}^{\rm qce}(u) - \mathcal{E}^{\rm a}(u) &= \sum_{\xi=K+1}^{\infty} \big\{\Phi_\xi^{\rm c}(u) - \Phi_\xi^{\rm a}(u)\big\}\\ &= \sum_{\xi=K+1}^{\infty} \frac{1}{2}\big\{\phi_2(2u'_\xi) + \phi_2(2u'_{\xi+1}) - \phi_2(u'_{\xi-1} + u'_\xi) - \phi_2(u'_{\xi+1} + u'_{\xi+2})\big\},\end{aligned}$$

from which it is easy to obtain, by Taylor expansion of ϕ_2, that the energy error can be bounded by

$$|\mathcal{E}^{\rm a}(u) - \mathcal{E}^{\rm qce}(u)| \lesssim \|u'''\|_{\ell^1(\tilde{\mathcal{C}})} + \|u''\|^2_{\ell^2(\tilde{\mathcal{C}})},$$

where $\tilde{\mathcal{C}} := \{K \le \xi < \infty\}$.

On the other hand, following the arguments in Section 2.2 we may estimate the error between the atomistic and QCE solutions in terms of the error in the first variation. Computing the error in the first variation of QCE gives

$$\begin{aligned}&\big\langle \delta\mathcal{E}^{\rm qce}(u) - \delta\mathcal{E}^{\rm a}(u), v\big\rangle\\ &\quad= -\tfrac{1}{2}\phi'_2(u'_K + u'_{K+1})v'_K + \tfrac{1}{2}\phi'_2(u'_{K+1} + u'_{K+2})v'_{K+2}\\ &\qquad+ \tfrac{1}{2}\big\{2\phi'_2(2u'_{K+1}) - \phi'_2(u'_K + u'_{K+1}) - \phi'_2(u'_{K+1} + u'_{K+2})\big\}v'_{K+1}\\ &\qquad+ \sum_{\xi=K+2}^{\infty} \big\{2\phi'_2(2u'_\xi) - \phi'_2(u'_\xi + u'_{\xi+1}) - \phi'_2(u'_{\xi-1} + u'_\xi)\big\}v'_\xi,\end{aligned} \tag{2.24}$$

from which we can obtain by Taylor's theorem and the Cauchy–Schwarz

inequality that

$$\left\langle \delta\mathcal{E}^{\rm qce}(u) - \delta\mathcal{E}^{\rm a}(u), v\right\rangle \lesssim \left(c_g + \|u'''\|_{\ell^2(\tilde{\mathcal{C}})} + \|u''\|^2_{\ell^4(\tilde{\mathcal{C}})}\right)\|v'\|_{\ell^2}, \tag{2.25}$$

where we (crudely) estimated the coupling error by

$$-\tfrac{1}{2}\phi_2'(u_K' + u_{K+1}')v_K' + \tfrac{1}{2}\phi_2'(u_{K+1}' + u_{K+2}')v_{K+2}' \lesssim c_g\|v'\|_{\ell^2}.$$

Here, c_g is some constant that is an estimate for the force acting on second-neighbour bonds.

To see that this upper bound is in fact attained, we consider for simplicity the case $f \equiv 0$. Then it is easy to check that $u^{\rm a} = u^{\rm c} = 0$ are solutions of, respectively, (2.4) and (2.10) (in this case the Cauchy–Born model is exact). However, it follows from (2.24) and $\delta\mathcal{E}^{\rm a}(0) = 0$ that

$$\left\langle \delta\mathcal{E}^{\rm qce}(0), v\right\rangle = \frac{\phi_2'(0)}{2}\left(v_{K+2}' - v_K'\right) = \sum_{\xi=1}^{\infty} G_\xi^K v_\xi', \tag{2.26}$$

where

$$G_\xi^K := \frac{\phi_2'(0)}{2}(\delta_{K+2,\xi} - \delta_{K,\xi}) \tag{2.27}$$

is called the 'ghost force' ($\delta_{i,j}$ is the Kronecker delta). Ghost forces are spurious forces observed in most energy-based a/c methods, which are entirely due to the coupling mechanism rather than a mismatch between the atomistic and continuum descriptions. They are one of the most widely discussed issues both in the engineering and mathematical a/c literature. Often, the notion of the ghost force as conjugate to displacement rather than conjugate to strain, $\mathcal{F}_\xi^{\text{ghost force}} := -(G_\xi^{K+1} - G_\xi^K)$, is used.

Upon testing with a compactly supported virtual displacement $\hat{v}$ satisfying $\hat{v}_0 = 0$ and $\|\hat{v}'\|_{\ell^2} = 1$ defined by

$$\hat{v}_\xi' := \frac{\operatorname{sign}(\phi_2'(0))}{\sqrt{2}}(\delta_{K+2,\xi} - \delta_{K,\xi}),$$

we obtain for $\phi_2'(0) \neq 0$ that

$$\sup_{\|v'\|_{\ell^2}=1} \left\langle \delta\mathcal{E}^{\rm qce}(0) - \delta\mathcal{E}^{\rm a}(0), v\right\rangle \geq \left\langle \delta\mathcal{E}^{\rm qce}(0) - \delta\mathcal{E}^{\rm a}(0), \hat{v}\right\rangle = \frac{|\phi_2'(0)|}{\sqrt{2}} \gtrsim c_g.$$

We now return to the case of nonlinear deformation, $f \neq 0$. If we assume, as in fact it is easy to prove, that $\delta\mathcal{E}^{\rm qce}$ is Lipschitz-continuous, then we obtain that

$$\begin{aligned} c_g &\lesssim \left\langle \delta\mathcal{E}^{\rm qce}(u^{\rm a}) - \delta\mathcal{E}^{\rm a}(u^{\rm a}), \hat{v}\right\rangle = \left\langle \delta\mathcal{E}^{\rm qce}(u^{\rm a}) - \delta\mathcal{E}^{\rm qce}(u^{\rm qce}), \hat{v}\right\rangle \\ &\lesssim \|(u^{\rm a} - u^{\rm qce})'\|_{\ell^2}\|\hat{v}'\|_{\ell^2} = \|(u^{\rm a} - u^{\rm qce})'\|_{\ell^2}. \end{aligned}$$

Thus, the interfacial 'ghost forces' are responsible for the fact that the QCE method creates an $O(1)$ error in the strains. A more detailed analysis of the

decay of the displacement and strain error away from the QCE interface is given by Dobson and Luskin (2009*a*) and by Ming and Yang (2009).

Stability of QCE

As in the case of the Cauchy–Born method, we briefly discuss the stability of the QCE method by focusing on homogeneous deformation. We can obtain

$$\begin{aligned}\big\langle \delta^2\mathcal{E}^{\rm qce}(0)v, v\big\rangle &= \phi_1''(0)\sum_{\xi=1}^{\infty}|v_\xi'|^2 + \phi_2''(0)\sum_{\xi=K+1}^{\infty}\tfrac{1}{2}\big(|2v_\xi'|^2+|2v_{\xi+1}'|^2\big)\\ &\quad+\phi_2''(0)\sum_{\xi=1}^{K}\tfrac{1}{2}\big(|v_{\xi-1}'+v_\xi'|^2+|v_{\xi+1}'+v_{\xi+2}'|^2\big)+\phi_2''(0)\tfrac{1}{2}|v_1'+v_2'|^2\\ &= \big\langle \delta^2\mathcal{E}^{\rm c}(0)v, v\big\rangle\\ &\quad+\phi_2''(0)\sum_{\xi=1}^{K}\tfrac{1}{2}\big(|v_{\xi-1}'+v_\xi'|^2+|v_{\xi+1}'+v_{\xi+2}'|^2-|2v_\xi'|^2-|2v_{\xi+1}'|^2\big)\\ &\quad+\phi_2''(0)\tfrac{1}{2}\big(|v_1'+v_2'|^2-|2v_1'|^2\big).\end{aligned}$$

Applying the parallelogram identity (2.17), we deduce that

$$\begin{aligned}&\tfrac{1}{2}\big(|v_{\xi-1}'+v_\xi'|^2+|v_{\xi+1}'+v_{\xi+2}'|^2-|2v_\xi'|^2-|2v_{\xi+1}'|^2\big)\\ &\qquad=|v_{\xi-1}'|^2-|v_\xi'|^2-|v_{\xi+1}'|^2+|v_{\xi+2}'|^2-\tfrac{1}{2}|v_{\xi-1}''|^2-\tfrac{1}{2}|v_{\xi+1}''|^2,\end{aligned}\tag{2.28}$$

and inserting this formula above, we arrive at

$$\begin{aligned}\big\langle \delta^2\mathcal{E}^{\rm qce}(0)v, v\big\rangle &= \big\langle \delta^2\mathcal{E}^{\rm c}(0)v, v\big\rangle - \phi_2''(0)\big(|v_K'|^2-|v_{K+2}'|^2\big)\\ &\quad-\phi_2''(0)\left(\sum_{\xi=1}^{K-1}|v_\xi''|^2+\tfrac{1}{2}|v_K''|^2+\tfrac{1}{2}|v_{K+1}''|^2\right).\end{aligned}$$

Thus, assuming that $\phi_2''(0)<0$, we obtain the lower bound

$$\big\langle \delta^2\mathcal{E}^{\rm qce}(0)v, v\big\rangle \geq \big\langle \delta^2\mathcal{E}^{\rm c}(0)v, v\big\rangle + \phi_2''(0)\|v'\|_{\ell^2}^2.$$

To obtain an upper bound for $\big\langle \delta^2\mathcal{E}^{\rm qce}(0)v, v\big\rangle/\|v'\|_{\ell^2}^2$, we test with the virtual displacement $\hat{v}$ satisfying $\hat{v}_0=0$ and $\hat{v}_\xi' := (\phi_2''(0))\delta_{K+2,\xi}$, and compute that

$$\big\langle \delta^2\mathcal{E}^{\rm qce}(0)\hat{v}, \hat{v}\big\rangle \leq \big\langle \delta^2\mathcal{E}^{\rm c}(0)\hat{v}, \hat{v}\big\rangle - \tfrac{1}{2}|\phi_2''(0)|\,\|\hat{v}\|_{\ell^2}^2.\tag{2.29}$$

Noting from (2.19) that $\delta^2\mathcal{E}^{\rm c}(0)$ exactly reproduces the stability of $\delta^2\mathcal{E}^{\rm a}(0)$, we obtain (for $\phi_2''(0)<0$) the result

$$\inf_{\|v'\|_{\ell^2}=1}\big\langle \delta^2\mathcal{E}^{\rm qce}(0)v, v\big\rangle \leq \inf_{\|v'\|_{\ell^2}=1}\big\langle \delta^2\mathcal{E}^{\rm a}(0)v, v\big\rangle - \tfrac{1}{2}|\phi_2''(0)|,\tag{2.30}$$

that is, the coercivity constant of the QCE Hessian is strictly smaller than that of the atomistic model. In particular, it may happen that the QCE

method is unstable even when both the atomistic and Cauchy–Born models are stable. We expand on this observation in the following remark.

Remark 2.3 ((in-)accuracy of the critical strain). Recalling from (2.1) that $\phi_i(s) := \phi(i\mathsf{A} + s)$, we see that $\phi_i''(0) = \phi''(i\mathsf{A})$. Reverting to this notation, and also recalling that $\phi''(2\mathsf{A})$ is always assumed to be negative, we have shown in (2.19) and (2.30) that

$$\begin{aligned} \inf_{\|v'\|_{\ell^2}=1} \left\langle \delta^2\mathcal{E}^{\mathrm{a}}(0)v, v\right\rangle &= \phi''(\mathsf{A}) + 4\phi''(2\mathsf{A}) \quad \text{and} \\ \inf_{\|v'\|_{\ell^2}=1} \left\langle \delta^2\mathcal{E}^{\mathrm{c}}(0)v, v\right\rangle &= \phi''(\mathsf{A}) + 4\phi''(2\mathsf{A}), \quad \text{but} \\ \inf_{\|v'\|_{\ell^2}=1} \left\langle \delta^2\mathcal{E}^{\mathrm{qce}}(0)v, v\right\rangle &\leq \phi''(\mathsf{A}) + 4.5\phi''(2\mathsf{A}). \end{aligned} \tag{2.31}$$

Consider now a quasi-static loading scenario where we increase the macroscopic strain A until the chain becomes unstable, that is, when the Hessian of the lattice energy functional becomes indefinite and the system reaches a bifurcation point. For the atomistic and Cauchy–Born models, it follows from (2.31) that this *critical strain* $\mathsf{A}_{\mathrm{crit}}$ is given by the condition $\phi''(\mathsf{A}_{\mathrm{crit}}) + 4\phi''(2\mathsf{A}_{\mathrm{crit}}) = 0$. This instability can be considered to be a simple model for fracture.

We see from (2.31) that the loss of positive-definiteness of $\delta^2\mathcal{E}^{\mathrm{qce}}(0)$ occurs at a critical strain $\mathsf{A}_{\mathrm{crit}}^{\mathrm{qce}} \leq \mathsf{B}$, where $\phi''(\mathsf{B}) + 4.5\phi''(2\mathsf{B}) = 0$, and it therefore follows that $\mathsf{A}_{\mathrm{crit}}^{\mathrm{qce}} < \mathsf{A}_{\mathrm{crit}}$. That is, the QCE method incorrectly predicts the load at which fracture occurs.

This effect is further exacerbated by the fact that the reference state is not an equilibrium of the QCE energy, and hence its stability is not characterized simply by the positive-definiteness of $\delta^2\mathcal{E}^{\mathrm{qce}}(0)$, but that of $\delta^2\mathcal{E}^{\mathrm{qce}}(u^{\mathrm{qce}})$. An analysis that also takes this effect into account is given in Dobson *et al.* (2010*a*). This analysis provides a theoretical basis to explain the numerical experiments reported by Miller and Tadmor (2009) and Van Koten, Li, Luskin and Ortner (2012), who observed that the QCE method incorrectly predicts lattice instability at a significantly reduced applied load.

2.5. Energy blending (B-QCE)

To overcome the significant interfacial error committed in the QCE method, Xiao and Belytschko (2004) proposed replacing the sharp transition from the atomistic to the continuum model with a smooth blending. We should not expect to remove the ghost forces entirely in this way, but we can hope that 'spreading' them will reduce the error.

Here, we present a variant of the blending approach that fits more closely into our general framework (Van Koten and Luskin 2011). We choose a

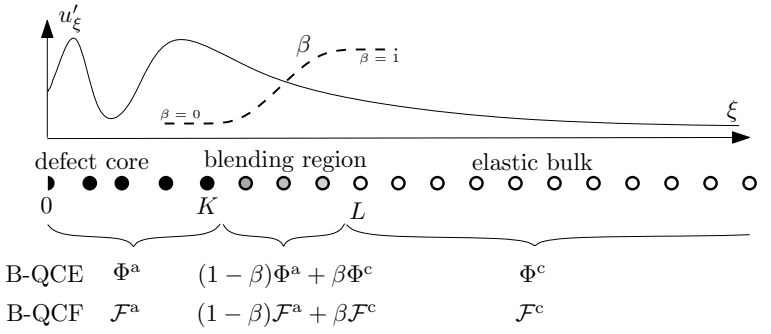

Figure 2.5. Illustration of the B-QCE and B-QCF methods.

blending function $\beta : \mathbb{Z}_+ \to [0,1]$ and define

$$\mathcal{E}^{\rm bqce}(u) := \sum_{\xi=0}^{\infty} \big\{(1-\beta(\xi))\Phi^{\rm a}_\xi(u) + \beta(\xi)\Phi^{\rm c}_\xi(u)\big\}. \tag{2.32}$$

For the purpose of implementation, we choose $K < L$ and assume that $\beta(\xi) = 0$ in $\{0,\dots,K\}$ and $\beta(\xi) = 1$ in $\{L, L+1, \dots\}$: that is, the smooth transition takes place between $\xi = K$ and L. We call $L - K$ the *blending width*. See Figure 2.5 for an illustration of this construction.

It is easy to rewrite (2.32) in the form

$$\mathcal{E}^{\rm bqce}(u) = \sum_{\xi=0}^{L} (1-\beta(\xi))\Phi^{\rm a}_\xi(u) + \int_K^\infty I\beta \cdot W(\nabla u)\,{\rm d}x, \tag{2.33}$$

where $I\beta(x)$ is the continuous piecewise affine interpolant of $\beta(\xi)$. The QCE energy is a special case of the B-QCE energy with β being given by the indicator function $\beta(\xi) = 0$ in $\{0,\dots,K\}$ and $\beta(\xi) = 1$ in $\{K+1,\dots\}$. In the B-QCE method, we seek

$$u^{\rm bqce} \in \arg\min \big\{\mathcal{E}^{\rm bqce}(u) - \langle f, u\rangle_{\mathbb{Z}_+}\big\}. \tag{2.34}$$

Reduction of ghost forces

We wish to explore, briefly, whether B-QCE indeed reduces the ghost forces, that is, the coupling error. To that end, it is convenient to use the fact that the B-QCE energy is an average of QCE energies with different interface positions (Van Koten and Luskin 2011). To see this, let $\mathcal{E}^{\rm qce}_\eta(u)$ denote the QCE energy with a/c interface at $K = \eta$. Then one readily checks that

$$\mathcal{E}^{\rm bqce}(u) = \sum_{\eta=K}^{L-1} (\beta(\eta+1) - \beta(\eta))\mathcal{E}^{\rm qce}_\eta(u).$$

We can then calculate that

$$\begin{aligned}\langle \delta\mathcal{E}^{\mathrm{bqce}}(0), v\rangle &= \sum_{\eta=K}^{L-1} \big\langle (\beta(\eta+1)-\beta(\eta))\delta\mathcal{E}^{\mathrm{qce}}_{\eta}(0), v\big\rangle \\ &= \sum_{\eta=K}^{L-1}\sum_{\xi=1}^{\infty}(\beta(\eta+1)-\beta(\eta))G^{\eta}_{\xi}v'_{\xi} \qquad (2.35)\\ &=: \sum_{\xi=1}^{\infty} G^{\mathrm{bqce}}_{\xi} v'_{\xi}.\end{aligned}$$

It follows from (2.27) that the B-QCE ghost force is given by

$$G^{\mathrm{bqce}}_{\xi} = \sum_{\eta=K}^{L-1}(\beta(\eta+1)-\beta(\eta))G^{\eta}_{\xi} = -\tfrac{1}{2}\phi'_2(0)\big(\beta''_{\xi-1}+\beta''_{\xi}\big).$$

We have thus shown that

$$\langle \delta\mathcal{E}^{\mathrm{bqce}}(0), v\rangle = -\tfrac{1}{2}\phi'_2(0)\sum_{\xi=1}^{\infty}\big(\beta''_{\xi-1}+\beta''_{\xi}\big)v'_{\xi}, \qquad (2.36)$$

from which we deduce that the B-QCE modelling error at $u^{\mathrm{a}} = 0$ is bounded by

$$\sup_{\|v'\|_{\ell^2}=1}\big\langle \delta\mathcal{E}^{\mathrm{bqce}}(0) - \delta\mathcal{E}^{\mathrm{a}}(0), v\big\rangle \le |\phi'_2(0)|\|\beta''\|_{\ell^2}. \qquad (2.37)$$

If we choose a piecewise linear blending function,

$$\beta(\xi) := \begin{cases} 0, & \xi \le K,\\ \frac{\xi-K}{L-K}, & K<\xi<L,\\ 1, & \xi \ge L,\end{cases}$$

then we obtain an $(L-K)^{-1}$ rate of modelling error reduction,

$$\sup_{\|v'\|_{\ell^2}=1}\big\langle \delta\mathcal{E}^{\mathrm{bqce}}(0) - \delta\mathcal{E}^{\mathrm{a}}(0), v\big\rangle \lesssim (L-K)^{-1}\sup_{\|v'\|_{\ell^2}=1}\big\langle \delta\mathcal{E}^{\mathrm{qce}}(0), v\big\rangle.$$

(Note that $\beta''_{\xi} = 0$, except at $\xi \in \{K, L\}$ where $\beta''_{\xi} = (L-K)^{-1}$.) That is, the blending approach does not remove but reduces the consistency error due to the ghost forces.

To improve the rate of error reduction, it follows from (2.37) that we should choose β to minimize $\|\beta''\|_{\ell^2}$ subject to the boundary conditions $\beta(\xi) = 0$ for $\xi \le K$ and $\beta(\xi) = 1$ for $\xi \ge L$, which is achieved for a cubic blending function with zero derivative at $\xi = K$ and $\xi = L$ (Van Koten and Luskin 2011, Luskin, Ortner and Van Koten 2013). The improved optimal rate of error reduction can be directly calculated by scaling to be $(L-K)^{-3/2}$.

Finally, we remark that a complete consistency and stability error analysis (see Van Koten and Luskin (2011), and Sections 6.2 and 7.2) reveals that

$$\|(u^{\mathrm{a}}-u^{\mathrm{bqce}})'\|_{\ell^2} \lesssim \|\beta''\|_{\ell^2}+\|\beta'\cdot(u^{\mathrm{a}})''\|_{\ell^2}+\|\beta\cdot(u^{\mathrm{a}})'''\|_{\ell^2}+\|\beta\cdot(u^{\mathrm{a}})''\|_{\ell^4}^2. \quad (2.38)$$

Stability of B-QCE

To understand why we should expect the B-QCE scheme to be stable, we present a brief analysis of the B-QCE Hessian at the reference state. More details are given in Van Koten and Luskin (2011). By a careful calculation, we can write it in the form

$$\begin{aligned}\big\langle \delta^2\mathcal{E}^{\mathrm{bqce}}(0)v,v\big\rangle &= \phi_1''(0)\sum_{\xi=1}^{\infty}|v_\xi'|^2+\phi_2''(0)\sum_{\xi=1}^{\infty}\beta(\xi)\tfrac{1}{2}\big(|2v_\xi'|^2+|2v_{\xi+1}'|^2\big)\\ &\quad+\phi_2''(0)\sum_{\xi=1}^{\infty}(1-\beta(\xi))\tfrac{1}{2}\big(|v_{\xi-1}'+v_\xi'|^2+|v_{\xi+1}'+v_{\xi+2}'|^2\big)\\ &\quad+\phi_2''(0)\tfrac{1}{2}|v_1'+v_2'|^2\\ &= \big\langle \delta^2\mathcal{E}^{\mathrm{c}}(0)v,v\big\rangle+\phi_2''(0)\Big\{\tfrac{1}{2}|v_1'+v_2'|^2+\sum_{\xi=1}^{\infty}(1-\beta(\xi))\\ &\quad\times\tfrac{1}{2}\big(|v_{\xi-1}'+v_\xi'|^2+|v_{\xi+1}'+v_{\xi+2}'|^2-|2v_\xi'|^2-|2v_{\xi+1}'|^2\big).\end{aligned}$$

Applying the identity (2.28), we arrive at

$$\begin{aligned}\big\langle \delta^2\mathcal{E}^{\mathrm{bqce}}(0)v,v\big\rangle &= \big\langle \delta^2\mathcal{E}^{\mathrm{c}}(0)v,v\big\rangle-\phi_2''(0)\sum_{\xi=1}^{\infty}(\beta_{\xi-1}''+\beta_\xi'')|v_\xi'|^2\\ &\quad-\phi_2''(0)\sum_{\xi=1}^{\infty}\big(1-\tfrac{1}{2}\beta(\xi-1)-\tfrac{1}{2}\beta(\xi+1)\big)|v_\xi''|^2.\end{aligned}$$

Thus, assuming again that $\phi_2''(0)<0$ and $\beta\in[0,1]$, we obtain that

$$\big\langle \delta^2\mathcal{E}^{\mathrm{bqce}}(0)v,v\big\rangle \geq \big\langle \delta^2\mathcal{E}^{\mathrm{c}}(0)v,v\big\rangle-2|\phi_2''(0)|\|\beta''\|_{\ell^\infty}\|v'\|_{\ell^2}^2. \quad (2.39)$$

Using the equivalence of the stability of $\delta^2\mathcal{E}^{\mathrm{a}}(0)$ and $\delta^2\mathcal{E}^{\mathrm{c}}(0)$ from (2.19), we can summarize these results as

$$\inf_{\|v'\|_{\ell^2}=1}\big\langle \delta^2\mathcal{E}^{\mathrm{bqce}}(0)v,v\big\rangle \geq \inf_{\|v'\|_{\ell^2}=1}\big\langle \delta^2\mathcal{E}^{\mathrm{a}}(0)v,v\big\rangle-2|\phi_2''(0)|\|\beta''\|_{\ell^\infty}. \quad (2.40)$$

By choosing β quasi-optimally as discussed above, we obtain that $\|\beta''\|_{\ell^\infty}\lesssim (L-K)^{-2}$, and hence we conclude that up to an error controllable by the blending width, we can guarantee stability of $\delta^2\mathcal{E}^{\mathrm{bqce}}(0)$.

2.6. Quasi-nonlocal (QNL) coupling

To conclude our discussion of ghost forces we show how, in the second-neighbour chain model, they can be removed altogether. The first method

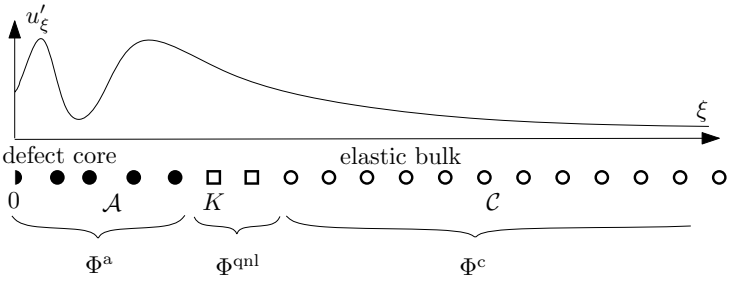

Figure 2.6. Illustration of the construction of the QNL method.

of this kind was formulated by Shimokawa *et al.* (2004). Here, we present a construction valid only for 1D pair interactions (Ortner 2011), employing an approximation of bonds rather than site energies:

$$\phi_2(u'_\xi + u'_{\xi+1}) \approx \tfrac{1}{2}\phi_2(2u'_\xi) + \tfrac{1}{2}\phi_2(2u'_{\xi+1}).$$

Taking the first variation on both sides above, at $u = 0$, we see that they are in fact equal:

$$\phi'_2(0)(v'_\xi + v'_{\xi+1}) = \tfrac{1}{2}\big\{\phi'_2(0)2v'_\xi + \phi'_2(0)2v'_{\xi+1}\big\}.$$

This immediately implies that the following construction exhibits no ghost forces: $\delta\mathcal{E}^{\rm qnl}(0) = 0$, where

$$\mathcal{E}^{\rm qnl}(u) := \mathcal{E}^{\rm a}(u) + \sum_{\xi=K+1}^{\infty} \big[\tfrac{1}{2}\big\{\phi_2(2u'_\xi) + \phi_2(2u'_{\xi+1})\big\} - \phi_2(u'_\xi + u'_{\xi+1})\big]. \tag{2.41}$$

Upon rearranging the sums, one may rewrite the QNL energy in the form

$$\mathcal{E}^{\rm qnl}(u) = \sum_{\xi=0}^{K-1} \Phi^{\rm a}_\xi(u) + \sum_{\xi=K}^{K+1} \Phi^{\rm qnl}_\xi(u) + \sum_{\xi=K+2}^{\infty} \Phi^{\rm c}_\xi(u), \tag{2.42}$$

where

$$\Phi^{\rm qnl}_K(u) := \tfrac{1}{2}\big\{\phi_1(u'_K) + \phi_2(u'_{K-1} + u'_K) + W(u'_{K+1})\big\}, \quad \text{and}$$
$$\Phi^{\rm qnl}_{K+1}(u) := \tfrac{1}{2}\big\{\phi_1(u'_{K+1}) + \phi_2(u'_K + u'_{K+1}) + W(u'_{K+2})\big\}$$

(see Figures 2.6 and 2.7). Equation (2.42) is the form of the QNL scheme as originally proposed by Shimokawa *et al.* (2004).

Thus, the QNL method has a highly localized interface correction, and in particular we observe that the QNL energy indeed reduces to the atomistic model in the atomistic region and to the Cauchy–Born model in the continuum region. The *interface atoms* $\{K, K+1\}$ are labelled 'quasi-nonlocal' (Shimokawa *et al.* 2004) since their interaction with the atomistic region is nonlocal but their interaction with the continuum region is local. We will

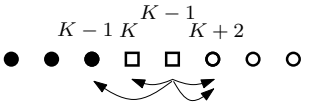

Figure 2.7. Modified interaction stencil used to construct the QNL method. Compare with the atomistic stencil of Figure 2.2.

consider couplings of the form (2.42) for more general interatomic potentials in Section 4.5.

To obtain an error estimate for the QNL method, we again compute the error in the first variation,

$$\begin{aligned}\big\langle \delta\mathcal{E}^{\rm qnl}(u) - \delta\mathcal{E}^{\rm a}(u), v\big\rangle \\ &= \sum_{\xi=K+2}^{\infty} \big\{2\phi_2'(2u_\xi') - \phi_2'(u_\xi' + u_{\xi+1}') - \phi_2'(u_{\xi-1}' + u_\xi')\big\} v_\xi' \\ &\quad + \big\{\phi_2'(2u_{K+1}') - \phi_2'(u_{K+1}' + u_{K+2}')\big\} v_{K+1}',\end{aligned}$$

and following the arguments leading to (2.15), we now obtain the first-order error estimate

$$\|(u^{\rm a} - u^{\rm qnl})'\|_{\ell^2} \lesssim \|(u^{\rm a})'''\|_{\ell^2(\mathcal{C})} + \|(u^{\rm a})''\|_{\ell^4(\mathcal{C})}^2 + |(u^{\rm a})_{K+1}''|, \tag{2.43}$$

where now $\mathcal{C} = \{K+1, \dots\}$. This is a clear potential improvement over the error in the B-QCE method, where there is an additional $\|\beta''\|_{\ell^2}$ term in the error estimate. We will more carefully distinguish the relative accuracy of B-QCE and QNL in Section 8.

Stability of QNL

As in the case of the Cauchy–Born and B-QCE models, we need to guarantee stability of the QNL method in order to make the error estimates discussed above rigorous. For the purpose of illustration, we again investigate stability of the QNL Hessian in the reference state,

$$\begin{aligned}\big\langle \delta^2\mathcal{E}^{\rm qnl}(0)v, v, \big\rangle = \phi_1''(0) \sum_{\xi=1}^{\infty} |v_\xi'|^2 + \phi_2''(0)|2v_1'|^2 + \phi_2''(0) \sum_{\xi=1}^{K} |v_\xi' + v_{\xi+1}'|^2 \\ + \phi_2''(0) \sum_{\xi=K+1}^{\infty} \big(\tfrac{1}{2}|v_\xi'|^2 + \tfrac{1}{2}|v_{\xi+1}'|^2\big).\end{aligned}$$

Applying the parallelogram identity (2.17) yields

$$\big\langle \delta^2\mathcal{E}^{\rm qnl}(0)v, v\big\rangle = \big\langle \delta^2\mathcal{E}^{\rm c}(0)v, v\big\rangle - \phi_2''(0) \sum_{\xi=1}^{K} |v_\xi''|^2.$$

For Lennard-Jones type interactions, we assume that $\phi_2''(0) < 0$, and hence it is easy to show (as in the Cauchy–Born case) that

$$\inf_{\|v'\|_{\ell^2}=1} \big\langle \delta^2\mathcal{E}^{\rm qnl}(0)v, v\big\rangle = \inf_{\|v'\|_{\ell^2}=1} \big\langle \delta^2\mathcal{E}^{\rm c}(0)v, v\big\rangle = \inf_{\|v'\|_{\ell^2}=1} \big\langle \delta^2\mathcal{E}^{\rm a}(0)v, v\big\rangle.$$

That is, the QNL Hessian $\delta^2\mathcal{E}^{\rm qnl}(0)$ is stable if and only if the atomistic and Cauchy–Born Hessians are stable.

2.7. Force-based coupling (QCF)

An a/c hybrid energy without ghost forces for general 2D/3D interface geometries has yet to be constructed and implemented. A popular alternative has been to construct a/c approximations based on coupling forces. In the most basic variant of this approach, one computes the (negative of the) force of each atom from either the atomistic or the continuum model:

$$\mathcal{F}_\xi^{\rm qcf}(u) := \begin{cases} \frac{\partial \mathcal{E}^{\rm a}(u)}{\partial u_\xi} = -\mathsf{S}^{\rm a}_{\xi+1}(u) + \mathsf{S}^{\rm a}_\xi(u), & \text{for } \xi = 1, \dots, K, \\ \frac{\partial \mathcal{E}^{\rm c}(u)}{\partial u_\xi} = -\partial_{\mathsf{F}} W(u'_{\xi+1}) + \partial_{\mathsf{F}} W(u'_\xi), & \text{for } \xi \geq K+1. \end{cases} \tag{2.44}$$

One then solves the nonlinear system

$$\mathcal{F}_\xi^{\rm qcf}(u) = f_\xi \quad \text{for all } \xi = 1, \dots, \infty. \tag{2.45}$$

It can be checked that $\mathcal{F}_\xi^{\rm qcf}(u)$ is not a conservative force (Dobson and Luskin 2008*a*), so it is not given by the Euler–Lagrange equation for an energy. Nonetheless, we can formulate (2.45) in 'variational form' as

$$\langle \mathcal{F}^{\rm qcf}(u), v\rangle_{\mathbb{Z}_+} = \langle f, v\rangle_{\mathbb{Z}_+} \quad \text{for all } v,\ v(0) = 0.$$

We estimate the modelling error following Makridakis, Ortner and Süli (2011). We obtain from summation by parts that

$$\begin{aligned} &\langle \mathcal{F}^{\rm qcf}(u), v\rangle_{\mathbb{Z}_+} \\ &\quad = -\sum_{\xi=1}^{K} \big\{\mathsf{S}^{\rm a}_{\xi+1}(u) - \mathsf{S}^{\rm a}_\xi(u)\big\} v_\xi - \sum_{\xi=K+1}^{\infty} \big\{\partial_{\mathsf{F}} W(u'_{\xi+1}) - \partial_{\mathsf{F}} W(u'_\xi)\big\} v_\xi \\ &\quad = \sum_{\xi=1}^{K+1} \mathsf{S}^{\rm a}_\xi(u) v'_\xi + \sum_{\xi=K+2}^{\infty} \partial_{\mathsf{F}} W(u'_\xi) v'_\xi + \big(\partial_{\mathsf{F}} W(u'_{K+1}) - \mathsf{S}^{\rm a}_{K+1}(u)\big) v_{K+1}. \end{aligned} \tag{2.46}$$

We thus obtain the second-order modelling error bound

$$\begin{aligned} &\langle \mathcal{F}^{\rm qcf}(u), v\rangle_{\mathbb{Z}_+} - \langle \delta\mathcal{E}^{\rm a}(u), v\rangle \\ &\quad = \sum_{\xi=K+2}^{\infty} \big\{\partial_{\mathsf{F}} W(u'_\xi) - \mathsf{S}^{\rm a}_\xi(u)\big\} v'_\xi + \big(\partial_{\mathsf{F}} W(u'_{K+1}) - \mathsf{S}^{\rm a}_{K+1}(u)\big) v_{K+1} \end{aligned} \tag{2.47}$$

$$
\begin{aligned}
&= \sum_{\xi=K+2}^{\infty} \big\{2\phi_2'(2u_\xi') - \phi_2'(u_{\xi-1}' + u_\xi') - \phi_2'(u_\xi' + u_{\xi+1}')\big\} v_\xi' \\
&\qquad + \big\{2\phi_2'(2u_{K+1}') - \phi_2'(u_K' + u_{K+1}') - \phi_2'(u_{K+1}' + u_{K+2}')\big\} v_{K+1} \\
&\lesssim \big\{\|u'''\|_{\ell^\infty(\tilde{\mathcal{C}})} + \|u''\|_{\ell^\infty(\tilde{\mathcal{C}})}^2\big\} \|v'\|_{\ell^1},
\end{aligned}
$$

where $\tilde{\mathcal{C}} = \{K, \ldots\}$, since we can use $v_0 = 0$ to bound

$$
|v_{K+1}| \leq \sum_{\xi=1}^{K+1} |v_\xi'| \leq \|v'\|_{\ell^1}.
$$

We note that the above estimate does not give a second-order modelling bound uniform in K in a discrete $W^{-1,2}$-seminorm since $|v_{K+1}|$ cannot be bounded by $\|v'\|_{\ell^2}$.

Even if we could prove a second-order modelling error bound in a discrete $W^{-1,2}$-seminorm that is uniform in K, this would not lead to the analogous error estimate. Indeed, it was shown in Dobson, Luskin and Ortner (2010*b*) that $\delta\mathcal{F}^{\mathrm{qcf}}(u)$ is not stable in the discrete $W^{1,p}$-seminorm for any $p < \infty$. It is somewhat technical to prove this, so instead we establish the slightly weaker result that $\delta\mathcal{F}^{\mathrm{qcf}}(u)$ is nearly always indefinite.

To see this, we take again $u = 0$, to obtain after some careful algebra that

$$
\langle \delta\mathcal{F}^{\mathrm{qcf}}(0)v, v\rangle_{\mathbb{Z}_+} = \langle \delta^2\mathcal{E}^{\mathrm{c}}(0)v, v\rangle - 4\phi_2''(0) \sum_{\xi=1}^{K} |v''(\xi)|^2 \tag{2.48}
$$

$$
+ \phi_2''(0)(v_{K+2}' - 2v_{K+1}' + v_K')v_{K+1}. \tag{2.49}
$$

Under the usual assumption that $\phi_2''(0) < 0$, the right-hand side of (2.48) is positive definite if and only if $\phi_1''(0) + 4\phi_2''(0) > 0$, but this is not sufficient to prove that $\langle \delta\mathcal{F}^{\mathrm{qcf}}(0)v, v\rangle$ is positive since (2.49) cannot be bounded by $\|v'\|_{\ell^2}^2$. Precisely, using the fact that

$$
\sup_{\|v'\|_{\ell^2}, v_0 = 0} |v_{K+1}| \approx K^{1/2},
$$

one can show that there exist positive constants C_1, C_2 such that

$$
\inf_{\|v'\|_{\ell^2}=1, v_0=0} \langle \delta\mathcal{F}^{\mathrm{qcf}}(0)v, v\rangle_{\mathbb{Z}_+} \leq C_1 - C_2 K^{1/2}.
$$

That is, for K sufficiently large (*i.e.*, for a sufficiently large atomistic region), $\delta\mathcal{F}^{\mathrm{qcf}}(0)$ cannot be positive definite.

However, using more general stability arguments, it can be shown that $\delta\mathcal{F}^{\mathrm{qcf}}(u)$ is in fact stable in the discrete $W^{1,\infty}$-seminorm (Dobson *et al.* 2010*b*) and hence it follows from (2.47) that

$$
\|(u^{\mathrm{a}} - u^{\mathrm{qcf}})'\|_{\ell^\infty} \lesssim \|(u^{\mathrm{a}})'''\|_{\ell^\infty(\mathcal{C})} + \|(u^{\mathrm{a}})''\|_{\ell^\infty(\mathcal{C})}^2. \tag{2.50}
$$

Remark 2.4. The non-symmetric and indefinite structure of the QCF method also presented a challenge to the efficient and reliable iterative solution of the QCF equations. Preconditioned linear stationary and GMRES methods have been studied in Luskin and Ortner (2012), Dobson, Luskin and Ortner (2011) and Dobson, Ortner and Shapeev (2012).

Ghost force correction (GFC)

At the time this article was written, the most popular publicly available a/c coupling software is the *Quasicontinuum Code*, which can be obtained from http://qcmethod.org/. At the core of this code lies the *ghost force correction* (GFC) *iteration*, which we briefly put into our context.

The GFC scheme is normally applied for computing quasi-static evolutions. In our context, we are given a family of external forces $\{f(t)\}_{t\in[0,1]}$, say, and aim to compute a continuous path

$$u^{\mathrm{a}}(t) \in \arg\min\left\{\mathcal{E}^{\mathrm{a}}(v) - \langle f(t), v\rangle\right\} \quad \text{for } t \in [0,1].$$

To compute this, Shenoy *et al.* (1999) propose the following iteration. Given an initial condition $u^{\mathrm{gfc}}(0)$ and a time step k, let

$$u_k^{\mathrm{gfc}}(jk) \in \arg\min\left\{\mathcal{E}^{\mathrm{qce}}(v) - \langle f(jk), v\rangle - \langle g_{j-1}, v\rangle\right\} \quad \text{for } j = 1, \ldots, 1/k.$$

where g_{j-1} is a dead-load correction that is intended to remove the ghost forces. Since the QCF operator has no ghost forces, a natural choice is

$$g(t_{j-1}) := \delta\mathcal{E}^{\mathrm{qce}}(u^{\mathrm{gfc}}(t_{j-1})) - \mathcal{F}^{\mathrm{qcf}}(u^{\mathrm{gfc}}(t_{j-1})),$$

which in particular ensures that g_{j-1} is concentrated in a small neighbourhood of the a/c interface.

Formally, it is straightforward to see that, if we interpolate u_k^{gfc} in time and if $u_k^{\mathrm{gfc}}(t) \to u(t)$ as $k \to 0$, then this limit solves the quasi-static QCF evolution,

$$\langle \mathcal{F}^{\mathrm{qcf}}(u(t)), v\rangle = \langle f(t), v\rangle \quad \text{for } t \in [0,1].$$

We therefore consider the GFC method as an iterative scheme to solve the QCF equation, and our analyses in the remainder of the paper will only focus on the latter.

This observation was first made by Dobson and Luskin (2008*b*) and Dobson *et al.* (2011), where further rigorous results on the GFC iteration and further discussions of the interesting challenges associated with solving the QCF equations can be found.

2.8. Force-based blending (B-QCF)

We can construct a blended version of QCF (B-QCF) that is positive definite with respect to the discrete $W^{1,2}$-seminorm (Li, Luskin and Ortner 2012)

(see Lu and Ming (2013) for a stability result in other topologies) by

$$\mathcal{F}_\xi^{\mathrm{bqcf}}(u) := \beta(\xi)\mathcal{F}_\xi^{\mathrm{a}}(u) + (1-\beta(\xi))\mathcal{F}_\xi^{\mathrm{c}}(u).$$

The consistency of the B-QCF method is intuitively clear since there is no interface coupling error. However we shall see in Section 6.4 that there are non-trivial technical issues to overcome, hence we postpone this discussion.

Here, we focus instead on the stability of the B-QCF method. With some work, following in part the discussions of stability of the Cauchy–Born, B-QCE and QCF methods, we can derive the identity (the details of this computation are also given in Section 7.3 and Li *et al.* (2012))

$$\langle \delta\mathcal{F}^{\mathrm{bqcf}}(0)u, u\rangle = \langle \delta^2\mathcal{E}^{\mathrm{bqce}}(0)u, u\rangle + \phi_2''(0)\big(\mathbf{R}+\mathbf{S}\big), \tag{2.51}$$

where $|\mathbf{R}| \lesssim \|\beta''\|_{\ell^\infty}\|u'\|_{\ell^2}^2$ and the (crucial) error term $\mathbf{S}$ is given by

$$\mathbf{S} := \sum_{\xi=1}^{\infty} \big(\beta'''_{\xi+1}\big) u_\xi u'_{\xi+1}, \tag{2.52}$$

which can be bounded by

$$|\mathbf{S}| \le \|\beta'''\|_{\ell^\infty}\|u\|_{\ell^2[K,L]}\|u'\|_{\ell^2}. \tag{2.53}$$

We can construct blending functions by the scaling $\beta(\xi) = \hat{\beta}\big(\frac{\xi-K}{L-K}\big)$, where $\hat{\beta} \in C^3$, that satisfy

$$\|\beta''\|_{\ell^\infty} \lesssim (L-K)^{-2} \quad \text{and} \quad \|\beta'''\|_{\ell^\infty} \lesssim (L-K)^{-3}. \tag{2.54}$$

At this stage, we require a Poincaré-type inequality for u to bound $\|u\|_{\ell^2[K,L]}$ in (2.53). Recalling that $u_0 = 0$ from antisymmetry, we obtain

$$\|u\|_{\ell^2[K,L]} \le (L-K)^{1/2}\|u-u_0\|_{\ell^\infty[K,L]} \lesssim (L-K)^{1/2}L^{1/2}\|u'\|_{\ell^2}.$$

We thus obtain that, for some non-negative constants C_R and C_S,

$$\begin{aligned}\langle \delta\mathcal{F}^{\mathrm{bqcf}}(0)u, u\rangle \ge{}& \langle \delta^2\mathcal{E}^{\mathrm{bqce}}(0)u, u\rangle \\ &- |\phi_2''(0)|\big(C_R(L-K)^{-2} + C_S(L-K)^{-5/2}L^{1/2}\big)\|u'\|_{\ell^2}^2.\end{aligned} \tag{2.55}$$

Utilizing the estimate (2.40) for the stability of $\delta^2\mathcal{E}^{\mathrm{bqce}}(0)$, we finally obtain

$$\begin{aligned}\inf_{\|v'\|_{\ell^2}=1} \langle \delta\mathcal{F}^{\mathrm{bqcf}}(0)u, u\rangle \ge{}& \inf_{\|v'\|_{\ell^2}=1} \big\langle \delta^2\mathcal{E}^{\mathrm{a}}(0)v, v\big\rangle \\ &- C\big\{(L-K)^{-2} + (L-K)^{-5/2}L^{1/2}\big\}.\end{aligned} \tag{2.56}$$

We can conclude that, by choosing a sufficiently large blending region and imposing the mild requirement $(L-K) \gg L^{1/5}$, then, up to a controllable error, $\delta\mathcal{F}^{\mathrm{bqcf}}(0)$ is positive-definite if and only if $\delta^2\mathcal{E}^{\mathrm{a}}(0)$ is positive-definite.

Detailed numerical tests for 1D and 2D problems exploring the dependence of stability of the B-QCF method on the blending width are reported

Table 2.1. Summary of stability results and error estimates formally derived in Section 2. Here, $e := u^{\rm a} - u^{\rm ac}$, and $\eta_p^{\rm cb} := \|(u^{\rm a})'''\|_{\ell^p(\tilde{\mathcal{C}})} + \|(u^{\rm a})''\|^2_{\ell^{2p}(\tilde{\mathcal{C}})}$.

Method	Stability	Error estimate
QCE (Section 2.4)	reduced stability in energy norm	$c_g \lesssim \|e'\|_{\ell^2} \lesssim c_g + \eta_2^{\rm cb}$ (zeroth-order at interface)
B-QCE (Section 2.5)	controllable stability error in energy norm	$\|e'\|_{\ell^2} \lesssim \|\beta''\|_{\ell^2} + \eta_2^{\rm cb}$ (blending dictates error)
QNL (Section 2.6)	sharp stability in energy norm	$\|e'\|_{\ell^2} \lesssim \|(u^{\rm a})''_K\| + \eta_2^{\rm cb}$ (first-order at interface)
QCF (Section 2.7)	unstable in discrete $W^{1,p}$-norms, $p < \infty$	$\|e'\|_{\ell^\infty} \lesssim \eta_\infty^{\rm cb}$ (no interface error)
B-QCF (Section 2.8)	controllable stability error in energy norm	$\|e'\|_{\ell^2} \lesssim \eta_2^{\rm cb}$ (no interface error; this is not proved in Section 2)

in Li, Luskin, Ortner and Shapeev (2013). Sharp stability results for the B-QCF method in a discrete H^2-type norm are established by Lu and Ming (2013).

2.9. Summary of results

We briefly summarize the main results that we derived in this section in Table 2.1. To simplify the presentation, we introduce notation for the error $e := u^{\rm a} - u^{\rm ac}$, and for the Cauchy–Born consistency error, $\eta_p^{\rm cb} := \|(u^{\rm a})'''\|_{\ell^p(\tilde{\mathcal{C}})} + \|(u^{\rm a})''\|^2_{\ell^{2p}(\tilde{\mathcal{C}})}$, for a suitably defined (method-dependent) continuum region $\tilde{\mathcal{C}}$.

3. Atomistic simulation

In this section, we introduce an atomistic model for an infinite crystal. Some care must be taken with the formulation of the appropriate function space setting, but it is well suited to discussion of *rates of convergence* for defect simulations. We will then approximate the full atomistic problem by a reduced atomistic problem in a finite domain, which can be solved numerically, and estimate the resulting error in terms of the computational cost.

As in Section 2, we shall again consider only antisymmetric displacements. In the set-up of the model, this will require some additional notation. However, this initial investment will pay off in our subsequent discussion and analysis of a/c couplings.

The proofs of the results presented in this chapter are not of immediate interest to a/c coupling. Hence we have postponed some of the proofs to the Appendix.

3.1. Lattice functions

We identify a lattice function $v : \mathbb{Z} \to \mathbb{R}$ with its continuous piecewise affine interpolant, with weak derivative ∇v, which is also the pointwise derivative in each interval $(\xi - 1, \xi)$.

In order to measure smoothness of discrete functions, we introduce a second interpolant $\tilde{v} \in C^{2,1}(\mathbb{R})$ as follows: $\tilde{v}$ is the unique continuous function such that, for all $\xi \in \mathbb{Z}$,

$$\tilde{v}|_{(\xi-1,\xi)} \text{ is a polynomial of degree 5,} \tag{3.1}$$

$$\tilde{v}(\xi) = v(\xi), \tag{3.2}$$

$$\nabla\tilde{v}(\xi) = \tfrac{1}{2}\big(v(\xi+1) - v(\xi-1)\big), \quad \text{and} \tag{3.3}$$

$$\nabla^2\tilde{v}(\xi) = v(\xi+1) - 2v(\xi) + v(\xi-1). \tag{3.4}$$

There exists a unique interpolant satisfying these conditions. It is easy to see that $\tilde{v}$ is quasi-optimal among all possible $C^{2,1}$-interpolants of v, in the following sense.

Proposition 3.1. Let $v : \mathbb{Z} \to \mathbb{R}$, and let $\hat{v} \in C^{2,1}$ satisfy $\hat{v}(\xi) = v(\xi)$ for all $\xi \in \mathbb{Z}$. Then

$$\|\nabla^j\tilde{v}\|_{L^p(\xi-1,\xi)} \lesssim \|\nabla^j\hat{v}\|_{L^p(\xi-2,\xi+1)} \quad \text{for all } p \in [1,\infty],\ \xi \in \mathbb{Z},\ j = 1,2,3.$$

Moreover,

$$\|\nabla v\|_{L^p(\xi-1,\xi)} \le \|\nabla\tilde{v}\|_{L^p(\xi-1,\xi)} \lesssim \|\nabla v\|_{L^p(\xi-2,\xi+1)} \quad \text{for all } p \in [1,\infty],\ \xi \in \mathbb{Z}.$$

Proof. See Appendix A. □

Remark 3.2. Our definition of $\tilde{v}$ is natural, but also arbitrary in that many alternative interpolants could be employed that yield qualitatively the same results. Our choice was made only for its simplicity.

Antisymmetric lattice displacements are functions $u : \mathbb{Z}_+ \to \mathbb{R}$, where $\mathbb{Z}_+ := \{0, 1, 2, \dots\}$. Throughout, we identify them with lattice functions on $\mathbb{Z}$ through the convention that $u(-\xi) = -u(\xi)$ for $\xi \in \mathbb{Z}_+$. We define the *spaces* of antisymmetric displacements by

$$\mathcal{U}_0 := \big\{u : \mathbb{Z}_+ \to \mathbb{R} \,\big|\, \operatorname{supp}(u) \text{ is bounded and } u(0) = 0\big\}, \quad \text{and}$$
$$\mathcal{U} := \big\{u : \mathbb{Z}_+ \to \mathbb{R} \,\big|\, \nabla u \in L^2 \text{ and } u(0) = 0\big\}.$$

We equip the space $\mathcal{U}$ with the H^1-seminorm $|u|_{H^1} = \|\nabla u\|_{L^2}$, which makes it a Hilbert space. After defining the energy functional in the next section, we will motivate why an H^1-type function space is natural.

Proposition 3.3. $\mathcal{U}_0$ is dense in $\mathcal{U}$.

Proof. See Appendix A. □

We conclude this section on lattice functions with definitions of the finite difference operators. We fix an *interaction range* $\mathcal{R} = \{\pm 1, \dots, \pm r_{\rm cut}\} \subset \mathbb{Z}$, where $r_{\rm cut} \in \mathbb{N}$ is fixed throughout. (We typically think of $2 \le r_{\rm cut} \le 4$.) For each $u \in \mathcal{U}$ and $\xi \in \mathbb{Z}_+$, we define the interaction stencil

$$Du(\xi) := \big(D_\rho u(\xi)\big)_{\rho\in\mathcal{R}}, \quad \text{where} \quad D_\rho u(\xi) := u(\xi+\rho) - u(\xi),$$

and where we employ the antisymmetric convention $u(-\xi) := -u(\xi)$; for example, $D_{-\rho}u(0) = -D_\rho u(0)$ and $D_{-2}u(1) = -2u(1)$.

Remark 3.4. We can relate the finite difference operators u'_ξ used in Section 2 for nearest neighbour and next-nearest neighbour interactions ($r_{\rm cut} = 2$) to the finite difference operators $D_\rho u(\xi) := u(\xi+\rho) - u(\xi)$ for more general interaction ranges $\rho \in \mathcal{R}$ by

$$\begin{aligned} u'_\xi &:= u(\xi) - u(\xi-1) = D_1 u(\xi-1) = -D_{-1}u(\xi), \\ u'_\xi + u'_{\xi-1} &= D_2 u(\xi-2) = -D_{-2}u(\xi). \end{aligned} \tag{3.5}$$

3.2. Atomistic energy

Let $V \in C^k(\mathbb{R}^{\mathcal{R}})$, $k \ge 2$, be the interatomic many-body site potential. For compact displacements $u \in \mathcal{U}_0$, we can then define

$$\mathcal{E}^{\rm a}(u) := \sum_{\xi=0}^{\infty} \Phi^{\rm a}_\xi(u), \quad \text{where} \quad \Phi^{\rm a}_\xi(u) := \begin{cases} V(Du(\xi)) - V(\mathbf{0}), & \xi \ge 1, \\ \frac{1}{2}\big(V(Du(\xi)) - V(\mathbf{0})\big), & \xi = 0. \end{cases}$$

Remark 3.5. For the next-nearest neighbour Lennard-Jones model studied in Section 2, we have from (2.2) and (3.5) that

$$\begin{aligned} V(g_{-2}, g_{-1}, g_1, g_2) &= \frac{1}{2}\sum_{\rho=1}^{2}[\phi(\rho\mathsf{A} + g_\rho) + \phi(\rho\mathsf{A} - g_{-\rho})] \\ &= \tfrac{1}{2}\big\{\phi_1(-g_{-1}) + \phi_1(g_1) + \phi_2(-g_{-2}) + \phi_2(g_2)\big\}, \end{aligned} \tag{3.6}$$

where $\phi_i(s) := \phi(i\mathsf{A} + s)$ and $\mathsf{A} > 0$ is the macroscopic stretch described in Section 2.1.

For the embedded atom model (Daw and Baskes 1984), we have

$$V(g_{-r_{\rm cut}},\dots,g_{r_{\rm cut}}) = \frac{1}{2}\sum_{\rho=1}^{r_{\rm cut}}\big[\phi(\rho\mathsf{A}+g_\rho)+\phi(\rho\mathsf{A}-g_{-\rho})\big] + \psi\left(\sum_{\rho=1}^{r_{\rm cut}}\big[\eta(\rho\mathsf{A}+g_\rho)+\eta(\rho\mathsf{A}-g_{-\rho})\big]\right), \tag{3.7}$$

where ψ is the embedding energy function and η is the electron density function.

Remark 3.6. The definition of $\mathcal{E}^{\rm a}$ employs the convention that u is extended to an antisymmetric displacement. Hence, we should confirm that this coincides with the natural definition

$$\mathcal{E}^{\rm a}(u) = \frac{1}{2}\sum_{\xi\in\mathbb{Z}}\big\{V(Du(\xi))-V(\mathbf{0})\big\}. \tag{3.8}$$

One can readily check that

$$D_\rho u(\xi) = -D_{-\rho}u(-\xi). \tag{3.9}$$

Hence, to obtain identity (3.8), we require that $V(\{g_\rho\}) = V(\{-g_{-\rho}\})$. Indeed, this is a natural condition, originating from lattice symmetries, that we will state as a standing assumption in (3.15).

Since $\Phi^{\rm a}_\xi$ is an energy difference from the reference state, the lattice sum is finite for compact displacements, and hence $\mathcal{E}^{\rm a}:\mathcal{U}_0\to\mathbb{R}$ is well-defined. $\mathcal{E}^{\rm a}(u)$ should be understood as the energy difference between the deformed state $y = y^{\mathsf{A}}+u$ and the reference state $y^{\mathsf{A}} = \mathsf{A}\mathbb{Z}$ (or $y^{\mathsf{A}}(\xi) = \mathsf{A}\xi$; similarly we will use $u^{\mathsf{F}}(\xi) = \mathsf{F}\xi$). The macroscopic stretch A is encoded in the definition of the potential V (see (2.1)).

We impose the far-field boundary condition $y(\xi)\sim y^{\mathsf{A}}(\xi)$ as $\xi\to\infty$, which, in terms of u, corresponds to $u(\xi)\sim 0$ as $\xi\to\infty$. Hence, $\mathcal{U}_0$ should be contained in any admissible displacement space. We now briefly explain why it is natural to take its closure with respect to the H^1-seminorm. From the proofs that we present in Appendix A, one can readily deduce that $|\mathcal{E}^{\rm a}(u)|\lesssim\|\nabla u\|_{L^2}^2$ for all $u\in\mathcal{U}_0$. Moreover, for the choice $V(Du(\xi)) = |D_1u(\xi)|^2+|D_2u(\xi)|^2$ this estimate is sharp (in general, it is sharp for all 'small' displacements). Consequently, $\mathcal{U}$ is the largest space to which $\mathcal{E}^{\rm a}$ can be extended continuously.

Proposition 3.7. $\mathcal{E}^{\rm a}:\mathcal{U}_0\to\mathbb{R}$ is continuous. In particular, there exists a unique continuous extension of $\mathcal{E}^{\rm a}$ to $\mathcal{U}$, which we still denote by $\mathcal{E}^{\rm a}$.

Proof. See Appendix A. □

From now on, we understand $\mathcal{E}^{\mathrm{a}}$ to be defined on $\mathcal{U}$. Next, we establish the differentiability of $\mathcal{E}^{\mathrm{a}}$. To that end, we introduce some notation for partial derivatives of V and Φ^{a}_ξ. For $\boldsymbol{\rho} = (\rho_1, \dots, \rho_j) \in \mathcal{R}^j$, $1 \le j \le k$, for $\boldsymbol{g} \in \mathbb{R}^{\mathcal{R}}$ and for $\xi \in \mathbb{Z}$, we define

$$V_{\boldsymbol{\rho}}(\boldsymbol{g}) := \frac{\partial^j V(\boldsymbol{g})}{\partial g_{\rho_1} \dots \partial g_{\rho_j}}, \quad \text{and analogously}$$

$$\Phi^{\mathrm{a}}_{\xi,\boldsymbol{\rho}}(u) := \begin{cases} V_{\boldsymbol{\rho}}(Du(\xi)), & \xi \in \mathbb{Z}_+ \setminus \{0\}, \\ \frac{1}{2} V_{\boldsymbol{\rho}}(Du(0)), & \xi = 0. \end{cases}$$

Note that for $\xi \ge r_{\mathrm{cut}}$, $\Phi^{\mathrm{a}}_{\xi,\rho}(u) = \partial \Phi^{\mathrm{a}}_\xi(u)/\partial u(\xi + \rho)$, and so forth, but for $\xi < r_{\mathrm{cut}}$ this is false.

We define bounds on partial derivatives

$$m(\boldsymbol{\rho}) := \prod_{i=1}^{j} |\rho_i| \sup_{\boldsymbol{g} \in \mathbb{R}^{\mathcal{R}}} \|V_{\boldsymbol{\rho}}(\boldsymbol{g})\| \quad \text{for } \boldsymbol{\rho} \in \mathcal{R}^j, \quad \text{and}$$

$$M^{(j,s)} := \sum_{\boldsymbol{\rho} \in \mathcal{R}^j} m(\boldsymbol{\rho}) |\boldsymbol{\rho}|^s_\infty,$$

where $\|\cdot\|$ denotes the ℓ^2-operator norm of a multilinear form and $|\boldsymbol{\rho}|_\infty := \max_{i=1,\dots,j} |\rho_i|$.

We shall assume throughout that the constants $M^{(j,s)}$ for $j = 1, \dots, k$ and $s \ge 0$ are finite. This assumption is in stark contrast to realistic interatomic potentials, which become singular as the distance between any two nuclei tends to zero. We make this assumption purely for the sake of convenience; removing it is not analytically challenging (see, *e.g.*, Ortner (2011) and Ortner and Theil (2013)) but complicates both the formulations and proofs of our results without introducing interesting conceptual ideas. To weaken the assumption, one may simply take the supremum of $\boldsymbol{g}$ over a *regime of interest*.

Remark 3.8. For most of our error analysis we will show how the constants in the estimates depend on the interaction potential by explicitly including prefactors of the form $M^{(j,s)}$. These prefactors in the estimates can be obtained by carefully tracing the dependence on the interaction potential in the proofs. Because this is tedious, we will in fact never carry out these details. However, it is important to be aware of this dependence, since the constants in the error estimates can be large (or even infinite) when the interaction decays slowly.

Lemma 3.9. $\mathcal{E}^{\rm a}$ is k times continuously Fréchet-differentiable, with variations

$$\langle \delta^j \mathcal{E}^{\rm a}(u)\boldsymbol{v}\rangle = \sum_{\xi\in\mathbb{Z}_+}\sum_{\boldsymbol{\rho}\in\mathcal{R}^j} \Phi^{\rm a}_{\xi,\boldsymbol{\rho}}(u)\prod_{i=1}^{j} D_{\rho_i}v_i(\xi) \quad \text{for all } \boldsymbol{v}\in\mathcal{U}_0^j, \tag{3.10}$$

for $j = 1,\dots,k$. Moreover, if $\sum_{i=1}^j \frac{1}{p_i} = 1$, then $\delta^j\mathcal{E}^{\rm a}$ satisfies the bound

$$\langle \delta^j \mathcal{E}^{\rm a}(u)\boldsymbol{v}\rangle \le M^{(j,0)}\prod_{i=1}^{j}\|\nabla v_i\|_{L^{p_i}} \quad \text{for all } \boldsymbol{v}\in\mathcal{U}_0^j. \tag{3.11}$$

Proof. See Appendix A. □

Remark 3.10. For test functions $v\in\mathcal{U}$, second and higher variations are well-defined via (3.10). First variations can be written as

$$\langle \delta\mathcal{E}^{\rm a}(u), v\rangle = \sum_{\xi\in\mathbb{Z}_+}\sum_{\rho\in\mathcal{R}} \big(\Phi^{\rm a}_{\xi,\rho}(u) - \Phi^{\rm a}_{\xi,\rho}(0)\big) D_\rho v(\xi). \tag{3.12}$$

Note that $\sum_{\xi\in\mathbb{Z}} D_\rho u(\xi) = 0$ for $u\in\mathcal{U}_0$, hence the constant $\Phi^{\rm a}_{\xi,\rho}(0)$ need not be subtracted. For $u\in\mathcal{U}$, (3.10) with $j=1$ may be ill-defined.

Remark 3.11 (far-field boundary condition). For $u\in\mathcal{U}$, the Cauchy–Schwarz inequality immediately implies that

$$|u(\xi)| \le \xi^{1/2}\|\nabla u\|_{L^2}. \tag{3.13}$$

Moreover, by checking that the displacement $u(\xi) := |\xi|^{1/2-\epsilon}$ belongs to $\mathcal{U}$ for $0<\epsilon<1/2$, we see that this bound is essentially sharp. This raises the question in which sense the far-field boundary condition $u\sim 0$ is still observed in the space $\mathcal{U}$. We interpret this as follows.

Let $y(\xi) := \mathsf{A}\xi + u(\xi)$ be the atomistic *deformation*, where $\mathsf{A}>0$ is a prescribed macroscopic stretch. Then (3.13) implies that

$$y(\xi) = \mathsf{A}\xi + u(\xi) \sim \mathsf{A}\xi \quad \text{as } |\xi|\to\infty, \tag{3.14}$$

which formally translates to $u(\xi)\sim 0$.

We remark that, in 2D, elements in the closure of $\mathcal{U}_0$ may still exhibit logarithmic growth, while in 3D they decay to zero uniformly due to the Gagliardo–Nirenberg–Sobolev embedding.

Symmetries of V

Since we are considering a single species of atoms it follows that permuting the atom positions should not change the total energy. Moreover, inversion of the atom positions about any point should also leave the energy invariant. It is therefore natural to assume that the site potential satisfies

$$V\big(\{-g_{-\rho}\}_{\rho\in\mathcal{R}}\big) = V\big(\{g_\rho\}_{\rho\in\mathcal{R}}\big) \quad \text{for all } \boldsymbol{g}\in\mathbb{R}^{\mathcal{R}}. \tag{3.15}$$

See, for example, the Lennard-Jones (3.6) and EAM (3.7) models. As a matter of fact, if only the global energy satisfies such a symmetry, but not the site potential, then one can construct a modified site potential that does satisfy (3.15): see Van Koten and Ortner (2012).

From (3.15), and the fact that $-\mathsf{F}(-\rho) = \mathsf{F}\rho$, it is easy to deduce that

$$V_{-\boldsymbol{\rho}}\big(\{\mathsf{F}\rho\}_{\rho\in\mathcal{R}}\big) = (-1)^j V_{\boldsymbol{\rho}}\big(\{\mathsf{F}\rho\}_{\rho\in\mathcal{R}}\big) \quad \text{for all } \boldsymbol{\rho}\in\mathcal{R}^j,\ \mathsf{F}\in\mathbb{R}. \tag{3.16}$$

This will be a useful property to exploit later on.

3.3. The variational problem

For the sake of simplicity, we consider only (antisymmetric) dead load external forces. This allows us to focus on the properties of the internal energies. We say that a lattice function $f : \mathbb{Z}_+ \to \mathbb{R}$ belongs to $\mathcal{U}^*$ if there exists a constant $\|f\|_{\mathcal{U}^*}$ such that

$$\langle f, v\rangle_{\mathbb{Z}_+} \le \|f\|_{\mathcal{U}^*}\|\nabla v\|_{L^2} \quad \text{for all } v\in\mathcal{U}_0.$$

In this case, the linear form $\langle f,\cdot\rangle_{\mathbb{Z}_+}$ can be extended to a bounded linear functional on $\mathcal{U}$. It is easy to see that $f\in\mathcal{U}^*$ if and only if there exists $g\in\ell^2(\mathbb{Z}_+)$ such that $D_{-1}g(\xi) = f(\xi)$ for $\xi\ge 1$.

Given $f\in\mathcal{U}^*$, we seek

$$u^{\mathrm{a}} \in \arg\min\big\{\mathcal{E}^{\mathrm{a}}(u) - \langle f, u\rangle_{\mathbb{Z}_+} \,\big|\, u\in\mathcal{U}\big\}. \tag{3.17}$$

We understand (3.17) as a *local minimization problem* that may have several or no solutions. If u^{a} solves (3.17), then it satisfies the Euler–Lagrange equation

$$\langle \delta\mathcal{E}^{\mathrm{a}}(u), v\rangle = \langle f, v\rangle_{\mathbb{Z}_+} \quad \text{for all } v\in\mathcal{U}. \tag{3.18}$$

Vice versa, if $u^{\mathrm{a}}\in\mathcal{U}$ satisfies (3.18) and in addition the second-order sufficient optimality condition

$$\langle \delta^2\mathcal{E}^{\mathrm{a}}(u^{\mathrm{a}})v, v\rangle \ge c_0\|\nabla v\|_{L^2}^2 \quad \text{for all } v\in\mathcal{U}, \tag{3.19}$$

for some $c_0 > 0$, then u^{a} is a solution to (3.17). We call such a solution a *strong local minimizer*. (Note that (3.19) is not a strong requirement: if u^{a} solves (3.17) then it automatically satisfies (3.19) with $c_0 = 0$.)

We shall not be concerned with a general existence theory of solutions to (3.17). However, we state the following trivial result.

Proposition 3.12. Suppose that $k\ge 3$ and that the reference state is strongly stable; that is, there exists $c_0 > 0$ such that

$$\langle \delta^2\mathcal{E}^{\mathrm{a}}(0)v, v\rangle \ge c_0\|\nabla v\|_{L^2}^2 \quad \text{for all } v\in\mathcal{U}.$$

Then there exists $\epsilon > 0$ such that, for all $f\in\mathcal{U}^*$ with $\|f\|_{\mathcal{U}^*} < \epsilon$, (3.17) has a strong local minimizer.

Proof. This result is an immediate consequence of the inverse function theorem. □

In order to analyse approximations to (3.17), we will need to exploit regularity properties of the solution u^{a}. To that end, we shall make the following *assumption.*

(DH) *Decay hypothesis.* There exists a strong local minimizer $u^{\mathrm{a}} \in \mathcal{U}$ of (3.17) and $\alpha > 1/2$, such that

$$\left|\nabla^j \tilde{u}^{\mathrm{a}}(x)\right| \le C_{\mathbf{DH}} x^{-\alpha+1-j}, \quad \text{for } x > r_0,\ j = 0,1,2,3. \tag{3.20}$$

Moreover, we assume that $|\nabla^j \tilde{f}(x)| \le C_{\mathbf{DH}} x^{-\alpha-1-j}$ for $j = 0,1,2$.

Remark 3.13. **(1)** The requirement that $\alpha > 1/2$ is due to the fact that, if $|\nabla u(x)| \sim x^{-\alpha}$ as $x \to \infty$, for $\alpha \le 1/2$, then $u \notin \mathcal{U}$. Thus, **(DH)** does not represent a significant restriction of generality.

(2) Formally, we expect that (3.20) holds provided that $|\nabla^j \tilde{f}(x)| \lesssim x^{-\alpha-1-j}$ for $j = 0,1$. A rigorous proof of this result is tedious, but not difficult. *Vice versa*, it is easy to see that (3.20) implies the stated decay for f, $j = 0,1$. The natural additional assumption that $|\nabla^2 \tilde{f}(x)| \lesssim x^{-\alpha-3}$ will be required in the external consistency estimate derived in Section 5.3.

3.4. Approximation from a finite domain

Since $\mathcal{U}$ is infinite-dimensional, (3.17) cannot be solved directly, hence we reduce the problem to a finite domain and estimate the resulting error. We fix $N \in \mathbb{N}$ and define the finite-dimensional displacement space

$$\mathcal{U}_N := \big\{ u \in \mathcal{U}_0 \,|\, u(\xi) = 0 \text{ for } \xi \ge N \big\}.$$

We approximate the exact variational problem (2.3) with

$$u^N \in \arg\min \big\{ \mathcal{E}^{\mathrm{a}}(u) - \langle f, u \rangle_{\mathbb{Z}_+} \,\big|\, u \in \mathcal{U}_N \big\}. \tag{3.21}$$

This formulation effectively reduces the infinite domain $\mathbb{Z}$ to the finite domain $\{0, \dots, N\}$.

Since (3.21) is a pure Galerkin approximation, we expect that the error is equivalent to the best approximation error. We define an approximation operator $\Pi_N : \mathcal{U} \to \mathcal{U}_N$ as follows:

$$\Pi_N u(\xi) := \begin{cases} u(\xi) - \frac{\xi}{N} u(N), & \xi = 0, \dots, N, \\ 0, & \xi > N. \end{cases}$$

It is straightforward to see that, if u satisfies **(DH)**, then

$$\|\nabla u - \nabla \Pi_N u\|_{L^2} \le C N^{1/2-\alpha}, \tag{3.22}$$

where C depends on α and on $C_{\mathbf{DH}}$. This motivates the following result.

Theorem 3.14. Let u^{a} be a strong local minimizer of (3.17) satisfying **(DH)** and (3.19). Then there exists $N_0 \in \mathbb{N}$ such that, for all $N \geq N_0$, there exists a strong local minimizer u^N of (3.21) satisfying

$$\|\nabla u^{\mathrm{a}} - \nabla u^N\|_{L^2} \leq \frac{C}{c_0} N^{1/2-\alpha},$$

where C depends on $M^{(2,0)}, \alpha$, and $C_{\mathbf{DH}}$; and c_0 is the coercivity constant from (3.19).

Proof. The result is an easy consequence of the quantitative inverse function theorem stated in Appendix B.

The Euler–Lagrange equation for (3.21) is

$$\langle \delta\mathcal{E}^{\mathrm{a}}(u^N), v\rangle = \langle f, v\rangle_{\mathbb{Z}_+} \quad \text{for all } v \in \mathcal{U}_N,$$

which can be written equivalently as

$$\langle \mathcal{G}_N(e), v\rangle := \langle \delta\mathcal{E}^{\mathrm{a}}(\Pi_N u^{\mathrm{a}} + e) - \delta\mathcal{E}^{\mathrm{a}}(u^{\mathrm{a}}), v\rangle = 0 \quad \text{for all } v \in \mathcal{U}_N, \tag{3.23}$$

where $e := u^N - \Pi_N u^{\mathrm{a}}$. We aim to solve (3.23) in $\mathcal{U}_N$. Since $\delta\mathcal{G}_N = \delta^2\mathcal{E}^{\mathrm{a}}(\Pi_N u^{\mathrm{a}} + \cdot)$ is Lipschitz (according to Lemma 3.9) we only need to show that $\|\mathcal{G}_N(0)\|_{\mathcal{U}_N^*}$ can be made arbitrarily small and that $\delta\mathcal{G}_N(0)$ is positive definite.

Using (3.11) and (3.22), we bound the residual by

$$\begin{aligned}\|\mathcal{G}_N(0)\|_{\mathcal{U}_N^*} &= \|\delta\mathcal{E}^{\mathrm{a}}(\Pi_N u^{\mathrm{a}}) - \delta\mathcal{E}^{\mathrm{a}}(u^{\mathrm{a}})\|_{\mathcal{U}_N^*} \\ &\leq M^{(2,0)}\|\nabla\Pi_N u^{\mathrm{a}} - \nabla u^{\mathrm{a}}\|_{L^2} \leq C M^{(2,0)} N^{1/2-\alpha}.\end{aligned}$$

In particular, $\|\mathcal{G}_N(0)\|_{\mathcal{U}_N^*} \to 0$ as $N \to \infty$.

Using again (3.11) and (3.22), and also the fact that $\|\nabla w\|_{L^\infty} \leq \|\nabla w\|_{L^2}$ for all $w \in \mathcal{U}$, we can also bound the coercivity constant of $\delta\mathcal{G}_N(0)$:

$$\begin{aligned}\langle \delta\mathcal{G}_N(0)v, v\rangle &= \langle \delta^2\mathcal{E}^{\mathrm{a}}(\Pi_N u^{\mathrm{a}})v, v\rangle \\ &\geq \langle \delta^2\mathcal{E}^{\mathrm{a}}(u^{\mathrm{a}})v, v\rangle - M^{(3,0)}\|\nabla\Pi_N u^{\mathrm{a}} - \nabla u^{\mathrm{a}}\|_{L^\infty}\|\nabla v\|_{L^2}^2 \\ &\geq \big(c_0 - C M^{(3,0)} N^{1/2-\alpha}\big)\|\nabla v\|_{L^2}^2.\end{aligned}$$

In particular, if N is sufficiently large, then

$$\langle \delta\mathcal{G}_N(0)v, v\rangle \geq \frac{c_0}{2}\|\nabla v\|_{L^2}^2 \quad \text{for all } v \in \mathcal{U}_N.$$

Combining these estimates and applying the inverse function theorem, Lemma B.1, we obtain the stated result. □

Remark 3.15. **(1)** Theorem 3.14 is an error estimate in terms of the *computational cost* required to solve (3.21). This motivates us to analyse a/c methods in terms of their computational cost as well.

(2) Theorem 3.14 can also be understood to establish that (3.17) is the *thermodynamic limit* of (3.21) as $N \to \infty$ and generalizations are therefore interesting. (i) If u^{a} does not satisfy the decay hypothesis **(DH)**, then Theorem 3.14 is still true, but without an explicit convergence rate. (ii) If we were to apply periodic boundary conditions to (3.21), then the approximation operator Π_N would still be admissible and hence, with only minor modifications, the result can be extended to this case. (iii) Moreover, the result can be readily extended to 2D/3D.

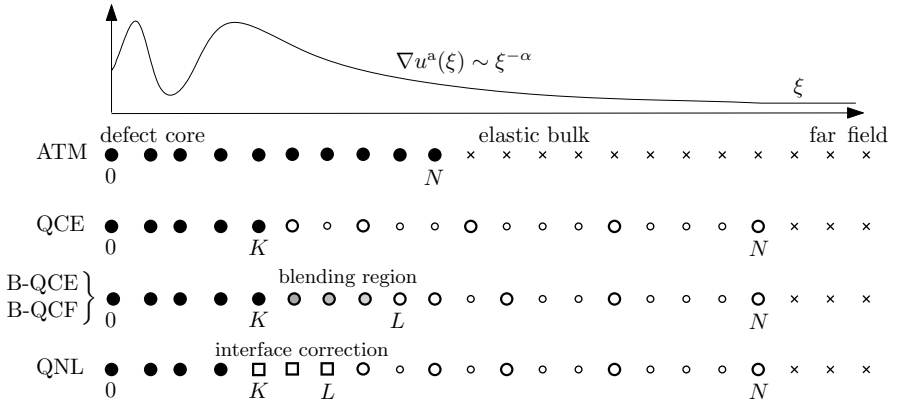

Figure 3.1. Illustration of the a/c coupling methods introduced in Section 4, and of the decay hypothesis **(DH)**. Black discs (•) indicate atoms described by the atomistic model; white discs (∘) indicate atoms modelled by the Cauchy–Born model; grey discs indicate the blending region used in the B-QCE and B-QCF methods; squares □ indicate atoms receiving special interface corrections as in QNL-type constructions. Finally, small white discs are atoms that are 'slaved' to the rep-atoms (large white discs) via P1 interpolation, and small crosses × are atoms removed via the far-field boundary condition.

4. Many-body finite-range atomistic-to-continuum coupling

In this section, we introduce the a/c couplings that we will analyse in the context of the atomistic model introduced in the previous section. We will point out the main approximations being made in the various a/c couplings and give an outline of our analytical approach, to motivate the subsequent analysis.

An illustration and summary of all a/c coupling methods, including the purely atomistic model (ATM), is given in Figure 3.1.

4.1. The quasicontinuum idea: Galerkin projection

In Section 2 we introduced a/c methods via the idea of coupling an atomistic to a continuum model. Here, we take an alternative point of view: we first

project $\mathcal{E}^{\rm a}$ onto a coarse subspace, and then apply further approximations to render the coarse optimization problem computable. Ultimately, the two philosophies lead to the same a/c coupling formulations.

We restrict displacements again to a computational domain $[0, N]$, $N \in \mathbb{N}$: see Section 3.4. Let $\mathcal{T}_h = \{T\}$ be a regular partition of $[0, N]$ into closed intervals T, with vertices $\mathcal{N}_h \subset \mathbb{Z}_+$ (or, *rep-atoms* in the language of the quasicontinuum method). We define the coarse displacement space by

$$\mathcal{U}_h := \big\{ u_h \in \mathcal{U}_N \,\big|\, u_h \text{ is piecewise affine with respect to } \mathcal{T}_h \big\}. \tag{4.1}$$

Elements of $\mathcal{U}_h$ are defined pointwise, but give rise to lattice functions through point evaluation. Since finite element nodes lie on lattice sites, this is compatible with our interpolation of lattice functions.

The philosophy of the *quasicontinuum* (QC) *method* is to retain the atomistic description, but restrict the admissible set to the *coarse space* $\mathcal{U}_h$:

$$u_h^{\rm qc} \in \arg\min \big\{ \mathcal{E}^{\rm a}(u_h) - \langle f, u_h \rangle_{\mathbb{Z}_+} \,\big|\, u_h \in \mathcal{U}_h \big\}. \tag{4.2}$$

Typically, one would let all atoms in the neighbourhood of a defect (in our case the origin) be finite element vertices (atomistic region), and rapidly coarsen the mesh in the surrounding bulk (continuum region). Thus, one would fully resolve the defect, but transition seamlessly to a coarse 'continuum-like' description of the far field.

The method (4.2) is formulated in the spirit of Galerkin approximations for nonlinear variational problems. Applying the standard arguments for approximations of this type, one can see that, if a solution $u^{\rm a}$ of (3.17) exists, and its best approximation from $\mathcal{U}_h$ lies 'sufficiently close', then a solution $u_h^{\rm qc}$ of (4.2) exists, satisfying Céa's lemma.

In 1D, the implementation of (4.2) can be achieved with $O(\#\mathcal{N}_h)$ complexity since the element interfaces are particularly simple. However, in 2D/3D the evaluation of $\mathcal{E}^{\rm a}(u_h)$ and $\delta\mathcal{E}^{\rm a}(u_h)$ for $u_h \in \mathcal{U}_h$ still requires summation over a number of lattice points proportional to the area of the element faces, which is much larger than $\#\mathcal{N}_h$. To make this precise: while displacement gradients ∇u_h are homogeneous inside elements $T \in \mathcal{T}_h$, the interaction stencils $Du_h(\xi)$ are only homogeneous ($Du_h(\xi) = \nabla u_h|_T \cdot \mathcal{R}$) in subsets of the elements T. Near element interfaces, one must resort to exact summation over all lattice sites. Thus, the cost of evaluating $\mathcal{E}^{\rm a}(u_h)$ and $\delta\mathcal{E}^{\rm a}(u_h)$ scales with the surface area of the mesh, which in 1D is $O(\#\mathcal{N}_h)$, but is significantly higher in 2D/3D.

In conclusion, while (4.2) is attractive from a theoretical perspective, it is not a practical scheme.

4.2. Finite element notation

Before we introduce the various many-body a/c couplings in the following subsections, we summarize a unified notation for finite element meshes.

We fix three mesh parameters K, L, $N \in \mathbb{N}$, $K \leq L \leq N/2$, where the computational domain is $[0, N]$. We choose a set of finite element nodes $\mathcal{N}_h = \{\nu_0, \ldots, \nu_{N_{\mathcal{T}_h}}\}$, for some $N_{\mathcal{T}_h} \in \mathbb{N}$, such that $\{0, \ldots, L, N\} \subset \mathcal{N}_h \subset \{0, \ldots, N\}$. The set of interior nodes is $\mathcal{N}_h^\circ := \mathcal{N}_h \setminus \{0, N\}$. The finite elements are given by $\mathcal{T}_h = \{[\nu_{j-1}, \nu_j] \,|\, j = 1, \ldots, J\}$. For each $T \in \mathcal{T}_h$, let $h_T := \operatorname{diam} T$. For each $x \in [0, N]$, $x \in \operatorname{int} T$, let $h(x) := h_T$. For $x > N$, let $h(x) := 1$.

The space of all continuous piecewise affine functions on $[0, N]$ is given by $\mathrm{P1}(\mathcal{T}_h)$, and the space of piecewise constant functions by $\mathrm{P0}(\mathcal{T}_h)$. The admissible finite element space $\mathcal{U}_h$ is defined by (4.1), and imposes the boundary condition $u_h(0) = u_h(N) = 0$.

Finally, for any function $v : \mathcal{N}_h \to \mathbb{R}$, let $I_h v : [0, N] \to \mathbb{R}$, $I_h v \in \mathrm{P1}(\mathcal{T}_h)$, denote its continuous piecewise affine interpolant,

$$I_h v(\zeta) := v(\zeta) \quad \text{for all } \zeta \in \mathcal{N}_h.$$

Coarse-graining the external forces
For $f, g : \mathcal{N}_h \to \mathbb{R}^J$, we define

$$\langle f, g \rangle_h := \int_0^N I_h(f \cdot g)\,\mathrm{d}x = \sum_{j=1}^{J} \tfrac{1}{2} h_T \big\{ f(\nu_{j-1}) \cdot g(\nu_{j-1}) + f(\nu_j) \cdot g(\nu_j) \big\}.$$

In all our a/c couplings, we shall approximate the potential of the external forces, $\langle f, u_h \rangle_{\mathbb{Z}_+}$, by its (coarse-grained) trapezoidal rule approximation, $\langle f, u_h \rangle_h$.

4.3. Cauchy–Born approximation and QCE method

In Section 4.1 we constructed a coarse-graining scheme that reduces the number of degrees of freedom, but still has a high computational cost for evaluating the energy and forces (at least its 2D/3D variants do). An analogy in continuum mechanics is that integrals occurring in Galerkin projections of nonlinear equations cannot be evaluated explicitly. In continuum mechanics, the solution to this issue is to employ quadrature rules to approximate the variational forms.

In the present case, since we are using P1 finite elements, the midpoint rule is a natural choice. For each 'large' element $T \in \mathcal{T}_h$ we choose an atomic site ξ_T near the centre of T and formally approximate

$$\sum_{\xi \in T} \Phi^{\mathrm{a}}_\xi(u_h) \approx \#(T \cap \mathbb{Z}) \Phi^{\mathrm{a}}_{\xi_T}(u_h) \approx |T| \Phi^{\mathrm{a}}_{\xi_T}(u_h),$$

where the issue of multiple counting of atoms at element boundaries is resolved at the second approximation step. If T is sufficiently large that

$\xi_T + \mathcal{R} \subset T$, then we obtain

$$\sum_{\xi \in T} \Phi^{\rm a}_\xi(u_h) \approx |T| W(\nabla u_{h|_T}), \quad \text{where} \quad W(\mathsf{F}) := V(Du^{\mathsf{F}}(0)) - V(\mathbf{0}), \tag{4.3}$$

(recall that $u^{\mathsf{F}}(\xi) := \mathsf{F}\xi$), which is called the *Cauchy–Born strain energy density function*, generalizing the definition (2.8) for the NNN Lennard-Jones model. This approximation is also suitable for smaller elements provided that u_h is approximately affine in a neighbourhood of each element T (*i.e.*, u_h is 'smooth'). This motivates the following construction.

In the energy-based quasicontinuum method (QCE method) of Tadmor *et al.* (1996), previously introduced in Section 2.4, we fix $r_{\rm cut} \leq K = L < N$. For each site $\xi = K+1, K+2, \ldots$, we define the Cauchy–Born site energy

$$\Phi^{\rm c}_\xi(u_h) := \int_{\xi-1/2}^{\xi+1/2} W(\nabla u_h)\,{\rm d}x.$$

Then the energy functional of the QCE method is defined by $\mathcal{E}^{\rm qce} : \mathcal{U}_h \to \mathbb{R}$, where

$$\mathcal{E}^{\rm qce}(u_h) := \sum_{\xi=0}^{K} \Phi^{\rm a}_\xi(u_h) + \sum_{\xi=K+1}^{N} \Phi^{\rm c}_\xi(u_h). \tag{4.4}$$

Since the QCE energy is given as a finite sum of C^k potentials, it follows that $\mathcal{E}^{\rm qce} \in C^k(\mathcal{U}_h)$.

The energy (4.4) can be rewritten in a format more natural for its implementation:

$$\mathcal{E}^{\rm qce}(u_h) = \sum_{\xi=0}^{K} \Phi^{\rm a}_\xi(u_h) + \int_{K+1/2}^{N} W(\nabla u_h)\,{\rm d}x. \tag{4.5}$$

In the QCE method, we approximate the atomistic problem (3.17) by

$$u_h^{\rm qce} \in \arg\min \left\{ \mathcal{E}^{\rm qce}(u_h) - \langle f, u_h \rangle_h \,\middle|\, u_h \in \mathcal{U}_h \right\}. \tag{4.6}$$

The patch test and the ghost force problem

A key motivation for the QCE method is that

$$\Phi^{\rm c}_\xi(u^{\mathsf{F}}) = \Phi^{\rm a}_\xi(u^{\mathsf{F}}) \quad \text{for all } \mathsf{F} \in \mathbb{R},\ \xi \geq K+1. \tag{4.7}$$

That is, the QCE site energies are exact under (locally) homogeneous deformations. We call (4.7) *local energy consistency*. As demonstrated in Section 2.4, it implies that $\mathcal{E}^{\rm qce}(u_h) \approx \mathcal{E}^{\rm a}(u)$ if u is 'smooth' in the continuum region and u_h is a 'good approximation' to u.

However, in order to ensure that minimizers of (4.6) approximate minimizers of (3.17), we require more stringent conditions (consistency and stability, which we touched upon in Section 2 and will discuss in more detail

in Section 4.7). Indeed, as shown in Section 2.4, the QCE method generally fails the *force patch test*, $\delta\mathcal{E}^{\rm qce}(0) \neq 0$, that is, $u_h = 0$ is not a critical point of (4.6). In other words, even if $u^{\rm a}$ is 'smooth', a solution $u_h^{\rm qce}$ to (4.6) develops an oscillation at the a/c interface that lowers the energy further. This effect *always* creates an $O(1)$ error in the QCE methods (Dobson and Luskin 2009*a*, Ming and Yang 2009).

Further remarks

(1) Whereas earlier literature on a/c coupling exists, the introduction of the QCE method by Tadmor *et al.* (1996) spawned a surge of activity in the field. In particular, the Cauchy–Born approximation appears to have been used for the first time in this context. An iterative correction of the interface inconsistency ('ghost forces') was suggested by the same group (Shenoy *et al.* 1999), which leads naturally into force-based coupling schemes, discussed in Sections 2.7, 2.8 and 4.6.

(2) We may also consider the 'pure Cauchy–Born' approximation,

$$u^{\rm c} \in \arg\min \left\{ \mathcal{E}^{\rm c}(u) - \langle f, u\rangle_{\mathbb{R}_+} \,\middle|\, u \in \dot{H}^1 \right\}, \tag{4.8}$$

where

$$\mathcal{E}^{\rm c}(u) = \int_0^\infty W(\nabla u)\,{\rm d}x,$$

$\langle f, u\rangle_{\mathbb{R}_+} = \int_0^\infty fu\,{\rm d}x$ provided that $f \cdot u$ is integrable, and $\dot{H}^1$ is a homogeneous Sobolev space ($u \in \dot{H}^1$ if and only if $u \in H^1_{\rm loc}$ and $\nabla u \in L^2$). This model goes back to the work of Cauchy (1882), who used it to derive symmetries of the tensor of linearized elasticity (the Cauchy relations). In the modern calculus of variations and PDE literature, the Cauchy–Born model has been analysed and discussed, for instance by Blanc, Le Bris and Lions (2002), Friesecke and Theil (2002), E and Ming (2007), and Makridakis and Süli (2013). Recently, Ortner and Theil (2013) have proved for both static and dynamic problems and general many-body interactions that the Cauchy–Born approximation is second-order accurate in a natural scaling limit.

(3) In this subsection we have only discussed the consequences of choosing a midpoint-type summation rule. However, we have approximated this further by the Cauchy–Born stored energy density. Lin (2007) shows that taking a cluster of atoms near the centre of each element leads to a first-order accurate method. Similarly, Gunzburger and Zhang (2010) consider discrete variants of higher-order quadrature rules. In both cases the transition to a fully refined mesh, which introduces substantial new algorithmic and analytical challenges, is not taken into account.

Knap and Ortiz (2001) as well as Eidel and Stukowski (2009) consider an entirely different class of summation rules, which are node-based rather

than element-based. These rules are, in principle, suited to transition to full atomistic resolution. However, Luskin and Ortner (2009) have shown that these node-based summation rules result in prohibitively large and uncontrollable consistency errors.

4.4. Energy blending (B-QCE)

We now generalize the energy blending approach described in Section 2.5. If we can 'spread' the QCE ghost force error over an interface region,

$$G(\xi) := \begin{cases} (L-K)^{-1}, & \xi = K, \dots, L-1, \\ 0, & \text{otherwise}, \end{cases} \quad \text{then } \|G\|_{\ell^2} = (L-K)^{-1/2}.$$

(However, $\|G\|_{\ell^1} = 1$ for all K, L.) In our consistency analysis in Section 6.2, we will in fact see that exploiting symmetries of the interaction potential reduces the coupling error by a factor of $(L-K)^{-3/2}$, provided that the blending function is chosen in an optimal way.

We now choose a blending function $\beta : [0, N] \to [0, 1]$ and define for $u_h \in \mathcal{U}_h$

$$\mathcal{E}^{\mathrm{bqce}}(u_h) := \sum_{\xi=0}^{N} \big\{ (1 - \beta(\xi)) \Phi_\xi^{\mathrm{a}}(u_h) + \beta(\xi) \Phi_\xi^{\mathrm{c}}(u_h) \big\}. \tag{4.9}$$

We choose $r_{\mathrm{cut}} < K < L < N$ and assume that $\beta(\xi) = 0$ in $[0, K]$ and $\beta(\xi) = 1$ in $[L, N]$; that is, the transition takes place between $\xi = K$ and L. It is then easy to rewrite (4.9) in the form

$$\mathcal{E}^{\mathrm{bqce}}(u_h) := \sum_{\xi=0}^{L} (1 - \beta(\xi)) \Phi_\xi^{\mathrm{a}}(u_h) + \int_K^N I_h \beta \cdot W(\nabla u_h) \, \mathrm{d}x. \tag{4.10}$$

Again, we observe that $\mathcal{E}^{\mathrm{bqce}} \in C^k(\mathcal{U}_h)$.

In the B-QCE method, we seek

$$u_h^{\mathrm{bqce}} \in \arg\min \big\{ \mathcal{E}^{\mathrm{bqce}}(u_h) - \langle f, u_h \rangle_h \,\big|\, u_h \in \mathcal{U}_h \big\}. \tag{4.11}$$

Further remarks

B-QCE shares the idea of a blending region with the bridging domain method (Belytschko and Xiao 2003), the AtC coupling method (Badia *et al.* 2008), the Arlequin method (Bauman *et al.* 2008, Prudhomme *et al.* 2008), and overlapping domain methods (Parks, Bochev and Lehoucq 2008, Seleson and Gunzburger 2010).

4.5. QNL-type methods

Concurrently with the introduction of blending methods, Shimokawa *et al.* (2004) introduced an approach that promised not just to reduce the ghost

forces but to remove them altogether. Their idea was to create a narrow transition region of 'quasi-nonlocal atoms' with modified site energies, so that their interaction with the atomistic region would have atomistic qualities (nonlocal) and their interaction with the continuum region would have continuum qualities (local). They proposed the *ansatz*

$$\begin{aligned}\mathcal{E}^{\rm qnl}(u_h) &:= \sum_{\xi=0}^{K} \Phi^{\rm a}_\xi(u_h) + \sum_{\xi=K+1}^{L-1} \Phi^{\rm i}_\xi(u_h) + \sum_{\xi=L}^{N} \Phi^{\rm c}_\xi(u_h) \\ &= \sum_{\xi=0}^{K} \Phi^{\rm a}_\xi(u_h) + \sum_{\xi=K+1}^{L-1} \Phi^{\rm i}_\xi(u_h) + \int_{L-1/2}^{N} W(\nabla u_h)\,{\rm d}x\end{aligned}$$

where $\Phi^{\rm i}_\xi$ is a modified site potential to be defined for $\xi = K+1, \dots, L-1$.

In the remainder of this article, we will allow the following general form of $\mathcal{E}^{\rm qnl}$, which also requires the definition of a site potential $\Phi^{\rm i}_L$:

$$\mathcal{E}^{\rm qnl}(u_h) = \sum_{\xi=0}^{K} \Phi^{\rm a}_\xi(u_h) + \sum_{\xi=K+1}^{L} \Phi^{\rm i}_\xi(u_h) + \int_{L}^{N} W(\nabla u_h)\,{\rm d}x. \tag{4.12}$$

(The previous definition of $\mathcal{E}^{\rm qnl}$ fits into this general form by defining the rightmost site potential to be $\Phi^{\rm i}_L(u_h) := \int_{L-1/2}^{L} W(\nabla u_h)\,{\rm d}x$.)

We have already seen an explicit example in Section 2.6, which suggests that this formulation can potentially lead to substantially improved accuracy. The key advantage over the B-QCE method is that we may be able to choose the interface width $L - K$ to be much smaller. However, this comes at the cost of a far more complex construction. Indeed, at the time of writing this article it is still not known whether methods of the type discussed in this section can be constructed for general many-body potentials and general interface geometries in 2D/3D.

The key new ingredient in (4.12) is the interface site energy $\Phi^{\rm i}_\xi$. We will later prove that it is sufficient to construct $\Phi^{\rm i}_\xi$ in such a way that the resulting energy satisfies the following force consistency condition.

(F) *Force consistency.* $\mathcal{F}^{\rm qnl}_\zeta(u^{\mathsf{F}}) = 0$ for all $\zeta \in \mathcal{N}_h^\circ,\ \mathsf{F} \in \mathbb{R}$,

where, here and throughout, we define

$$\mathcal{F}^{\rm qnl}_\zeta(u_h) := \frac{\partial \mathcal{E}^{\rm qnl}(u_h)}{\partial u_h(\zeta)},$$

and remark that due to the finite interaction range, $\mathcal{F}^{\rm qnl}_\xi(u^{\mathsf{F}})$ is well-defined despite the fact that $u^{\mathsf{F}} \notin \mathcal{U}_h$. (It is more common to define a force as $\mathcal{F}_\zeta = -\frac{\partial \mathcal{E}}{\partial u_h(\zeta)}$, but for notational convenience we have not followed this convention.)

The geometry reconstruction idea

The second key idea of Shimokawa *et al.* (2004) was to define the interface site energy Φ^{i} in terms of the original atomistic site energy Φ^{a}, but with 'reconstructed' atom positions. Rephrased in our notation, they proposed setting

$$\Phi^{\mathrm{i}}_\xi(u_h) := V\big(\tilde{D}u_h(\xi)\big) - V(\mathbf{0}) \quad \text{for } \xi = K+1, \dots, L-1, \tag{4.13}$$

where $\tilde{D}u_h(\xi) = \{\tilde{D}_\rho u_h(\xi)\}_{\rho\in\mathcal{R}}$ is a modified finite difference stencil. (Note the abuse of notation: $\tilde{D}_\rho$ may in fact be ξ-dependent.) The rationale is to allow interface atoms to interact via atomistic rules (nonlocally) with their neighbours in the atomistic region, and by continuum rules (locally) with their neighbours in the continuum region.

For example, suppose that $\mathcal{R} = \{\pm1, \pm2\}$. Then this intuition leads us to define $L = K + 3$, and

$$\tilde{D}u(\xi) = \big\{D_{-2}u(\xi), D_{-1}u(\xi), D_1u(\xi), 2D_1u(\xi)\big\} \quad \text{for } \xi = K+1, K+2. \tag{4.14}$$

It is straightforward to check that the resulting a/c coupling satisfies the force consistency condition **(F)**.

Note, however, that this idea does not extend to third neighbour interactions: if $\mathcal{R} = \{\pm1, \pm2, \pm3\}$, $L = K + 4$, and

$$\tilde{D}u(\xi) = \big\{D_{-3}u(\xi), D_{-2}u(\xi), D_{-1}u(\xi), D_1u(\xi), 2D_1u(\xi), 3D_1u(\xi)\big\},$$

then there is generally a ghost force acting on the atom $\xi = K + 1$, and possibly others.

E, Lu and Yang (2006) proposed a more general form of the stencil $\tilde{D}u(\xi)$ with free parameters that are then to be fitted in order to satisfy **(F)**. This idea was further generalized by Ortner and Zhang (2012) to

$$\tilde{D}u(\xi) = \left\{ \sum_{\varsigma\in\mathcal{R}} C_{\xi,\rho,\varsigma} D_\varsigma u(\xi) \right\}_{\rho\in\mathcal{R}}.$$

It turns out that, with this *ansatz*, **(F)** reduces to a linear system of equations that is independent of F and V. It is unknown at present whether this system has a solution for general a/c interfaces in 2D/3D; see E *et al.* (2006) and Ortner and Zhang (2012) for more details.

The reflection method

We now present a construction proposed by Ortner, Shapeev and Zhang (2013) (in a slightly different context this was previously proposed by Langwallner, Ortner and Süli (2013)) which is valid for general many-body interactions in 1D. Unfortunately there appears to be no straightforward generalization to 2D/3D.

The idea is to apply a reflection boundary condition to the atomistic region, thus decoupling it from the continuum region. We fix $K > 0$, set $L := K + r_{\rm cut}$, and for each $v \in \mathcal{U}$ define its antisymmetric reflection about the interface L,

$$\begin{cases} v^*(\xi) := v(\xi), & 0 \le \xi \le L, \\ v^*(L+\rho) := 2v(L) - v(L-\rho), & 1 \le \rho \le r_{\rm cut}. \end{cases} \tag{4.15}$$

Then we define

$$\begin{aligned} \mathcal{E}^{\rm rfl}(u) &:= \mathcal{E}^*(u) + \int_L^\infty W(\nabla u)\,{\rm d}x, \quad \text{where} \\ \mathcal{E}^*(u) &:= \sum_{\xi=0}^{L-1} \Phi^{\rm a}_\xi(u^*) + \tfrac{1}{2}\Phi^{\rm a}_L(u^*). \end{aligned} \tag{4.16}$$

It is easy to see that $\mathcal{E}^{\rm rfl}$ can be rewritten in the form (4.12).

We will now rewrite $\mathcal{E}^*$ in a more convenient form, in terms of a periodic cell energy, from which it will become immediately obvious that $\mathcal{E}^{\rm rfl}$ satisfies the force-consistency condition **(F)**. This construction follows Langwallner *et al.* (2013, Section 3.3).

First, we redefine the reflection operator by

$$u^*(\xi + 2L\eta) := 2\eta u(L) + u(\xi), \quad \text{for all } \xi \in \{-L, \dots, L\} \text{ and } \eta \in \mathbb{Z}. \tag{4.17}$$

One can readily check that (4.17) is an extension of the earlier definition:

$$u^*(L+\rho) = u^*\big([-L+\rho] + 2L\big) = 2u(L) + u(-L+\rho) = 2u(L) - u(L-\rho).$$

To understand (4.17), we rewrite $u(\xi) = \mathsf{G}\xi + w(\xi)$ where $\mathsf{G} = u(L)/L$ and $w(\pm L) = 0$ (recall the antisymmetric extension of u across the origin). Then w^* is simply a $2L$-periodic extension of $w|_{\{-L+1,\dots,L\}}$ and

$$u^*(\xi + 2L\eta) = \mathsf{G}(\xi + 2L\eta) + w(\xi).$$

Thus, we see that $Du^*(\xi)$ is $2L$-periodic.

Lemma 4.1. Let u^* be defined by (4.17), then

$$\mathcal{E}^*(u) = \tfrac{1}{2} \sum_{\xi=-L+1}^{L} V(Du^*(\xi)) + C^*, \tag{4.18}$$

where $C^* = -2LV(0)$.

Proof. We have already seen in (3.9) that $D_\rho u(\xi) = -D_{-\rho} u(-\xi)$ for all $\xi \in \mathbb{Z}$ due to the antisymmetry of the displacement. One readily checks

that the extension u^* preserves antisymmetry. It now follows immediately from the symmetry of V (3.15) that

$$\mathcal{E}^*(u) = \tfrac{1}{4}V(Du^*(-L)) + \tfrac{1}{2}\sum_{\xi=-L+1}^{L-1} V(Du^*(\xi)) + \tfrac{1}{4}V(Du^*(L)) + C^*.$$

Since Du^* is $2L$-periodic, it follows that $V(Du^*(-L)) = V(Du^*(L))$ and hence the result follows. □

We now use the representation (4.18) to prove **(F)**. In Section 7 we will also see that this representation leads to a straightforward proof of stability of $\mathcal{E}^{\rm rfl}$.

Corollary 4.2. $\mathcal{E}^{\rm rfl}$ satisfies **(F)**.

Proof. Fix $v \in \mathcal{U}_0$. Using the form of $\mathcal{E}^*$ derived in Lemma 4.1, we obtain

$$\langle \delta\mathcal{E}^*(u^{\mathsf{F}}), v\rangle = \tfrac{1}{2}\sum_{\xi=-L+1}^{L}\sum_{\rho\in\mathcal{R}} V_\rho(\mathsf{F}\mathcal{R})D_\rho v^*(\xi). \tag{4.19}$$

Now let $v(\xi) = \mathsf{G}\xi + w(\xi)$, where $\mathsf{G} = v(L)/L$. Then w^* is periodic and hence (4.19) implies that $\langle \delta\mathcal{E}^*(u^{\mathsf{F}}), w\rangle = 0$. Hence, we obtain

$$\begin{aligned}\langle \delta\mathcal{E}^*(u^{\mathsf{F}}), v\rangle &= \langle \delta\mathcal{E}^*(u^{\mathsf{F}}), u^{\mathsf{G}}\rangle + \langle \delta\mathcal{E}^*(u^{\mathsf{F}}), w\rangle \\ &= \tfrac{1}{2}(2L)\sum_{\rho\in\mathcal{R}} V_\rho \mathsf{G}\rho = L\partial_{\mathsf{F}}W(\mathsf{F})\mathsf{G} = \partial_{\mathsf{F}}W(\mathsf{F})v(L).\end{aligned}$$

Inserting this result into the definition of $\delta\mathcal{E}^{\rm rfl}$, we obtain

$$\langle \delta\mathcal{E}^{\rm rfl}(u^{\mathsf{F}}), v\rangle = \partial_{\mathsf{F}}W(\mathsf{F})v(L) + \int_L^\infty \nabla v\,{\rm d}x = 0.$$

This clearly implies **(F)**. □

Further remarks

(1) One often also demands that the QNL interface correction satisfies a local energy consistency condition (see E *et al.* (2006) and Ortner and Zhang (2012)):

(E) *Local energy consistency.* $\Phi^{\rm i}_\xi(u^{\mathsf{F}}) = \Phi^{\rm a}_\xi(u^{\mathsf{F}})$ for all $\mathsf{F} \in \mathbb{R}$, $\xi = K+1, \dots, L-1$.

However, it is straightforward to show (Ortner 2012, § 6.4.3) that **(F)** implies a weaker global version of **(E)**. It is therefore unclear whether the condition **(E)** is required at all, except of course to approximate absolute energies. Indeed, we shall not use it in our subsequent 1D analysis.

(2) As remarked above, it is unknown whether the general geometric consistency equations have a solution. It is clear from comparing the number of parameters to the number of equations that the corresponding linear operator must have a non-trivial kernel. It would therefore be interesting to augment the consistency equations with additional constraints that induce further desirable properties of the resulting a/c coupling.

(3) For 2D pair interactions, Shapeev (2011) has provided a remarkably simple explicit construction of an a/c coupling satisfying **(F)**, which does not use the ideas of geometric reconstruction. Unfortunately the construction cannot be applied to general many-body interactions, but it has proved useful for the *analysis* of a/c couplings of many-body interactions (Ortner 2012). We will also frequently apply 1D variants of these ideas throughout our consistency analysis. A recent idea applicable to 3D pair interactions is presented in Makridakis, Mitsoudis and Rosakis (2012).

4.6. Force-based a/c coupling

We have so far described two a/c couplings that reduce or remove the ghost force. While the construction of the B-QCE method is straightforward for general a/c interfaces in 2D/3D, the construction of energy-based a/c couplings without ghost forces in 2D/3D remains a challenging open problem.

An alternative is to construct a/c couplings for the forces, and to accept a non-conservative force field. The simplest method of this type is the force-based quasicontinuum (QCF) method. Let $K = L$, and define

$$\mathcal{F}_\zeta^{\rm qcf}(u_h) := \begin{cases} \frac{\partial \mathcal{E}^{\rm a}(u_h)}{\partial u_h(\zeta)}, & \zeta \in \{1, \dots, K\}, \\ \frac{\partial \mathcal{E}^{\rm c}(u_h)}{\partial u_h(\zeta)}, & \zeta \in \mathcal{N}_h^\circ \setminus \{1, \dots, K\}. \end{cases} \tag{4.20}$$

Then we aim to solve the nonlinear system

$$\big\langle \mathcal{F}^{\rm qcf}(u_h), v_h \big\rangle = \langle f, v_h \rangle_h \quad \text{for all } v_h \in \mathcal{U}_h, \tag{4.21}$$

where

$$\langle \mathcal{F}^{\rm qcf}(u_h), v_h \rangle = \sum_{\zeta \in \mathcal{N}_h^\circ} \mathcal{F}_\zeta^{\rm qcf}(u_h) v_h(\zeta).$$

This scheme is naturally free of ghost forces: $\mathcal{F}_\zeta^{\rm qcf}(u^{\mathsf{F}}) = 0$ for all finite element nodes $\zeta \in \mathcal{N}_h^\circ$.

The first analysis of the QCF method (Dobson *et al.* 2010*b*) revealed that while the operator is naturally consistent, its stability is a subtle issue. For example, it was shown that $\delta \mathcal{F}^{\rm qcf}(0)$ is nearly *always* indefinite and never uniformly stable as an operator from $\mathcal{U}_h$ to $\mathcal{U}_h^*$. This not only makes the stability analysis in 2D/3D particularly challenging, but in fact it is currently unknown whether the QCF method is stable in any suitable function space setting.

To overcome this difficulty, Lu and Ming (2013) proposed applying the blending idea behind the B-QCE method to the QCF method. For earlier variants of force-based blending see Fischmeister *et al.* (1989), Kohlhoff *et al.* (1991) and Badia *et al.* (2007). To introduce this scheme, let $K < L$ and $\beta : \mathbb{R} \to [0,1]$ with $\beta = 0$ in $[0,K]$ and $\beta = 1$ in $[L,N]$, and define

$$\mathcal{F}_\zeta^{\rm bqcf}(u_h) := (1-\beta(\zeta))\frac{\partial \mathcal{E}^{\rm a}(u_h)}{\partial u_h(\zeta)} + \beta(\zeta)\frac{\partial \mathcal{E}^{\rm c}(u_h)}{\partial u_h(\zeta)}. \tag{4.22}$$

In the blended QCF (B-QCF) method, we aim to solve the nonlinear system

$$\big\langle \mathcal{F}_\zeta^{\rm bqcf}(u_h), v_h \big\rangle = \langle f, v_h \rangle_h \quad \text{for all } v_h \in \mathcal{U}_h.$$

Like the QCE and B-QCE methods, the QCF and the B-QCF methods are straightforward to implement, using purely atomistic and purely continuum finite element assembly techniques.

4.7. Formal outline of the error analysis

The fundamental theorem of numerical analysis states, loosely speaking, that *consistency* and *stability* imply convergence. A key motivation of this article is to flesh out this principle in the non-standard setting of a/c coupling methods. In the present section, we outline a general framework, in order to motivate the analysis of Sections 5–8.

Let $\mathcal{F}^{\rm ac} \in C^{k-1}(\mathcal{U}_h; \mathcal{U}_h^*)$ be the force operator associated with one of the a/c coupling methods that we constructed in the previous sections; that is, solutions of the a/c coupling under consideration satisfy

$$\langle \mathcal{F}^{\rm ac}(u_h^{\rm ac}), v_h \rangle = \langle f, v_h \rangle_h \quad \text{for all } v_h \in \mathcal{U}_h. \tag{4.23}$$

We now turn (4.23) into an *error equation*. We first assume the existence of an atomistic solution $u^{\rm a}$ to (3.17). Next, we define a quasi-best approximation $\Pi_h u^{\rm a} \in \mathcal{U}_h$ (Section 5). Accepting the decay hypothesis (3.20), assuming that K is sufficiently large and the finite element mesh sufficiently fine, we will obtain that $\Pi_h u^{\rm a}$ is 'close' to $u^{\rm a}$. Let $e_h := u_h^{\rm ac} - \Pi_h u^{\rm a}$; then (4.23) is equivalent to

$$\begin{aligned} \big\langle \mathcal{F}^{\rm ac}(\Pi_h u^{\rm a} + e_h) - \mathcal{F}^{\rm ac}(\Pi_h u^{\rm a}), v_h \big\rangle &= \big\langle \delta\mathcal{E}^{\rm a}(u^{\rm a}) - \mathcal{F}^{\rm ac}(\Pi_h u^{\rm a}), v_h \big\rangle \\ &\quad - \big\{ \langle f, v_h \rangle_{\mathbb{Z}_+} - \langle f, v_h \rangle_h \big\} \\ &=: \langle \eta_{\rm int}^{\rm ac}, v_h \rangle - \langle \eta_{\rm ext}, v_h \rangle, \end{aligned} \tag{4.24}$$

where $\eta_{\rm int}^{\rm ac}$ is the consistency error arising from the approximation of the internal energy and $\eta_{\rm ext}$ the consistency error arising from the approximation of the external forces.

If $\eta_{\rm int}^{\rm ac} = \eta_{\rm ext} = 0$, then a solution to (4.24) is $e_h = 0$. Thus, if $\eta_{\rm int}^{\rm ac}$ and $\eta_{\rm ext}$ are sufficiently 'small', and if the linearization of the right-hand side of

Table 4.1.

Error contribution	Origin	Approximation parameter(s)
far-field error	reduction to finite domain	N
coarsening error	finite element discretization	h
Cauchy–Born modelling error	replacing the atomistic model with continuum model in $[L, N]$	L
coupling error	interface treatment	K, L, β

(4.24) is an isomorphism (we will prove in Section 7 that $\langle \delta\mathcal{F}^{\rm ac}(\Pi_h u^{\rm a})v, v\rangle \geq (C^{\rm stab})^{-1}\|\nabla v\|_{L^2}^2$), then we expect from the inverse function theorem that a locally unique solution e_h to (4.24) exists, and that

$$\|\nabla e_h\|_{L^2} \leq C^{\rm stab}\big(\|\eta_{\rm int}^{\rm ac}\|_{\mathcal{U}_h^*} + \|\eta_{\rm ext}\|_{\mathcal{U}_h^*}\big), \tag{4.25}$$

where

$$\|\eta\|_{\mathcal{U}_h^*} := \sup_{v_h \in \mathcal{U}_h\setminus\{0\}} \frac{\langle \eta, v_h\rangle}{\|\nabla v_h\|_{L^2}}. \tag{4.26}$$

We will analyse the consistency errors in Section 6. We will split the error contributions as shown in Table 4.1. While the coarsening error is a standard component of classical finite element error analysis, the combination with the continuum modelling error and in particular the interfacial error requires new ideas. We will obtain consistency error estimates, similar to those in Section 2, depending on the smoothness of $u^{\rm a}$, the mesh coarsening, the computational domain size, and possibly other approximation parameters.

Next, we will analyse the stability of a/c schemes in Section 7. We shall prove for the B-QCE, B-QCF, and QNL methods that the approximation parameters can be chosen in such a way that positivity of $\delta^2\mathcal{E}^{\rm a}(u^{\rm a})$ (see (3.19)) implies positivity of $\delta\mathcal{F}^{\rm ac}(\Pi_h u^{\rm a})$.

Next, we will optimize all approximation parameters to obtain consistency error estimates, purely in terms of the computational cost,

$$\|\eta_{\rm int}^{\rm ac}\|_{\mathcal{U}_h^*} + \|\eta_{\rm ext}\|_{\mathcal{U}_h^*} \lesssim N_{\mathcal{T}_h}^{-\beta},$$

for some exponent $\beta > 0$. We will also translate the stability results from Section 7 to this setting, showing that if $N_{\mathcal{T}_h}$ is sufficiently large then $\delta\mathcal{F}^{\rm ac}(\Pi_h u^{\rm a})$ is stable.

Finally, in Section 8 we will make the formal argument presented in this subsection fully rigorous. We will obtain results of the form: Let $u^{\rm a}$ be a strongly stable solution of (3.17) satisfying **(DH)**. Then for $N_{\mathcal{T}_h}$ sufficiently large there exists a solution $u^{\rm ac}$ of (4.23) satisfying $\|\nabla u^{\rm ac} - \nabla u^{\rm a}\|_{L^2} \lesssim N_{\mathcal{T}_h}^{-\beta}$.

5. Coarsening error

Our first step in the error analysis is an analysis of the finite element coarsening error. The results in this section are fairly standard, and hence we only give brief summaries of certain auxiliary results that we require later on. Proofs are given, for the sake of completeness, in the Appendix.

5.1. Best approximation operator

Recall the definition of the nodal interpolation operator I_h from Section 4.2. Since I_h does not map $\mathcal{U}$ to $\mathcal{U}_h$, and to avoid any error contributions from the atomistic region (and possibly a neighbourhood of the interface region), we define

$$\Pi_h u(x) := \begin{cases} I_h u(x), & x \in [0, L + r_{\rm cut}], \\ I_h u(x) - \frac{x-L-r_{\rm cut}}{N-L-r_{\rm cut}} u(N), & x \in [L + r_{\rm cut}, N]. \end{cases}$$

With this definition, $\Pi_h u \in \mathcal{U}_h$ for all $u : \mathcal{N}_h \to \mathbb{R}$.

In our coarsening error analysis below, it will be useful to split the interpolant into $\Pi_h u = I_h u + (\Pi_h u - I_h u)$. Hence, we separately estimate the interpolation errors as follows.

Lemma 5.1. Let $T \in \mathcal{T}_h$, $T \subset [L, N]$ and $u \in \mathcal{U}$. Then

$$\|\nabla \tilde{u} - \nabla I_h u\|_{L^2(T)} \lesssim h_T \|\nabla^2 \tilde{u}\|_{L^2(T)}. \tag{5.1}$$

If, in addition, u satisfies **(DH)**, $L \leq N/2$ and $N \geq r_0$, then

$$\left|\nabla I_h u(x) - \nabla \Pi_h u(x)\right| \lesssim \begin{cases} 0, & x \in [0, L + r_{\rm cut}], \\ N^{-\alpha}, & x \in [L + r_{\rm cut}, N]. \end{cases} \tag{5.2}$$

Proof. The first result follows from Poincaré's inequality.

To prove the second estimate, we first note that $\nabla I_h u = \nabla \Pi_h u = \nabla u$ in $[0, L + r_{\rm cut}]$. In $[L + r_{\rm cut}, N]$ we have

$$\left|\nabla I_h u - \nabla \Pi_h u\right| = (N - L)^{-1} |u(N)| \lesssim (N - L)^{-1} N^{1-\alpha} \lesssim N^{-\alpha}. \qquad \square$$

5.2. Coarsening error of the internal forces

The first variation of the continuum energy contribution $\int_L^N W(\nabla u)\,\mathrm{d}x$ is given by

$$v \mapsto \int_L^N \partial_{\mathsf{F}} W(\nabla u) \nabla v \,\mathrm{d}x.$$

The following lemma estimates the error contribution from this operator induced by finite element coarsening and reduction to a finite domain.

Lemma 5.2. Let $u \in \mathcal{U}$ satisfy **(DH)**, $N > r_0$, and $0 < L \leq N/2$. Then

$$\left| \int_L^N \big(\partial_{\mathsf{F}} W(\nabla \Pi_h u) - \partial_{\mathsf{F}} W(\nabla \tilde{u})\big) \nabla v_h \, \mathrm{d}x \right| \\ \lesssim M^{(2,0)} \big(\|h \nabla^2 \tilde{u}\|_{L^4}^2 + N^{-\alpha+1/2} \big) \|\nabla v_h\|_{L^2} \quad \text{for all } v_h \in \mathrm{P1}(\mathcal{T}_h).$$

Proof. See Appendix A.2. □

Remark 5.3. **(1)** We observe that we require at least $\alpha > 1/2$ in order to control the far-field error, which is precisely the assumption we made in (3.20). Recall though that this is no severe restriction since a displacement gradient $\nabla u(x)$ with $\nabla u(x) \sim x^{-\alpha}$ as $x \to \infty$ belongs to L^2 if and only if $\alpha > 1/2$.

(2) The nodal interpolation error enters the coarsening error only as a quadratic term $\|h \nabla^2 \tilde{u}\|_{L^4}^2$. This effect is related to the well-known 1D superconvergence property that the nodal interpolant is at the same time the Ritz projection.

5.3. Coarsening error of external forces

We now turn towards the consistency error due to the approximation of the external potential $\langle f, v_h \rangle_{\mathbb{Z}_+}$ by the trapezoidal rule $\langle f, v_h \rangle_h$. The main challenge in this analysis is to avoid the use of the Poincaré inequality $\|v_h\|_{L^2} \lesssim N \|\nabla v_h\|_{L^2}$ at all costs (we will point out the relevant step in the proof of Proposition 5.4 in Appendix A.2). A common approach in unbounded domains is to employ weighted Poincaré inequalities instead. This yields the following result.

Proposition 5.4. Let $L > 1$ and suppose that $h(x) \leq \kappa x$ for almost every $x \in [L, N]$. Then there exists a constant C_κ such that

$$\|\eta_{\mathrm{ext}}\|_{\mathcal{U}_h^*} = \big\| \langle f, \cdot \rangle_{\mathbb{Z}_+} - \langle f, \cdot \rangle_h \big\|_{\mathcal{U}_h^*} \\ \lesssim \big\| h^2 \nabla \tilde{f} \big\|_{L^2(L,\infty)} + \frac{C_\kappa}{\log L} \big\| h^2 \omega \nabla^2 \tilde{f} \big\|_{L^2(L,\infty)},$$

where $\omega(x) := x \log x$.

Proof. See Appendix A.2. □

Remark 5.5. The proof of Proposition 5.4 reveals that for practical meshes one should expect $C_\kappa \eqsim \kappa$, hence it is important to control the bound $h(x) \leq \kappa x$. In Section 8, we shall optimize the finite element grid to balance the far-field error and interpolation error contributions with the best approximation error. For the quasi-optimal mesh scaling that we will derive, we will be able to make this bound explicit.

6. Consistency

Recall from Section 4.7 that the *internal consistency error*, associated with a displacement $u \in \mathcal{U}$, is given by a linear form

$$\left\langle \eta^{\rm ac}_{\rm int}(u), v_h \right\rangle := \left\langle \delta\mathcal{E}^{\rm a}(u) - \mathcal{F}^{\rm ac}(\Pi_h u), v_h \right\rangle,$$

where $\mathcal{F}^{\rm ac}$ is the force operator associated with one of the a/c coupling methods constructed in Section 4.

In the present section, we establish consistency error bounds associated with the model approximations (reminiscent of variational crimes in finite element methods) in the various a/c coupling schemes. These will then be combined with the coarsening error bounds derived in Section 5.2 to yield qualitatively sharp bounds on $\eta^{\rm ac}_{\rm int}$ in the $\mathcal{U}_h^*$-norm defined in (4.26) (a discrete H^{-1}-type norm).

6.1. Weak form of the atomistic model and Cauchy–Born modelling error

For a sharp consistency error analysis, it is useful to develop convenient 'weak forms' of the first variations of the atomistic, continuum, and a/c models. The canonical representation (3.12) of $\delta\mathcal{E}^{\rm a}$ is not immediately useful since the occurrence of the test function is nonlocal. In the following, we derive an alternative weak formulation, employing an atomistic notion of stress.

The idea is to localize the finite differences $D_\rho v(\xi)$ by rewriting them as *bond integrals*. A conceptually straightforward mechanism to achieve this is to simply take the derivatives of $\mathcal{E}^{\rm a}$ with respect to the discrete strains u'_ξ. However, this technique is restricted to 1D. Instead, we present a simplified 1D variant of a construction that was developed for the construction and analysis of a/c coupling methods in 2D/3D (see Section 6.6 for more details on this discussion).

We define the weighted characteristic function of a bond $(\xi, \xi+\rho)$ by

$$\chi^{\mathbb{R}}_{\xi,\rho}(x) := \begin{cases} |\rho|^{-1}, & x \in \operatorname{int}(\operatorname{conv}\{\xi, \xi+\rho\}), \\ \frac{1}{2}|\rho|^{-1}, & x \in \{\xi, \xi+\rho\}, \\ 0, & \text{otherwise.} \end{cases}$$

We then obtain for $D_\rho v(\xi) := v(\xi+\rho) - v(\xi)$ that

$$D_\rho v(\xi) = \int_\xi^{\xi+\rho} \frac{\rho}{|\rho|} \nabla v \, {\rm d}x = \int_{\mathbb{R}} \rho \chi^{\mathbb{R}}_{\xi,\rho} \nabla v \, {\rm d}x. \tag{6.1}$$

To express $D_\rho v(\xi)$ as an integral over $\mathbb{R}_+$, we use that $\nabla v(-x) = \nabla v(x)$ for all $v \in \mathcal{U}$ to obtain

$$D_\rho v(\xi) = \int_{\mathbb{R}} \rho \chi^{\mathbb{R}}_{\xi,\rho} \nabla v \, {\rm d}x = \int_{\mathbb{R}_+} \rho \chi_{\xi,\rho} \nabla v \, {\rm d}x, \tag{6.2}$$

where

$$\chi_{\xi,\rho}(x) := \chi^{\mathbb{R}}_{\xi,\rho}(x) + \chi^{\mathbb{R}}_{\xi,\rho}(-x).$$

Inserting this representation into (3.12) yields

$$\big\langle \delta\mathcal{E}^{\mathrm{a}}(u), v\big\rangle = \int_{\mathbb{R}_+} \left\{ \sum_{\rho\in\mathcal{R}} \rho \sum_{\xi\in\mathbb{Z}_+} \Phi^{\mathrm{a}}_{\xi,\rho}(u)\chi_{\xi,\rho}(x) \right\} \nabla v \,\mathrm{d}x.$$

Thus we obtain the following result.

Proposition 6.1. Let $u \in \mathcal{U}$, and $v \in \mathcal{U}_0$. Then

$$\big\langle \delta\mathcal{E}^{\mathrm{a}}(u), v\big\rangle = \int_{\mathbb{R}} \mathsf{S}^{\mathrm{a}}(u;x)\nabla v(x)\,\mathrm{d}x,$$

where the *atomistic stress function* S^{a} is defined by

$$\mathsf{S}^{\mathrm{a}}(u;x) := \sum_{\rho\in\mathcal{R}} \sum_{\xi\in\mathbb{Z}_+} \rho\Phi^{\mathrm{a}}_{\xi,\rho}(u)\chi_{\xi,\rho}(x). \tag{6.3}$$

Since the sum defining $\mathsf{S}^{\mathrm{a}}(u;x)$ is finite (the sum over ξ only needs to be taken over $\mathbb{Z}_+ \cap [x - r_{\mathrm{cut}}, x + r_{\mathrm{cut}}]$), S^{a} is well-defined and $k-1$ times continuously differentiable with respect to u. It is also clear from the definition that $x \mapsto \mathsf{S}^{\mathrm{a}}(u;x)$ is constant on each interval $(\eta, \eta+1)$, $\eta \in \mathbb{Z}_+$.

Moreover, if u is locally homogeneous, that is, $u(\xi) = \mathsf{F}\xi$ in $[x - 2r_{\mathrm{cut}}, x + 2r_{\mathrm{cut}}]$, then

$$\begin{aligned}\mathsf{S}^{\mathrm{a}}(u;x) = \mathsf{S}^{\mathrm{a}}(u^{\mathsf{F}};x) &= \sum_{\rho\in\mathcal{R}} \sum_{\xi\in\mathbb{Z}_+} \rho V_\rho(\mathsf{F}\mathcal{R})\chi_{\xi,\rho}(x) \\ &= \sum_{\rho\in\mathcal{R}} \rho V_\rho(\mathsf{F}\mathcal{R}) = \partial_{\mathsf{F}} W(\mathsf{F}),\end{aligned} \tag{6.4}$$

where we used the fact that $\sum_{\xi\in\mathbb{Z}_+} \chi_{\xi,\xi+\rho}(x) = 1$ (see Lemma 6.3 below). Since $\mathsf{S}^{\mathrm{a}} = \partial_{\mathsf{F}} W$ under locally homogeneous deformations, it follows easily that the Cauchy–Born stress is first-order consistent with the atomistic stress. By exploiting symmetries of the interaction potential, we can even prove that it is second-order consistent at bond midpoints.

Theorem 6.2. Let $u \in W^{3,\infty}_{\mathrm{loc}}$ and $x \in \frac{1}{2} + \mathbb{Z}_+$, $x > 2r_{\mathrm{cut}}$. Then

$$\big|\mathsf{S}^{\mathrm{a}}(u;x) - \partial_{\mathsf{F}} W(\nabla u(x))\big| \lesssim M^{(2,2)}\|\nabla^3 u\|_{L^\infty(\nu_x)} + M^{(3,2)}\|\nabla^2 u\|^2_{L^\infty(\nu_x)},$$

where $\nu_x := [x + \frac{1}{2} - 2r_{\mathrm{cut}}, x - \frac{1}{2} + 2r_{\mathrm{cut}}]$.

Proof. We note that $\mathsf{S}^{\mathrm{a}}(u;x)$ is defined for $x \in \mathbb{R}_+$ from the restriction of $u \in W^{3,\infty}_{\mathrm{loc}}$ to the nodes $\xi \in \mathbb{Z}_+$. The result is proved by Taylor expansion of the nonlocal terms in the definition of S^{a}, and exploiting the symmetries of the interaction potential.

The sum over ξ in (6.3) is only taken over $\xi \in N_x := \{x+\frac{1}{2}-r_{\rm cut}, \dots, x-\frac{1}{2}+r_{\rm cut}\}$, but the finite differences $D_\rho u(\xi)$, for $\xi \in N_x$ depend on the neighbourhoods ν_x defined in the statement of the theorem. In order to keep the notation concise, we define

$$\epsilon_2 := \|\nabla^2 u\|_{L^\infty(\nu_x)} \quad \text{and} \quad \epsilon_3 := \|\nabla^3 u\|_{L^\infty(\nu_x)}.$$

We will suppress all arguments where possible. For example, we define $\Phi^{\rm a}_{\xi,\rho} := \Phi^{\rm a}_{\xi,\rho}(u)$ and $V_\rho := V_\rho(\nabla u(x)\cdot\mathcal{R})$. Moreover, we often suppress dependence of constants on the potential, which can be readily reconstructed.

We begin by expanding $D_\varsigma u(\xi)$, for $\xi \in N_x, \varsigma \in \mathcal{R}$,

$$D_\varsigma u(\xi) = \nabla_\varsigma u(x) + \nabla^2 u(x)\varsigma\big(\xi - x + \tfrac{1}{2}\varsigma\big) + O(\epsilon_3),$$

which, together with the fact that $D_\varsigma u(\xi) - \nabla_\varsigma u(x) = O(\epsilon_2)$, allows us to expand $\Phi^{\rm a}_{\xi,\rho}$:

$$\begin{aligned}\Phi^{\rm a}_{\xi,\rho} &= V_\rho + \sum_{\varsigma\in\mathcal{R}} V_{\rho\varsigma}\cdot\big(D_\varsigma u(\xi) - \nabla_\varsigma u(x)\big) + O(\epsilon_2^2)\\ &= V_\rho + \nabla^2 u \sum_{\varsigma\in\mathcal{R}} \varsigma V_{\rho\varsigma}\cdot\big(\xi - x + \tfrac{1}{2}\varsigma\big) + O(\epsilon_2^2+\epsilon_3). \qquad (6.5)\end{aligned}$$

Inserting (6.5) into (6.3), recalling (6.4) and applying (6.6) and (6.7) with $\eta := x - 1/2$, yields

$$\begin{aligned}\mathsf{S}^{\rm a}(u;x) - \partial\!\mathsf{F}W(\nabla u(x)) &= \left\{\sum_{\rho\in\mathcal{R}} \rho V_\rho \sum_{\xi\in\mathbb{Z}} \chi_{\xi,\rho} - \partial\!\mathsf{F}W(\nabla u)\right\}\\ &\quad + \nabla^2 u \sum_{\rho,\varsigma\in\mathcal{R}} \rho\varsigma V_{\rho\varsigma} \sum_{\xi\in\mathbb{Z}} \chi_{\xi,\rho}\left(\xi - x + \frac{\varsigma}{2}\right) + O(\epsilon_2^2+\epsilon_3)\\ &= \left\{\sum_{\rho\in\mathcal{R}} \rho V_\rho - \partial\!\mathsf{F}W(\nabla u)\right\}\\ &\quad + \nabla^2 u \sum_{\rho,\varsigma\in\mathcal{R}} \rho\varsigma V_{\rho\varsigma}\left(x - \frac{\rho}{2} - x + \frac{\varsigma}{2}\right) + O(\epsilon_2^2+\epsilon_3)\\ &= \nabla^2 u \frac{1}{2}\sum_{\rho\varsigma\in\mathcal{R}} \rho\varsigma V_{\rho\varsigma}(\varsigma-\rho) + O(\epsilon_2^2+\epsilon_3).\end{aligned}$$

Applying the symmetry $V_{\rho,\varsigma} = V_{-\rho,-\varsigma}$ (see (3.16)) we obtain that

$$\sum_{\rho\varsigma\in\mathcal{R}} \rho\varsigma V_{\rho\varsigma}(\varsigma-\rho) = \sum_{\rho\in\mathcal{R}_+}\sum_{\varsigma\in\mathcal{R}} \rho\varsigma V_{\rho\varsigma}\big[(\varsigma-\rho)+(-\varsigma+\rho)\big] = 0.$$

This concludes the proof of the result. □

Lemma 6.3. Let $x \in (\eta, \eta+1)$ for some $\eta \in \mathbb{Z}_+$ and $\rho \in \mathbb{Z} \setminus \{0\}$. Then

$$\sum_{\xi \in \mathbb{Z}_+} \chi_{\xi,\rho}(x) = 1. \tag{6.6}$$

If, moreover, $x > r_{\rm cut}$, then

$$\sum_{\xi \in \mathbb{Z}_+} \chi_{\xi,\rho}(x) \cdot \xi = \left(\eta + \frac{1}{2} - \frac{\rho}{2}\right). \tag{6.7}$$

Proof. Suppose first that $x > r_{\rm cut}$. If $\rho > 0$, then

$$\sum_{\xi \in \mathbb{Z}_+} \chi_{\xi,\rho}(x) = \frac{1}{\rho} \sum_{j=1}^{\rho} 1 = 1 \quad \text{and}$$

$$\sum_{\xi \in \mathbb{Z}_+} \chi_{\xi,\rho}(x)\xi = \frac{1}{\rho} \sum_{j=1}^{\rho} (\eta - j) = \frac{1}{\rho}\left(\rho\eta - \frac{\rho(\rho+1)}{2}\right) = \eta + \frac{1}{2} - \frac{\rho}{2}.$$

For $\rho < 0$ an analogous argument applies.

If $0 < x < r_{\rm cut}$ and $\rho < 0$, then the same argument gives

$$\sum_{\xi \in \mathbb{Z}} \chi^{\mathbb{R}}_{\xi,\rho}(x) = 1.$$

Moreover, one readily checks that

$$\sum_{\xi \in \mathbb{Z}} \chi^{\mathbb{R}}_{\xi,\rho}(x) = \sum_{\xi \in \mathbb{Z}_+} \chi_{\xi,\rho}(x). \qquad \square$$

Corollary 6.4 (Cauchy–Born modelling error). If $u \in \mathcal{U}$ and $L \geq 2r_{\rm cut}$, then

$$\int_L^N \big(\mathsf{S}^{\rm a}(u) - \partial_{\mathsf{F}} W(\nabla \tilde{u})\big) \nabla v_h \, {\rm d}x$$
$$\lesssim \big(M^{(3,3)} \|\nabla^3 \tilde{u}\|_{L^2(\nu)} - M^{(2,3)} \|\nabla^2 \tilde{u}\|^2_{L^4(\nu)}\big) \|\nabla v_h\|_{L^2(L,N)} \quad \text{for all } v_h \in \mathcal{U}_h,$$

where $\nu := (L - 2r_{\rm cut} + 1, N + 2r_{\rm cut})$.

Proof. Let $\bar{x} := \eta - 1/2$, $\eta \in \mathbb{Z}_+$. Then, recalling that $\mathsf{S}^{\rm a}(u)$ is piecewise constant and that $\tilde{u}|_{\mathbb{Z}_+} = u$,

$$\int_{\eta-1}^{\eta} \big(\mathsf{S}^{\rm a}(u) - \partial_{\mathsf{F}} W(\nabla \tilde{u})\big) \nabla v_h \, {\rm d}x = \Big\{ \big[\mathsf{S}^{\rm a}(\tilde{u}; \bar{x}) - \partial_{\mathsf{F}} W(\nabla \tilde{u}(\bar{x}))\big]$$
$$+ \int_{\eta-1}^{\eta} \big[\partial_{\mathsf{F}} W(\nabla \tilde{u}(\bar{x})) - \partial_{\mathsf{F}} W(\nabla \tilde{u}(x))\big] \, {\rm d}x \Big\} \nabla v_h. \tag{6.8}$$

Applying Theorem 6.2, the local norm-equivalence for polynomials of degree 5,

$$\|\nabla^j \tilde{u}\|_{L^\infty(\eta-1,\eta)} \lesssim \|\nabla^j \tilde{u}\|_{L^2(\eta-1,\eta)},$$

and the embedding $\ell^2 \subset \ell^\infty$, we obtain

$$\begin{aligned}\left|\mathsf{S}^{\mathrm{a}}(\tilde{u};\bar{x}) - \partial_{\mathsf{F}} W(\nabla\tilde{u}(\bar{x}))\right| &\lesssim \|\nabla^3\tilde{u}\|_{L^\infty(\nu_{\bar{x}})} + \|\nabla^2\tilde{u}\|^2_{L^\infty(\nu_{\bar{x}})}\\ &\lesssim \|\nabla^3\tilde{u}\|_{L^2(\nu_{\bar{x}})} + \|\nabla^2\tilde{u}\|^2_{L^4(\nu_{\bar{x}})}.\end{aligned}$$

Moreover, using the fact that the midpoint rule is second-order accurate,

$$\begin{aligned}\left|\int_{\eta-1}^{\eta} \big(\partial_{\mathsf{F}} W(\nabla\tilde{u}(\bar{x})) - \partial_{\mathsf{F}} W(\nabla\tilde{u}(x))\big)\,\mathrm{d}x\right| &\lesssim \|\nabla^2\partial_{\mathsf{F}} W(\nabla\tilde{u}(x))\|_{L^1(\eta-1,\eta)}\\ &\lesssim \|\nabla^3\tilde{u}\|_{L^1(\eta-1,\eta)} + \|\nabla^2\tilde{u}\|^2_{L^2(\eta-1,\eta)}\\ &\lesssim \|\nabla^3\tilde{u}\|_{L^2(\eta-1,\eta)} + \|\nabla^2\tilde{u}\|^2_{L^4(\eta-1,\eta)}.\end{aligned}$$

Inserting these estimates into (6.8) yields

$$\begin{aligned}&\left|\int_{\eta-1}^{\eta} \big(\mathsf{S}^{\mathrm{a}}(u) - \partial_{\mathsf{F}} W(\nabla\tilde{u})\big)\nabla v_h\,\mathrm{d}x\right|\\ &\qquad\lesssim \big(\|\nabla^3\tilde{u}\|_{L^2(\nu_{\bar{x}})} + \|\nabla^2\tilde{u}\|^2_{L^4(\nu_{\bar{x}})}\big)\|\nabla v_h\|_{L^2(\eta-1,\eta)},\end{aligned}$$

where we recall that $\nu_{\bar{x}} = (\eta - 2r_{\mathrm{cut}}, \eta - 1 + 2r_{\mathrm{cut}})$.

Summing over all $\eta = L+1, \ldots, N$, applying Hölder's inequality, and noting that any interval $(\xi-1,\xi)$ intersects with at most $4r_{\mathrm{cut}}$ neighbourhoods $\nu_{\bar{x}}$, we obtain

$$\int_L^N \big(\mathsf{S}^{\mathrm{a}}(u) - \partial_{\mathsf{F}} W(\nabla\tilde{u})\big)\nabla v_h\,\mathrm{d}x \lesssim \big(\|\nabla^3\tilde{u}\|_{L^2(\nu)} + \|\nabla^2\tilde{u}\|^2_{L^4(\nu)}\big)\|\nabla v_h\|_{L^2(L,N)},$$

where $\nu := \bigcup_{\bar{x}\in[L,N]} \nu_{\bar{x}}$. This definition of ν is equivalent to the one given in the statement of the result. □

Further remarks

(1) The consistency proof in this section mimics an analogous proof valid in general dimensions by Ortner and Theil (2013), which builds on ideas of Shapeev (2011) and Ortner (2012). The atomistic stress function S^{a} and its 2D/3D generalizations are closely connected to a notion of stress defined by Hardy (1982). A recent general account of stress in molecular mechanics simulations is given by Admal and Tadmor (2010).

(2) The prefactors $M^{(j,3)}$ cannot be immediately derived from Theorem 6.2, but can only be obtained if the dependence of the interaction neighbourhoods of tuples of pairs and triples of bonds occurring in the proof of Theorem 6.2 are carefully traced. We refer to Ortner and Theil (2013) for further details.

6.2. Consistency of the B-QCE method

Recall from the definition of the B-QCE method in Section 4.4 that we assumed $0 < K < L \leq N/2$ and that $\nabla\beta = 0$ in $[0, K] \cup [L, N]$. In addition, we will assume that $K \geq r_0 + 2r_{\rm cut} + 1$.

Motivated by the derivation of the atomistic stress in Section 6.1, we derive a similar notion of stress for the BQCE method. The natural form of the first variation of $\mathcal{E}^{\rm bqce}$ is

$$\langle \delta\mathcal{E}^{\rm bqce}(u_h), v_h\rangle = \sum_{\xi=0}^{L}(1-\beta(\xi)) \sum_{\rho\in\mathcal{R}} \Phi^{\rm a}_{\xi,\rho}(u_h) D_\rho v_h(\xi) + \int_K^N I_h\beta \cdot \partial_{\mathsf{F}} W(\nabla u_h)\cdot\nabla v_h \,{\rm d}x \quad \text{for all } u_h, v_h \in \mathcal{U}_h.$$

Following closely the calculations in Section 6.1 yields the following result. Note that, since we assumed that $\{0, \dots, L\} \subset \mathcal{N}_h$, the apparent h-dependence in the definition of $\mathsf{S}^{\rm bqce}$ through $I_h\beta$ is not an actual dependence.

Proposition 6.5. Let $u_h, v_h \in \mathcal{U}_h$. Then

$$\langle \delta\mathcal{E}^{\rm bqce}(u_h), v_h\rangle = \int_0^N \mathsf{S}^{\rm bqce}(u_h)\nabla v_h \,{\rm d}x, \quad \text{where} \tag{6.9}$$

$$\mathsf{S}^{\rm bqce}(u_h; x) := \sum_{\rho\in\mathcal{R}}\sum_{\xi\in\mathbb{Z}_+} (1-\beta(\xi))\chi_{\xi,\rho}(x)\Phi^{\rm a}_{\xi,\rho}(u_h)\rho + I_h\beta(x)\cdot\partial_{\mathsf{F}}W(\nabla u_h(x)).$$

We immediately obtain a result stating that the consistency error vanishes in a core atomistic region.

Lemma 6.6. Let $u \in \mathcal{U}$. Then

$$\mathsf{S}^{\rm a}(u; x) = \mathsf{S}^{\rm bqce}(\Pi_h u; x) \quad \text{for } x \in (0, K - r_{\rm cut} + 1).$$

Proof. This result follows immediately from (6.9) and the fact that $u = \Pi_h u$ in $[0, L]$. □

We begin by analysing the error in a simplified version of the B-QCE stress, where $I_h\beta$ is replaced with β.

Lemma 6.7 (stress consistency). For $\tilde{u} \in W^{1,\infty}_{\rm loc}$ and $x \in \mathbb{R}$, let

$$\tilde{\mathsf{S}}^{\rm bqce}(\tilde{u}; x) := \sum_{\rho\in\mathcal{R}}\sum_{\xi\in\mathbb{Z}_+} (1-\beta(\xi))\chi_{\xi,\rho}(x)\Phi^{\rm a}_{\xi,\rho}(\tilde{u})\rho + \beta(x)\partial_{\mathsf{F}}W(\nabla\tilde{u}(x)).$$

If $\tilde{u} \in W^{3,\infty}_{\rm loc}$ and $x \in \frac{1}{2} + \mathbb{Z}$, $x \geq K - r_{\rm cut} + 1$, then

$$\begin{aligned}\left|\mathsf{S}^{\rm a}(\tilde{u}; x) - \tilde{\mathsf{S}}^{\rm bqce}(\tilde{u}; x)\right| \lesssim M^{(1,2)} \|\nabla^2 \beta\|_{L^\infty(\nu_x)} + M^{(2,2)} |\nabla \beta(x) \nabla^2 \tilde{u}(x)| \\ + M^{(3,2)} \|\nabla^2 \tilde{u}\|^2_{L^\infty(\nu_x)} + M^{(2,2)} \|\nabla^3 \tilde{u}\|_{L^\infty(\nu_x)},\end{aligned}$$

where we recall that $\nu_x = [x + \frac{1}{2} - 2r_{\rm cut}, x - \frac{1}{2} + 2r_{\rm cut}]$.

Proof. We begin by writing out

$$\mathsf{S}^{\rm a} - \tilde{\mathsf{S}}^{\rm bqce} = \sum_{\rho \in \mathcal{R}} \rho \sum_{\xi \in \mathbb{Z}} \beta(\xi) \Phi^{\rm a}_{\xi,\rho} \chi_{\xi,\rho} - \beta \partial_{\mathsf{F}} W, \tag{6.10}$$

and observe the similarity to the Cauchy–Born stress error $\mathsf{S}^{\rm a} - \partial_{\mathsf{F}} W$. In the present case, we need to expand both $\Phi^{\rm a}_{\xi,\rho}$, using (6.5), and

$$\beta(\xi) = \beta + \nabla \beta \cdot (\xi - x) + O(\delta_2),$$

where $\delta_2 := \|\nabla^2 \beta\|_{L^\infty(\nu_x)}$, which yields

$$\begin{aligned}\mathsf{S}^{\rm a} - \tilde{\mathsf{S}}^{\rm bqce} &= \sum_{\rho \in \mathcal{R}} \rho \sum_{\xi \in \mathbb{Z}_+} \big[\beta + \nabla \beta \cdot (\xi - x)\big] \Phi^{\rm a}_{\xi,\rho} \chi_{\xi,\rho} - \beta \partial_{\mathsf{F}} W + O(\delta_2) \\ &= \beta \big[\mathsf{S}^{\rm a} - \partial_{\mathsf{F}} W\big] + \nabla \beta \sum_{\rho \in \mathcal{R}} \rho \sum_{\xi \in \mathbb{Z}_+} (\xi - x) \Phi^{\rm a}_{\xi,\rho} \chi_{\xi,\rho} + O(\delta_2).\end{aligned}$$

Inserting the expansion (6.5) for $\Phi^{\rm a}_{\xi,\rho}$, recalling that $V_{\boldsymbol{\rho}} = V_{\boldsymbol{\rho}}(D\tilde{u}(\xi))$, and applying Theorem 6.2 to estimate $\mathsf{S}^{\rm a} - \partial_{\mathsf{F}} W$ gives

$$\begin{aligned}\mathsf{S}^{\rm a} - \tilde{\mathsf{S}}^{\rm bqce} = \nabla \beta \sum_{\rho \in \mathcal{R}} \rho V_\rho \sum_{\xi \in \mathbb{Z}_+} \chi_{\xi,\rho} \cdot (\xi - x) \\ + \nabla \beta \, \nabla^2 y \sum_{\rho,\varsigma \in \mathcal{R}} \rho_\varsigma V_{\rho\varsigma} \sum_{\xi \in \mathbb{Z}_+} \chi_{\xi,\rho} \cdot (\xi - x) \big(\xi - x + \tfrac{\varsigma}{2}\big) \\ + O(\delta_2 + \epsilon_2^2 + \epsilon_3).\end{aligned}$$

Performing similar computations as in the proof of Theorem 6.2, in particular taking into account the symmetry $V_{-\rho} = -V_\rho$, we observe that the first group on the right-hand side vanishes. Thus, we obtain

$$\left|\mathsf{S}^{\rm a} - \tilde{\mathsf{S}}^{\rm bqce}\right| \lesssim \delta_2 + |\nabla \beta \nabla^2 y| + \epsilon_2^2 + \epsilon_3,$$

which is the required result. □

We can now easily derive the global consistency error estimate for the B-QCE method.

Theorem 6.8. Let $u \in \mathcal{U}$ satisfy **(DH)**. Then

$$\begin{aligned}\big\|\eta_{\rm int}^{\rm bqce}(u)\big\|_{\mathcal{U}_h^*} &\lesssim M^{(1,3)}\|\nabla^2\beta\|_{L^2} + M^{(2,2)}\|\nabla\beta\nabla^2\tilde{u}\|_{L^2} \\ &\quad + M^{(2,3)}\|\nabla^3\tilde{u}\|_{L^2(\Omega^{\rm c})} + M^{(3,3)}\|h\nabla^2\tilde{u}\|_{L^4(\Omega^{\rm c})}^2 + M^{(2,0)}N^{1/2-\alpha},\end{aligned}$$

where $\Omega^{\rm c} := (K - 2r_{\rm cut}, \infty)$. (Recall that $h(x) = 1$ for $x > N$.)

Proof. Let $K' := K - r_{\rm cut} + 1$ and assume that $\|\nabla v_h\|_{L^2} = 1$. Using Proposition 6.5 and Lemma 6.6, we split the consistency error into

$$\begin{aligned}\big\langle \delta\mathcal{E}^{\rm a}(u) - \delta\mathcal{E}^{\rm bqce}(\Pi_h u), v_h\big\rangle &= \int_{K'}^{N} \big(\mathsf{S}^{\rm a}(u) - \mathsf{S}^{\rm bqce}(\Pi_h u)\big)\nabla v_h \,{\rm d}x \\ &= \int_{K'}^{N} \big(\tilde{\mathsf{S}}^{\rm bqce}(\tilde{u}) - \mathsf{S}^{\rm bqce}(\Pi_h u)\big)\nabla v_h \,{\rm d}x \\ &\qquad + \int_{K'}^{N} \big(\mathsf{S}^{\rm a}(u) - \tilde{\mathsf{S}}^{\rm bqce}(\tilde{u})\big)\nabla v_h \,{\rm d}x \\ &=: \eta_1 + \eta_2. \end{aligned} \tag{6.11}$$

Estimating η_1. Since the nodal values of β and $I_h\beta$ are the same, the discrete components of $\mathsf{S}^{\rm bqce}$ and $\tilde{\mathsf{S}}^{\rm bqce}$ are identical, and only the continuous components remain. Hence, and also using $\Pi_h u = u = I_h\tilde{u}$ in $[0, L + 2r_{\rm cut}]$, we can split the group η_1 further into

$$\begin{aligned}\eta_1 &= \int_K^N \big(\beta\,\partial_{\mathsf{F}}W(\nabla\tilde{u}) - I_h\beta\,\partial_{\mathsf{F}}W(\nabla\Pi_h u)\big)\nabla v_h \,{\rm d}x \\ &= \int_K^L (\beta - I_h\beta)\partial_{\mathsf{F}}W(\nabla u)\nabla v_h \,{\rm d}x \\ &\qquad + \int_K^L \beta\big(\partial_{\mathsf{F}}W(\nabla\tilde{u}) - \partial_{\mathsf{F}}W(\nabla I_h\tilde{u})\big)\nabla v_h \,{\rm d}x \\ &\qquad + \int_L^N \big(\partial_{\mathsf{F}}W(\nabla\tilde{u}) - \partial_{\mathsf{F}}W(\nabla\Pi_h u)\big)\nabla v_h \,{\rm d}x \\ &=: \eta_{1,1} + \eta_{1,2} + \eta_{1,3}.\end{aligned}$$

Using an interpolation error estimate for β, the term $\eta_{1,1}$ can be bounded by

$$\eta_{1,1} \lesssim \|\nabla^2\beta\|_{L^2}.$$

The term $\eta_{1,3}$ is analysed in Lemma 5.2. The term $\eta_{1,2}$ can be estimated similarly as the coarsening error in Lemma 5.2, but now the first term in the expansion must be taken into account, resulting in

$$\eta_{1,2} \lesssim \|\nabla\beta\,\nabla^2\tilde{u}\|_{L^2(K,L)} + \|\nabla^2\tilde{u}\|_{L^4(K,L)}^2.$$

Combining these estimates yields

$$\eta_1 \lesssim \|\nabla^2\beta\|_{L^2} + \|\nabla\beta\,\nabla^2\tilde{u}\|_{L^2} + \|h\nabla^2\tilde{u}\|_{L^4(K,N)}^2.$$

Estimating η_2. Applying Lemma 6.7 and then arguing analogously as in the proof of Theorem 6.4, we obtain the bound

$$\eta_2 \lesssim \|\nabla^2\beta\|_{L^2} + \|\nabla\beta\nabla^2\tilde{u}\|_{L^2} + \|\nabla^3\tilde{u}\|_{L^2(\Omega^c)} + \|\nabla^2\tilde{u}\|^2_{L^4(\Omega^c)}.$$

We obtain the stated result by combining the estimates for η_1 and for η_2. □

Optimizing the blending function

Under the decay hypothesis **(DH)**, one can readily check that the dominant consistency error contribution in the B-QCE method is the interface coupling error term $\|\nabla^2\beta\|_{L^2}$. This term originates from the smeared-out ghost forces. A natural question at this point is how one should choose β to minimize this consistency error contribution.

Recall that we have assumed that $\beta = 0$ in $[0, K]$ and $\beta = 1$ in $[L, N]$. Thus, we must solve the variational problem

$$\min \|\nabla^2\beta\|_{L^2(K,L)} \quad \text{subject to} \quad \beta(K) = \beta'(K) = \beta'(L) = 0, \text{ and } \beta(L) = 1.$$

The solution to this problem is the cubic polynomial

$$\beta^*(x) = \begin{cases} 0, & x \in [0, K], \\ \hat{\beta}\big(\frac{x-K}{L-K}\big), & x \in [K, L], \\ 1, & x > L, \end{cases} \quad \text{where} \quad \hat{\beta}(s) = 3s^2 - 2s^3. \tag{6.12}$$

One may now readily check that

$$\|\nabla^2\beta^*\|_{L^2} = (L-K)^{-3/2}\|\nabla^2\hat{\beta}\|_{L^2(0,1)} = \sqrt{12}(L-K)^{-3/2}. \tag{6.13}$$

In particular, we see again that the consistency error can be controlled by increasing the blending width.

We summarize further properties of β that will be useful throughout the remainder of the paper.

Lemma 6.9. Let β^* be given by (6.12) and $p \in [1, \infty]$. Then

$$\|\nabla\beta^*\|_{L^p} \lesssim (L-K)^{-1/p'}, \qquad \|\nabla^2\beta^*\|_{L^p} \lesssim (L-K)^{-1-1/p'}, \tag{6.14}$$

$$\|\nabla\sqrt{\beta^*}\|_{L^\infty} \lesssim (L-K)^{-1}, \qquad \|\nabla\sqrt{1-\beta^*}\|_{L^\infty} \lesssim (L-K)^{-1}. \tag{6.15}$$

Proof. The two estimates in (6.14) can be shown with the same scaling argument as (6.13).

To establish (6.15), we first note that, for $s \in [0, 1]$,

$$\sqrt{\hat{\beta}(s)} = s\sqrt{3-2s} \quad \text{and} \quad \sqrt{1-\hat{\beta}(s)} = (1-s)\sqrt{1+2s},$$

that is, $\sqrt{\hat{\beta}}$ and $\sqrt{1-\hat{\beta}}$ are both Lipschitz. Hence, (6.15) follows from an analogous scaling argument. □

Setting $\beta = \beta^*$ in Theorem 6.8, and inserting (6.14) into the consistency estimate (dropping the constants for simplicity), we obtain

$$\begin{aligned}\left\|\eta_{\rm int}^{\rm bqce}\right\|_{\mathcal{U}_h^*} \lesssim (L-K)^{-3/2} + (L-K)^{-1}\|\nabla^2\tilde{u}\|_{L^2(K,L)} \\ + \|\nabla^3\tilde{u}\|_{L^2(\Omega^{\rm c})} + \|h\nabla^2\tilde{u}\|^2_{L^4(\Omega^{\rm c})} + N^{1/2-\alpha}.\end{aligned} \tag{6.16}$$

Further remarks

(1) The first analysis of the B-QCE method (for 1D pair interactions) was given by Van Koten and Luskin (2011). In that paper, the consistency estimates follow the lines of the analysis in Ortner (2011) and Section 2. Our approach in the present section is a simplified 1D variant of the 2D/3D analysis in Li *et al.* (2013).

(2) Since we only attempted to obtain qualitative estimates, our Theorem 6.8 hides the fact that nearest-neighbour interactions do not generate a ghost force in 1D and hence do not contribute to the modelling error. Thus, the prefactor for the dominant error term, $\|\nabla^2\beta\|_{L^2}$, can be considered small (Van Koten and Luskin 2011). However, in 2D/3D, this observation is no longer valid (Ortner and Zhang 2012).

(3) To obtain (6.14) it is not necessary to use the 'optimal' blending function (6.12). Through a straightforward scaling argument one can see that $\hat{\beta}$ may be replaced by any function that is twice continuously differentiable and satisfies the same boundary conditions. However, the bounds (6.15) crucially enter the stability analysis.

6.3. Consistency of QNL-type methods

In Section 4.5 we introduced a general setting for the construction of force-consistent methods and have presented some explicit constructions as well, in particular the second-neighbour QNL method (4.14) and the reflection method (4.16). Rather than focusing on any particular variant, we shall show that *all* methods of the form (4.12), satisfying force-consistency **(F)** and the following additional technical assumptions, are first-order consistent at the interface.

We shall require two additional restrictions on the interface site energies, which we call the locality and scaling conditions.

(L) *Locality.* $\Phi^{\rm i}_\xi(u_h)$ is a k times continuously differentiable function of the interaction stencil $Du_h(\xi) = (D_\rho u_h(\xi))_{\rho\in\mathcal{R}}$. Moreover, $\Phi^{\rm i}_{\xi,\rho} \equiv 0$ for $\xi + \rho > L$.

(S) *Scaling.* $|\Phi^{\rm i}_{\xi,\boldsymbol{\rho}}(u)| \lesssim c(\boldsymbol{\rho})$, for $\boldsymbol{\rho} \in \mathcal{R}^j$, $j = 2, 3$, where

$$\sum_{\boldsymbol{\rho}\in\mathcal{R}^j} |\boldsymbol{\rho}|^s \prod_{i=1}^{j} |\rho_i| c(\boldsymbol{\rho}) \lesssim M^{(j,s)} \quad \text{for } 0 \le s \le 3.$$

Both the locality and scaling conditions ensure that the qualitative analytical properties of the interface potentials are similar to those of the atomistic potential. Both conditions can be weakened, but they are, at least in some form, necessary to obtain the following results (Ortner 2012). Both conditions are satisfied for the reflection method (4.16) and for the geometric reconstruction scheme discussed in Section 4.5, provided that the reconstruction coefficients $C_{\xi,\rho\varsigma}$ satisfy a uniform bound.

We begin, once again, by deriving a weak form of the first variation.

Proposition 6.10. For $u_h \in \mathcal{U}_h$, we have that

$$\big\langle \delta\mathcal{E}^{\rm qnl}(u_h), v_h \big\rangle = \int_0^N \mathsf{S}^{\rm qnl}(u_h; x) \nabla v_h \,{\rm d}x \quad \text{for all } v_h \in \mathcal{U}_h, \tag{6.17}$$

where, for $u \in W^{1,\infty}_{\rm loc}$, we define

$$\mathsf{S}^{\rm qnl}(u;x) := \begin{cases} \sum_{\rho\in\mathcal{R}} \sum_{\xi=0}^{K} \chi_{\xi,\rho}(x) \rho \Phi^{\rm a}_{\xi,\rho}(u) \\ \quad + \sum_{\rho\in\mathcal{R}} \sum_{\xi=K+1}^{L} \chi_{\xi,\rho}(x) \rho \Phi^{\rm i}_{\xi,\rho}(u), & \text{for a.e. } x < L, \\ \partial_{\mathsf{F}} W(\nabla u(x)), & \text{for a.e. } x > L. \end{cases} \tag{6.18}$$

Proof. The proof of this result is analogous to the derivation of the atomistic stress, using the form (4.12) of the QNL energy, and the locality assumption **(L)**. □

The next lemma establishes the key properties of $\mathsf{S}^{\rm qnl}$ required to derive the modelling error estimate.

Lemma 6.11. Let $u \in W^{1,\infty}_{\rm loc}$. Then

$$\mathsf{S}^{\rm qnl}(u;x) = \mathsf{S}^{\rm a}(u;x), \qquad \text{for a.e. } x \in [0, K - r_{\rm cut}], \tag{6.19}$$

$$\mathsf{S}^{\rm qnl}(u;x) = \partial_{\mathsf{F}} W(\nabla u), \quad \text{for a.e. } x \in [L, N], \tag{6.20}$$

$$\mathsf{S}^{\rm qnl}(u^{\mathsf{F}};x) = \partial_{\mathsf{F}} W(\mathsf{F}), \qquad \text{for a.e. } x \in \mathbb{R}_+. \tag{6.21}$$

Proof. Throughout, we assume that $x \notin \mathbb{Z}$. To prove (6.19), we note that, for $x \le K - r_{\rm cut}$, $\chi_{\xi,\rho}(x) \neq 0$ only when $\xi \le K$. Hence, (6.3) and (6.18) imply (6.19).

The property (6.20) follows immediately from the definition (6.18) of $\mathsf{S}^{\rm qnl}$.

To prove property (6.21), we observe that the force consistency condition **(F)** on page 437 can be restated as

$$\langle \delta\mathcal{E}^{\rm qnl}(u^{\mathsf{F}}), v_h \rangle = \int_0^N \mathsf{S}^{\rm qnl}(u^{\mathsf{F}}) \nabla v_h \,{\rm d}x = 0 \quad \text{for all } v_h \in \mathcal{U}_h,\ \mathsf{F} \in \mathbb{R}.$$

Since $\mathsf{S}^{\rm qnl}$ is a piecewise constant function, this is only possible if $\mathsf{S}^{\rm qnl}(u^{\mathsf{F}};x)$ is constant. Since $\mathsf{S}^{\rm qnl}(u^{\mathsf{F}};x) = \partial_{\mathsf{F}} W(\mathsf{F})$ in the continuum region, (6.21) follows. □

Next, we show that (6.21) implies a first-order error estimate on the a/c stress function. Note, however, that the stress error is second-order in the continuum region and vanishes in the atomistic region.

Lemma 6.12. Let $u \in W^{2,\infty}_{\mathrm{loc}}$. Then for almost every $x \in [K - r_{\mathrm{cut}}, L]$,

$$|\mathsf{S}^{\mathrm{qnl}}(u;x) - \mathsf{S}^{\mathrm{a}}(u;x)| \lesssim M^{(2,1)} \|\nabla^2 u\|_{L^\infty(\nu_x \setminus [0, K - r_{\mathrm{cut}}])}. \tag{6.22}$$

Proof. The result is a consequence of the Lipschitz estimate

$$\big|\mathsf{S}^{\mathrm{qnl}}(u;x) - \mathsf{S}^{\mathrm{qnl}}(v;x)\big| \lesssim \|\nabla u - \nabla v\|_{L^\infty(\nu_x)}.$$

However, to remove the dependence on the atomistic region, we proceed more carefully. Since the bounds on derivatives of Φ^{i} are now part of the approximation, we have to trace this dependence carefully. We assume, without loss of generality, that $|\rho||\varsigma|c(\rho,\varsigma) \gtrsim m(\rho,\varsigma)$ (see condition **(S)**).

Let $x \in [K - r_{\mathrm{cut}}, L] \setminus \mathbb{Z}$. Then

$$\begin{aligned}\mathsf{R}(u;x) &:= \mathsf{S}^{\mathrm{qnl}}(u;x) - \mathsf{S}^{\mathrm{a}}(u;x) \\ &= \sum_{\rho \in \mathcal{R}} \rho \sum_{\xi = K+1}^{L} \chi_{\xi,\rho}(x)\big(\Phi^{\mathrm{i}}_{\xi,\rho}(u) - \Phi^{\mathrm{a}}_{\xi,\rho}(u)\big).\end{aligned}$$

From (6.21), we know that $\mathsf{R}(u^{\mathsf{F}};x) = 0$ for all $\mathsf{F} \in \mathbb{R}$, and hence we can instead estimate

$$\begin{aligned}\big|\mathsf{R}(u;x)\big| &= \big|\mathsf{R}(u;x) - \mathsf{R}(u^{\mathsf{F}};x)\big| \\ &\le \sum_{\rho \in \mathcal{R}} |\rho| \sum_{\xi = K+1}^{L} \chi_{\xi,\rho}\big\{\big|\Phi^{\mathrm{i}}_{\xi,\rho}(u) - \Phi^{\mathrm{i}}_{\xi,\rho}(u^{\mathsf{F}})\big| + \big|\Phi^{\mathrm{a}}_{\xi,\rho}(u) - \Phi^{\mathrm{a}}_{\xi,\rho}(u^{\mathsf{F}})\big|\big\}.\end{aligned}$$

With the choice $\mathsf{F} := \nabla u(x)$, and for $\xi \in \nu_x \setminus [0,K]$, we can further bound

$$\begin{aligned}\big|\Phi^{\mathrm{i}}_{\xi,\rho}(u) - \Phi^{\mathrm{i}}_{\xi,\rho}(u^{\mathsf{F}})\big| &\le \sum_{\varsigma \in \mathcal{R}} c(\rho,\varsigma)\big|D_\varsigma u(\xi) - \nabla u(x)\varsigma\big| \\ &\lesssim |\xi - x| \sum_{\varsigma \in \mathcal{R}} |\varsigma| c(\rho,\varsigma) \|\nabla^2 u\|_{L^\infty(\nu_x \setminus [0, K - r_{\mathrm{cut}}])}.\end{aligned}$$

An analogous bound is satisfied by $|\Phi^{\mathrm{a}}_{\xi,\rho}(u) - \Phi^{\mathrm{a}}_{\xi,\rho}(u^{\mathsf{F}})|$.

Combining these estimates, and applying **(S)**, we obtain

$$\begin{aligned}\big|\mathsf{R}(u;x)\big| &\lesssim \|\nabla^2 u\|_{L^\infty(\nu_x \setminus [0, K - r_{\mathrm{cut}}])} \sum_{\rho,\varsigma \in \mathcal{R}} |\rho||\varsigma| c(\rho,\varsigma) \sum_{\xi = K+1}^{\infty} \chi_{\xi,\rho} |\xi - x| \\ &\lesssim M^{(2,1)} \|\nabla^2 u\|_{L^\infty(\nu_x \setminus [0, K - r_{\mathrm{cut}}])}.\end{aligned}$$

This concludes the proof of the result. □

Theorem 6.13. Let $u \in \mathcal{U}$ satisfy **(DH)** and let $K > r_{\rm cut}, N > r_0$. Then

$$\begin{aligned}\big\|\eta^{\rm qnl}_{\rm int}\big\|_{\mathcal{U}_h^*} \lesssim\ & M^{(2,2)}\|\nabla^2\tilde{u}\|_{L^2(K-r_{\rm cut},L)} \\ & + M^{(2,3)}\|\nabla^3\tilde{u}\|_{L^2(L-2r_{\rm cut},\infty)} + M^{(3,3)}\|h\nabla^2\tilde{u}\|^2_{L^4(L-2r_{\rm cut},\infty)} \\ & + M^{(2,0)}N^{1/2-\alpha}.\end{aligned}$$

Proof. The result can be proved along similar lines to Theorem 6.8. We simply remark that the term $M^{(2,2)}\|\nabla^2\tilde{u}\|_{L^2([K-r_{\rm cut},L])}$ is due to the first-order consistency in the a/c interface established in Lemma 6.12, while the remaining terms are due to the Cauchy–Born modelling and coarsening errors. □

Further remarks

The key result in this section is (6.21). Although it is straightforward to prove in 1D, it is in fact non-trivial. In particular, this property of the a/c stress is in general false in 2D/3D, due to the fact that $\mathsf{S}^{\rm qnl}$ may contain divergence-free components (Ortner and Zhang 2012). A divergence-free 'corrector' must therefore be added to the the a/c stress $\mathsf{S}^{\rm qnl}$, which leads to a modified stress function $\hat{\mathsf{S}}^{\rm qnl}(u)$. In 2D, one can exploit the characterization of discrete divergence-free tensor fields due to Arnold and Falk (1989) to characterize the difference $\mathsf{S}^{\rm qnl}(u^{\mathsf{F}}) - \mathsf{S}^{\rm a}(u^{\mathsf{F}})$ and construct such a corrector. This was carried out explicitly for a model problem by Ortner and Zhang (2012). A general result was established by Ortner (2012), which established first-order consistency for a general class of a/c couplings satisfying the force consistency **(F)**, locality **(L)**, and scaling conditions **(S)**.

It is, at present, an open question whether a similar result holds in 3D too. Moreover, even the 2D result (Ortner 2012) is not completely general. For example, it requires that the atomistic region is connected. (Although our framework includes this assumption as well, it is in fact not required in 1D.)

6.4. Consistency of the B-QCF method

We now turn to the consistency analysis of the B-QCF method, the only non-conservative scheme that we consider. We can again employ many of the ideas we developed in the previous sections. However, some interesting new effects appear. These can already be seen in the weak form of the B-QCF force operator in the following lemma.

We remark that we can replace I_h with I_1 (the nodal interpolant with respect to the atomistic grid $\mathbb{Z}_+$) in the following lemma.

Lemma 6.14. Let $u_h, v_h \in \mathcal{U}_h$. Then

$$\begin{aligned}\big\langle \mathcal{F}^{\mathrm{bqcf}}(u_h), v_h\big\rangle &= \big\langle \delta\mathcal{E}^{\mathrm{a}}(u_h), I_h((1-\beta)v_h)\big\rangle + \big\langle \delta\mathcal{E}^{\mathrm{c}}(u_h), I_h(\beta v_h)\big\rangle \qquad (6.23)\\ &= \int_0^N \big\{ \mathsf{S}^{\mathrm{a}}(u_h)\nabla I_h\big((1-\beta)v_h\big) + \partial_{\mathsf{F}} W(\nabla u_h)\nabla I_h(\beta v_h)\big\}\,\mathrm{d}x.\end{aligned}$$

Proof. From (4.22) and the definition of the weak form below (4.21), we obtain

$$\begin{aligned}\big\langle \mathcal{F}^{\mathrm{bqcf}}(u_h), v_h\big\rangle &= \sum_{\zeta\in\mathcal{N}_h} \left\{ (1-\beta(\zeta))\frac{\partial \mathcal{E}^{\mathrm{a}}(u_h)}{\partial u_h(\zeta)} + \beta(\zeta)\frac{\partial \mathcal{E}^{\mathrm{c}}(u_h)}{\partial u_h(\zeta)} \right\} \cdot v_h(\zeta)\\ &= \sum_{\zeta\in\mathcal{N}_h} \frac{\partial \mathcal{E}^{\mathrm{a}}(u_h)}{\partial u_h(\zeta)} \cdot I_h\big((1-\beta)v_h\big)(\zeta) + \sum_{\zeta\in\mathcal{N}_h} \frac{\partial \mathcal{E}^{\mathrm{c}}(u_h)}{\partial u_h(\zeta)} \cdot I_h(\beta v_h)(\zeta)\\ &= \big\langle \delta\mathcal{E}^{\mathrm{a}}(u_h), I_h((1-\beta)v_h)\big\rangle + \big\langle \delta\mathcal{E}^{\mathrm{c}}(u_h), I_h(\beta v_h)\big\rangle.\end{aligned}$$

The representation of $\delta\mathcal{E}^{\mathrm{a}}$ given in terms of the stress S^{a} in Proposition 6.1 and the standard weak form of $\delta\mathcal{E}^{\mathrm{c}}$ yield the stated result. □

As a consequence, we obtain the following form of the internal B-QCF consistency error.

Lemma 6.15. Let $u \in \mathcal{U}$ and suppose that $\{0, \dots, L + r_{\mathrm{cut}}\} \subset \mathcal{N}_h$. Then

$$\big\langle \eta_{\mathrm{int}}^{\mathrm{bqcf}}(u), v_h\big\rangle = \int_K^N \big(\mathsf{S}^{\mathrm{a}}(u) - \partial_{\mathsf{F}} W(\nabla \Pi_h u)\big)\nabla I_h(\beta v_h)\,\mathrm{d}x \quad \text{for all } v_h \in \mathcal{U}_h.$$

Proof. Under the assumption that $\{0, \dots, L + r_{\mathrm{cut}}\} \subset \mathcal{N}_h$, we have that $\Pi_h u = u$ in $[0, L + r_{\mathrm{cut}}]$, which implies that $\mathsf{S}^{\mathrm{a}}(\Pi_h u; x) = \mathsf{S}^{\mathrm{a}}(u; x)$ for $x \in [0, L]$. Hence, Lemma 6.14 yields

$$\begin{aligned}\big\langle \eta_{\mathrm{int}}^{\mathrm{bqcf}}(u), v_h\big\rangle &= \big\langle \mathcal{F}^{\mathrm{bqcf}}(\Pi_h u) - \delta\mathcal{E}^{\mathrm{a}}(u), v_h\big\rangle\\ &= \int_0^N \big\{ \mathsf{S}^{\mathrm{a}}(u)\nabla I_h\big((1-\beta)v_h\big) + \partial_{\mathsf{F}} W(\nabla \Pi_h u)\nabla I_h(\beta v_h) - \mathsf{S}^{\mathrm{a}}(u)\nabla v_h\big\}\,\mathrm{d}x\\ &= \int_0^N \big(\partial_{\mathsf{F}} W(\nabla \Pi_h u) - \mathsf{S}^{\mathrm{a}}(u)\big)\nabla I_h(\beta v_h)\,\mathrm{d}x.\end{aligned}$$

Since $\beta = 0$ in $[0, K]$, the result follows. □

We see from Lemma 6.15 that we can use our techniques from previous sections to bound the residual in terms of $\|\nabla(\beta v_h)\|_{L^2}$. However, we need a bound in terms of $\|\nabla v_h\|_{L^2}$. This is provided by the next lemma.

Lemma 6.16. Suppose that β is defined globally with $\beta \in W^{1,\infty}$, and suppose that $|\nabla\beta| \le 1$. Then

$$\|\nabla I_h(\beta v_h)\|_{L^2} \lesssim \big\{1 + \|x^{1/2}\nabla\beta\|_{L^2}\big\}\|\nabla v_h\|_{L^2} \quad \text{for all } v_h \in \mathcal{U}_h.$$

Proof. In order to evaluate the gradient of the product, we add and subtract $\nabla(v_h I_h \beta)$:

$$\|\nabla I_h(\beta v_h)\|_{L^2} \leq \|\nabla(v_h I_h \beta)\|_{L^2} + \|\nabla(v_h I_h \beta) - \nabla I_h(v_h \beta)\|_{L^2}. \tag{6.24}$$

The error term can be controlled in terms of $\nabla^2(v_h I_h \beta)$ (understood in the piecewise sense),

$$\begin{aligned}\|\nabla(v_h I_h \beta) - \nabla I_h(v_h \beta)\|_{L^2} &\lesssim \|\nabla^2(v_h I_h \beta)\|_{L^2} = 2\|\nabla v_h \nabla I_h \beta\|_{L^2} \\ &\lesssim \|\nabla I_h \beta\|_{L^\infty} \|\nabla v_h\|_{L^2} \leq \|\nabla \beta\|_{L^\infty} \|\nabla v_h\|_{L^2} \\ &\leq \|\nabla v_h\|_{L^2},\end{aligned}$$

where in the last line we used the assumption that $|\nabla \beta| \leq 1$.

The first term on the right-hand side of (6.24) can be bounded by

$$\|\nabla(v_h I_h \beta)\|_{L^2} \leq \|\nabla \beta \cdot v_h\|_{L^2(K,L)} + \|\nabla v_h\|_{L^2}.$$

Using the fact that $v_h(0) = 0$, Hölder's inequality implies

$$|v_h(x)| \leq x^{1/2} \|\nabla v_h\|_{L^2(0,x)}.$$

Hence we estimate

$$\|\nabla \beta \cdot v_h\|_{L^2(K,L)} \leq \|x^{1/2} \nabla \beta\|_{L^2(K,L)} \|\nabla v_h\|_{L^2}.$$

Combining the computations above, we obtain the stated result. □

We are now ready to prove the consistency result for the B-QCF method.

Theorem 6.17. Let $u \in \mathcal{U}$ satisfy the decay hypothesis **(DH)**, let $|\nabla \beta| \leq 1$ and let $L > K > 2r_{\rm cut}$. Then

$$\begin{aligned}\big\|\eta_{\rm int}^{\rm bqcf}(u)\big\|_{\mathcal{U}_h^*} \leq \big(1 + \|x^{1/2} \nabla \beta\|_{L^2}\big)\big\{&M^{(2,3)} \|\nabla^3 \tilde{u}\|_{L^2(K-2r_{\rm cut},\infty)} \\ &+ M^{(3,3)} \|h \nabla^2 \tilde{u}\|^2_{L^4(K-2r_{\rm cut},\infty)} + M^{(2,0)} N^{1/2-\alpha}\big\}.\end{aligned}$$

Proof. Applying Corollary 6.4 and Lemma 5.2 to the representation of $\eta_{\rm int}^{\rm bqcf}$ derived in Lemma 6.15, we obtain

$$\begin{aligned}\langle \eta_{\rm int}^{\rm bqcf}(u), v_h \rangle \lesssim \big\{&\|\nabla^3 \tilde{u}\|_{L^2(K-2r_{\rm cut},N+2r_{\rm cut})} + \|h \nabla^2 \tilde{u}\|^2_{L^4(K-2r_{\rm cut},N+2r_{\rm cut})} \\ &+ N^{1/2-\alpha}\big\} \|\nabla(\beta v_h)\|_{L^2}.\end{aligned}$$

Employing Lemma 6.16 yields the stated consistency error estimate. □

Suppose now that we use the blending function $\beta = \beta^*$ defined in (6.12). Then we have

$$\|\nabla \beta\|_{L^2} \lesssim (L - K)^{-1/2}$$

and hence

$$\|x^{1/2} \nabla \beta\|_{L^2} \lesssim L^{1/2} (L - K)^{-1/2},$$

and this cannot be improved upon. Thus, using the optimal blending function, the estimate (6.14) becomes

$$\begin{aligned}\big\|\eta_{\rm int}^{\rm bqcf}\big\|_{\mathcal{U}_h^*} \lesssim\ & \big(1+L^{1/2}(L-K)^{-1/2}\big)\big\{\|\nabla^3\tilde{u}\|_{L^p(K-2r_{\rm cut},\infty)} \\ & + \|h\nabla^2\tilde{u}\|^2_{L^{2p}(K-2r_{\rm cut},\infty)} + N^{1/2-\alpha}\big\}.\end{aligned} \tag{6.25}$$

In order to remove the prefactor dependence on the blending width, we must choose $L \geq cK$, $c > 1$. We will return to this point when we optimize all the approximation parameters in Section 8.

Further remarks

(1) The consistency analysis of the B-QCF method follows the more general multi-dimensional analysis in Li *et al.* (2013). Previous results in this direction can be found in Dobson *et al.* (2010*b*), Makridakis *et al.* (2011) and Lu and Ming (2013).

(2) Since H^1-stability for the QCF method (without blending) is false (Dobson *et al.* 2010*b*), the first error estimates for the QCF method were given in the $W^{1,\infty}$-seminorm and hence the consistency error was estimated in $W^{-1,\infty}$. Similarly, the consistency analysis of Lu and Ming (2013) is performed in the L^2-norm, which (in our scaling) is even weaker than the $W^{-1,\infty}$-norm.

The main difficulty in these analytical settings is to extend the analyses to realistic 2D/3D situations with defects, where $W^{1,\infty}$-regularity or H^2-regularity is likely to be false. Conversely, in the convenient (and natural) energy norm, the original QCF method is unstable. However, Li *et al.* (2012) showed that B-QCF is stable in the energy norm, which motivates our choice of analysing B-QCF in the framework of the present paper.

(3) If we had not imposed antisymmetry of the displacements, then we would not have the boundary condition $v_h(0) = 0$ available, but only $v_h(N) = 0$, and hence Lemma 6.16 would become

$$\|\nabla I_h(\beta v_h)\|_{L^2} \lesssim (1 + N^{1/2}(L-K)^{-1/2})\|\nabla v_h\|_{L^2}.$$

This is clearly a problem, since it would require an $O(N)$ blending region to control this prefactor. However, it is purely a 1D artefact. Indeed, analogous estimates in 2D and 3D (Li *et al.* 2013) show that the prefactor can be efficiently controlled.

6.5. Summary of consistency estimates

For the reader's convenience, we summarize all consistency estimates in Table 6.1. For each entry, we write the coupling error in the first line, the coarsening and Cauchy–Born modelling errors in the second line, and the

Table 6.1. Summary of consistency error estimates. For each entry, we write the coupling error in the first line, the coarsening and Cauchy–Born modelling errors in the second line, and the far-field error in the third line.

a/c method	$\|\eta^{\rm ac}_{\rm int}(u)\|_{\mathcal{U}_h^*} \lesssim$	Reference
B-QCE (Section 4.4)	$\|\nabla^2\beta\|_{L^2} + \|\nabla\beta\nabla^2\tilde{u}\|_{L^2}$ $+\|\nabla^3\tilde{u}\|_{L^2(\Omega^{\rm c})} + \|h\nabla^2\tilde{u}\|^2_{L^2(\Omega^{\rm c})}$ $+N^{1/2-\alpha}$	Theorem 6.8
QNL (Section 4.5)	$\|\nabla^2\tilde{u}\|_{L^2(K-r_{\rm cut},L)}$ $+\|\nabla^3\tilde{u}\|_{L^2(\Omega^{\rm c})} + \|h\nabla^2\tilde{u}\|^2_{L^2(\Omega^{\rm c})}$ $+N^{1/2-\alpha}$	Theorem 6.13
B-QCF (Section 4.6)	0 $+\|\nabla^3\tilde{u}\|_{L^2(\Omega^{\rm c})} + \|h\nabla^2\tilde{u}\|^2_{L^2(\Omega^{\rm c})}$ $+N^{1/2-\alpha}$	Theorem 6.17 and (6.25)

far-field error in the third line. For the B-QCF method, we assume that a blending function and choice of K, L was used for which the prefactor becomes $O(1)$.

6.6. Remarks on extensions to 2D/3D

The key concept in our consistency analyses is the representations of first variations of the atomistic and coupling energies in terms of stress functions ('weak forms'). To derive these, we employed a splitting of long-range finite differences in terms of local gradients (see (6.1)),

$$D_\rho v(\xi) = \int_{\mathbb{R}_+} \rho\, \chi_{\xi,\rho} \nabla v(x)\, {\rm d}x. \tag{6.26}$$

As a matter of fact, this technicality is not entirely necessary (though still convenient) in 1D since the stress in 1D can be simply defined as the derivative with respect to the gradient, for example,

$$\mathsf{S}^{\rm a}\big(u; \eta + \tfrac{1}{2}\big) = \frac{\partial \mathcal{E}^{\rm a}(u)}{\partial D_1 u(\eta)},$$

due to the fact that there is a one-to-one mapping between u and $D_1 u$. This was employed, for example, by Makridakis *et al.* (2011) for the analysis of the QCF method and the construction of a non-conservative scheme in divergence form. Our main reason for employing (6.26) in the present work is to mimic the extension of our results to 2D/3D.

The main difficulty in extending (6.26) to 2D/3D is that line integrals and volume integrals are no longer identical. A striking result of Shapeev (2011) showed that this need not be a problem: if T is a triangle with vertices belonging to $\mathbb{Z}^2$, $\rho \in \mathbb{Z}^2$, and $\chi_T(x) = 1$ if $x \in \mathrm{int}T$, $\chi_T(x) = 1/2$ if $x \in \partial T$, then

$$\sum_{\xi \in \mathbb{Z}^2} \int_{t=0}^{1} \chi_T(\xi + t\rho)\, \mathrm{d}t = |T|.$$

This *bond-density formula* enables the generalization of various 1D results to 2D, including the construction and rigorous analysis of the bond-splitting scheme (2.41); see Shapeev (2011) and Ortner and Shapeev (2013).

Unfortunately, the result is false in 3D, and moreover, there appears to be no analogue of (6.7) even in 2D, which makes it more difficult to exploit the symmetries of the interaction potential. An attempt to generalize it through the use of mollification operators (Ortner and Shapeev 2012) proved highly useful for the analysis of the Cauchy–Born approximation (Ortner and Theil 2013) as well as the B-QCE and B-QCF methods (Li *et al.* 2013), but has not led to a practical a/c coupling even for pair potentials. A promising approach based on yet another variant of writing finite differences as volume integrals and employing a family of interpolants of discrete functions (rather than a single interpolant) was proposed by Makridakis *et al* (2012). The techniques introduced therein may also provide an alternative avenue for the analysis of a/c coupling in 2D/3D.

7. Stability

The previous section was devoted to consistency estimates for the three main a/c methods. This section is devoted to the second fundamental ingredient for the error analysis: the stability of the linearized a/c operators $\delta\mathcal{F}^{\mathrm{ac}} \in \{\delta^2\mathcal{E}^{\mathrm{bqce}}, \delta^2\mathcal{E}^{\mathrm{qnl}}, \delta\mathcal{F}^{\mathrm{bqcf}}\}$. Assuming that $u \in \mathcal{U}$ is a strongly stable state satisfying (3.19), that is,

$$\langle \delta^2\mathcal{E}^{\mathrm{a}}(u^{\mathrm{a}})v, v\rangle \geq c_0\|\nabla v\|_{L^2}^2 \quad \text{for all } v \in \mathcal{U},$$

we will show that

$$\langle \delta\mathcal{F}^{\mathrm{ac}}(u)v, v\rangle \geq \big(c_0 - \epsilon\big)\|\nabla v\|_{L^2}^2,$$

where ϵ is a stability error that is controllable in terms of the approximation parameters.

7.1. Stability of the continuum model

In this preparatory section, we review the classical observation that stability of the atomistic model implies stability of the Cauchy–Born model. To state the result, we extend the definition of Hessians to general homogeneous

displacements $u = u^{\mathsf{F}}$ and $v \in \mathcal{U}$, by the same formula (3.10). This is well-defined since we have assumed that the second partial derivatives of V are bounded. We then define

$$\gamma^{\mathrm{a}}(\mathsf{F}) := \inf_{\substack{v \in \mathcal{U}_0 \\ \|\nabla v\|_{L^2} = 1}} \langle \delta^2 \mathcal{E}^{\mathrm{a}}(u^{\mathsf{F}}) v, v \rangle.$$

Lemma 7.1. $\gamma^{\mathrm{a}}(\mathsf{F}) \leq \partial_{\mathsf{F}}^2 W(\mathsf{F})$ for all $\mathsf{F} \in \mathbb{R}$.

Proof. Recall from (4.8) that $\mathcal{E}^{\mathrm{c}}(u) = \int_0^\infty W(\nabla u)\,\mathrm{d}x$. Then

$$\langle \delta^2 \mathcal{E}^{\mathrm{c}}(u^{\mathsf{F}}) v, v \rangle = \int_0^\infty \partial_{\mathsf{F}}^2 W(\mathsf{F}) |\nabla v|^2 \,\mathrm{d}x \quad \text{for } v \in W^{1,\infty}_{\mathrm{loc}},\ \nabla v \in L^2.$$

The proof uses the fact that $\mathcal{E}^{\mathrm{c}}$ is the scaling limit of $\mathcal{E}^{\mathrm{a}}$ and the scale invariance of the continuum model.

We fix an antisymmetric function $v \in C_0^\infty(\mathbb{R}), v \neq 0$, compactly supported, and define

$$v_R(x) := Rv(x/R).$$

Then $\nabla v_R(x) = (\nabla v)(x/R)$ and $\nabla^2 v_R(x) = R^{-1}(\nabla^2 v)(x/R)$. Using these properties, it is easy to show (see Hudson and Ortner (2012) for details) that

$$\left| \frac{\langle \delta^2 \mathcal{E}^{\mathrm{a}}(u^{\mathsf{F}}) v_R, v_R \rangle}{\|\nabla v_R\|_{L^2}^2} - \frac{\langle \delta^2 \mathcal{E}^{\mathrm{c}}(u^{\mathsf{F}}) v_R, v_R \rangle}{\|\nabla v_R\|_{L^2}^2} \right| \to 0 \quad \text{as } R \to \infty,$$

$$\text{and} \quad \frac{\langle \delta^2 \mathcal{E}^{\mathrm{c}}(u^{\mathsf{F}}) v_R, v_R \rangle}{\|\nabla v_R\|_{L^2}^2} = \frac{\langle \delta^2 \mathcal{E}^{\mathrm{c}}(u^{\mathsf{F}}) v, v \rangle}{\|\nabla v\|_{L^2}^2} = \partial_{\mathsf{F}}^2 W(\mathsf{F}).$$

Hence, we obtain

$$\gamma^{\mathrm{a}}(\mathsf{F}) \leq \lim_{R \to \infty} \frac{\langle \delta^2 \mathcal{E}^{\mathrm{a}}(u^{\mathsf{F}}) v_R, v_R \rangle}{\|\nabla v_R\|_{L^2}^2} = \partial_{\mathsf{F}}^2 W(\mathsf{F}). \qquad \square$$

Corollary 7.2. Suppose there exists *any* $u \in \mathcal{U}$ satisfying the strong stability condition (3.19). Then $\partial_{\mathsf{F}}^2 W(0) \geq c_0$.

Proof. Let $v \in \mathcal{U}_0$ with $v(\xi) = 0$ for $0 \leq \xi \leq r_{\mathrm{cut}}$, and let

$$v_R(\xi) := \begin{cases} 0, & 0 \leq \xi \leq R, \\ v(\xi - R), & \xi \geq R. \end{cases}$$

Then it is easy to see that

$$\langle \delta^2 \mathcal{E}^{\mathrm{a}}(u) v_R, v_R \rangle \to \langle \delta^2 \mathcal{E}^{\mathrm{a}}(0) v, v \rangle \quad \text{as } R \to \infty.$$

Hence, we deduce that for any v such that $v(\xi) = 0$ for $0 \le \xi \le r_{\rm cut}$,

$$\langle \delta^2 \mathcal{E}^{\rm a}(0) v, v \rangle \ge c_0 \|\nabla v\|_{L^2}^2.$$

Slightly modifying the proof of Lemma 7.1, we obtain that $\partial_{\mathsf{F}}^2 W(0) \ge c_0$. □

Further remarks

As mentioned above, the result $\gamma^{\rm a}(\mathsf{F}) \le \partial_{\mathsf{F}}^2 W(\mathsf{F})$ is classical and can be found in standard textbooks, for example Wallace (1998). The proof reducing the argument to only two ingredients (the fact that the Cauchy–Born model is the scaling limit of the atomistic model, and the scale-invariance of the continuum model) was given by Hudson and Ortner (2012). An interesting question that seems to have gone largely unnoticed is under which conditions the atomistic and continuum stability regions coincide. That is, when does $\partial_{\mathsf{F}}^2 W(\mathsf{F}) > 0$ imply $\gamma^{\rm a}(\mathsf{F}) > 0$? For materials where this condition holds, the Cauchy–Born model can be expected to correctly predict the onset of defect nucleation or other types of singularities.

7.2. Stability of B-QCE

The second variation of $\mathcal{E}^{\rm bqce}$ is given by

$$\begin{aligned} \langle \delta^2 \mathcal{E}^{\rm bqce}(u) v, v \rangle = &\sum_{\xi \in \mathbb{Z}_+} (1 - \beta(\xi)) \sum_{\rho, \varsigma \in \mathcal{R}} \Phi_{\xi, \rho\varsigma}(u) D_\rho v(\xi) D_\varsigma v(\xi) \\ &+ \int_0^\infty I_h \beta \cdot \partial_{\mathsf{F}}^2 W(\nabla u) |\nabla v|^2 \, {\rm d}x. \end{aligned} \tag{7.1}$$

If we assume that $\delta^2 \mathcal{E}^{\rm a}(u) > 0$, then this suggests that the atomistic component of $\delta^2 \mathcal{E}^{\rm bqce}(u)$ might be positive as well. Moreover, Lemma 7.1 suggests that $\partial_{\mathsf{F}}^2 W(\nabla u) > 0$, in which case the continuum component of $\delta^2 \mathcal{E}^{\rm bqce}(u)$ would also be positive. To make this intuition precise, we will 'split' the test function v into an atomistic and continuum component, using the following lemma.

Lemma 7.3. Let $\beta \in C^{1,1}(0, \infty)$, with $0 \le \beta \le 1$. For each $v \in \mathcal{U}$, there exists $v^{\rm a}, v^{\rm c} \in \mathcal{U}$ such that

$$\big| \sqrt{1 - \beta(\xi)} D_\rho v(\xi) - D_\rho v^{\rm a}(\xi) \big| \le C_1 \big\| \nabla \sqrt{1 - \beta} \big\|_{L^\infty} \|\nabla v\|_{L^2(\nu_\xi)}, \tag{7.2}$$

$$\big| \sqrt{I_h \beta(x)} \nabla v(x) - \nabla v^{\rm c}(x) \big| \le C_2 \big\| \nabla \sqrt{\beta} \big\|_{L^\infty} |\nabla v(x)|, \quad \text{and} \tag{7.3}$$

$$|\nabla v^{\rm a}|^2 + |\nabla v^{\rm c}|^2 = |\nabla v|^2, \tag{7.4}$$

where C_1 may depend on $r_{\rm cut}$, but C_2 is a generic constant. In particular, $\nabla v^{\rm a}(x) = 0$ for $x \ge L$ and $\nabla v^{\rm c}(x) = 0$ for $x \le K$.

Proof. Let $\psi(x) := \sqrt{1-\beta(x)}$ and assume, without loss of generality, that $\rho > 0$. Then,

$$\begin{aligned}\sqrt{1-\beta(\xi)}D_\rho v(\xi) &= \psi(\xi)\sum_{\eta=\xi}^{\xi+\rho-1} D_1 v(\eta)\\ &= \sum_{\eta=\xi}^{\xi+\rho-1}\psi(\eta)D_1 v(\eta) + \sum_{\eta=\xi}^{\xi+\rho-1}\big(\psi(\xi)-\psi(\eta)\big)D_1 v(\eta).\end{aligned}$$

If we define $v^{\rm a}$ by $v^{\rm a}(0) = 0$ and $D_1 v^{\rm a}(\eta) = \psi(\eta)D_1 v(\eta)$, then we obtain

$$\sum_{\eta=\xi}^{\xi+\rho-1}\psi(\eta)D_1 v(\eta) = D_\rho v^{\rm a}(\xi),$$

and hence

$$\big|\sqrt{1-\beta}D_\rho v(\xi) - D_\rho v^{\rm a}(\xi)\big| \le |\rho|^{3/2}\|\nabla\psi\|_{L^\infty}\|\nabla v\|_{L^2(\xi,\xi+\rho)}.$$

This establishes (7.2). The proof of (7.3) is analogous, with $v^{\rm c}$ defined by $D_1 v^{\rm c}(\xi) = \sqrt{\beta(\xi)}D_1 v(\xi)$.

With these definitions (7.4) is an immediate consequence. □

It is of course possible that $\|\nabla\sqrt{1-\beta}\|_{L^\infty}$ or $\|\nabla\sqrt{\beta}\|_{L^\infty}$ are unbounded. However, if we choose $\beta = \beta^*$ defined in (6.12), then, employing (6.15), the estimates (7.2) and (7.3) become

$$\big|\sqrt{1-\beta(\xi)}D_\rho v(\xi) - D_\rho v^{\rm a}(\xi)\big| \lesssim (L-K)^{-1}\|\nabla v\|_{L^2(\nu_\xi)}, \quad \text{and}$$
$$\big|\sqrt{I_h\beta(x)}\nabla v(x) - \nabla v^{\rm c}(x)\big| \lesssim (L-K)^{-1}|\nabla v(x)|.$$

Thus, the following result shows that the coercivity constant of the B-QCE Hessian can be controlled in terms of the atomistic region size and the blending width.

Theorem 7.4. Let $u \in \mathcal{U}$ satisfy **(DH)** as well as the stability condition (3.19) and let $K \ge r_0$. Then

$$\big\langle \delta^2\mathcal{E}^{\rm bqce}(u)v, v\big\rangle \ge \big[c_0 - C\epsilon^{\rm bqce}\big]\|\nabla v\|_{L^2}^2 \quad \text{for all } v \in \mathcal{U}_0,$$

where

$$\epsilon^{\rm bqce} := \max\big(\|\nabla\sqrt{1-\beta}\|_{L^\infty}, \|\nabla\sqrt{\beta}\|_{L^\infty}, K^{-\alpha}\big),$$

and $C \lesssim M^{(2,2)} + C_{\mathbf{DH}}M^{(3,0)}$ is independent of all approximation parameters.

If $\beta = \beta^*$, then $\epsilon^{\rm bqce} \lesssim \max((L-K)^{-1}, K^{-\alpha})$.

Proof. Let $\epsilon_1 := \max(\|\nabla\sqrt{1-\beta}\|_{L^\infty}, \|\nabla\sqrt{\beta}\|_{L^\infty})$. Applying the estimates (7.2) and (7.3) to (7.1), we obtain

$$\langle \delta^2\mathcal{E}^{\mathrm{bqce}}(u)v, v\rangle \geq \sum_{\xi\in\mathbb{Z}_+}\sum_{\rho,\varsigma\in\mathcal{R}} \big\{\Phi_{\xi,\rho\varsigma}(u)D_\rho v^{\mathrm{a}}(\xi)D_\varsigma v^{\mathrm{a}}(\xi) - C'_{1,\rho\varsigma}\epsilon_1\|\nabla v\|^2_{L^2(\nu_\xi)}\big\} + \int_0^\infty \big\{\partial_{\mathsf{F}}^2 W(\nabla u) - C'_2\epsilon_1\big\}|\nabla v^{\mathrm{c}}|^2\,\mathrm{d}x, \tag{7.5}$$

where $C'_{1,\rho\varsigma}, C'_2$ are independent of any approximation parameters. Since $\nabla v^{\mathrm{c}} = 0$ in $(0,K)$, and using also Lemma 7.1,

$$\partial_{\mathsf{F}}^2 W(\nabla u) \geq \partial_{\mathsf{F}}^2 W(0) - C'_3K^{-\alpha} \geq c_0 - C'_3K^{-\alpha},$$

where C'_3 depends only on $M^{(3,0)}$ and on $C_{\mathbf{DH}}$.

Estimating the overlaps from the terms $\|\nabla v^{\mathrm{a}}\|_{L^2(\nu_\xi)}$, and using the fact that $|\nabla v^{\mathrm{c}}| \leq |\nabla v|$, gives

$$\langle \delta^2\mathcal{E}^{\mathrm{bqce}}(u)v, v\rangle \geq \langle \delta^2\mathcal{E}^{\mathrm{a}}(u)v^{\mathrm{a}}, v^{\mathrm{a}}\rangle + c_0\|\nabla v^{\mathrm{c}}\|^2_{L^2} - C\epsilon\|\nabla v\|^2_{L^2},$$

where $\epsilon := \max(\epsilon_1, K^{-\alpha})$. Now we use the stability of the atomistic model and property (7.4), to conclude that

$$\begin{aligned}\langle \delta^2\mathcal{E}^{\mathrm{bqce}}(u)v, v\rangle &\geq c_0\|\nabla v^{\mathrm{a}}\|^2_{L^2} + c_0\|\nabla v^{\mathrm{c}}\|^2_{L^2} - C\epsilon\|\nabla v\|^2_{L^2}\\ &= \big[c_0 - C\epsilon\big]\|\nabla v\|^2_{L^2}.\end{aligned}$$

□

7.3. Stability of B-QCF

The stability analysis of the B-QCF method uses similar ideas to that of the B-QCE method. The key difference is where the blending function occurs in the Jacobian. From (6.23) we immediately obtain, for $u_h, v_h \in \mathcal{U}_h$,

$$\begin{aligned}\big\langle \delta\mathcal{F}^{\mathrm{bqcf}}(u_h)v_h, v_h\big\rangle &= \big\langle \delta^2\mathcal{E}^{\mathrm{a}}(u_h)v_h, (1-\beta)v_h\big\rangle + \big\langle \delta^2\mathcal{E}^{\mathrm{c}}(u_h)v_h, I_h(\beta v_h)\big\rangle\\ &= \sum_{\xi\in\mathbb{Z}_+}\sum_{\rho,\varsigma\in\mathcal{R}} \Phi_{\xi,\rho\varsigma}(u)D_\rho v_h(\xi)D_\varsigma\big[(1-\beta)v_h\big](\xi)\\ &\quad + \int_{\mathbb{R}^+} \partial_{\mathsf{F}}^2 W(\nabla u)\nabla v_h \nabla I_h[\beta v_h]\,\mathrm{d}x.\end{aligned}$$

Next, we note that $I_h[\beta v_h] = I_1[\beta v_h]$ for all $v_h \in \mathcal{U}_h$, where I_1 denotes the piecewise affine interpolant with respect to the atomistic mesh $\mathbb{Z}_+$. Therefore, we can extend the definition of $\delta\mathcal{F}^{\mathrm{bqcf}}$ naturally to $u, v \in \mathcal{U}$, by

$$\begin{aligned}\big\langle \delta\mathcal{F}^{\mathrm{bqcf}}(u)v, v\big\rangle &= \big\langle \delta^2\mathcal{E}^{\mathrm{a}}(u)v, (1-\beta)v\big\rangle + \big\langle \delta^2\mathcal{E}^{\mathrm{c}}(u)v, I_1(\beta v)\big\rangle \qquad (7.6)\\ &= \sum_{\xi\in\mathbb{Z}_+}\sum_{\rho,\varsigma\in\mathcal{R}} \Phi_{\xi,\rho\varsigma}(u)D_\rho v(\xi)D_\varsigma\big[(1-\beta)v\big](\xi)\\ &\quad + \int_{\mathbb{R}^+} \partial_{\mathsf{F}}^2 W(\nabla u)\nabla v \nabla I_1[\beta v]\,\mathrm{d}x.\end{aligned}$$

This will simplify the subsequent stability analysis.

We will now rewrite $\delta\mathcal{F}^{\rm bqce}$ in terms of $\delta^2\mathcal{E}^{\rm bqce}$ and a controllable error. The intuition behind the first intermediate step is the simple observation that $D_\varsigma[(1-\beta)v(\xi)] \approx -\varsigma\nabla\beta(\xi)v(\xi) + (1-\beta(\xi))D_\varsigma v(\xi)$.

Lemma 7.5. Let $u \in \mathcal{U}$ satisfy **(DH)** with $K - r_{\rm cut} \geq r_0$, and let $\|\nabla\beta\|_{L^\infty} \leq 1$. Then, for $v \in \mathcal{U}_h$,

$$\langle \delta\mathcal{F}^{\rm bqcf}(u)v, v\rangle \geq \langle \delta^2\mathcal{E}^{\rm bqce}(u)v, v\rangle + \langle Sv, v\rangle - C_1\epsilon_1\|\nabla v\|_{L^2}^2,$$

where $\epsilon_1 := \max(\|\nabla\beta\|_{L^\infty}K^{-\alpha}, \|\nabla^2\beta\|_{L^\infty})L^{1/2}(L-K)^{1/2}$, $C_1 \lesssim M^{(2,2)} + M^{(3,1)}$, and

$$\langle Sv, v\rangle := \sum_{\xi\in\mathbb{Z}_+} \nabla\beta(\xi)v(\xi) \sum_{\rho,\varsigma\in\mathcal{R}} \varsigma V_{\rho\varsigma}(0)\big\{\rho D_1 v(\xi) - D_\rho v(\xi)\big\}. \tag{7.7}$$

Proof. Let $\delta_j := \|\nabla^j\beta\|_{L^\infty}$. Using the Taylor expansion

$$\beta(\xi+\varsigma) = \beta(\xi) + \varsigma\nabla\beta(\xi) + O(\delta_2),$$

we can compute

$$\begin{aligned} D_\varsigma\big[(1-\beta)v\big](\xi) = (1-\beta(\xi))D_\varsigma v(\xi) - \varsigma\nabla\beta(\xi)v(\xi) \\ - \varsigma\nabla\beta(\xi)D_\varsigma v(\xi) - O(\delta_2)\cdot\big(v(\xi) + D_\varsigma v(\xi)\big). \end{aligned}$$

Inserting this estimate into (7.6), it is easy to get

$$\begin{aligned} \langle \delta^2\mathcal{E}^{\rm a}(u)v, (1-\beta)v\rangle = \sum_{\xi\in\mathbb{Z}_+}(1-\beta(\xi)) \sum_{\rho,\varsigma\in\mathcal{R}} \Phi_{\xi,\rho\varsigma}(u)D_\rho v(\xi)D_\varsigma v(\xi) \\ - \sum_{\xi\in\mathbb{Z}_+} \nabla\beta(\xi)v(\xi) \sum_{\rho,\varsigma\in\mathcal{R}} \varsigma\Phi_{\xi,\rho\varsigma}(u)D_\rho v(\xi) \\ - C_1'(\delta_1+\delta_2)\|\nabla v\|_{L^2}^2 - C_1'\delta_2\|v\|_{L^2(K,L)}\|\nabla v\|_{L^2}, \end{aligned} \tag{7.8}$$

where $C_1' \lesssim M^{(2,2)}$.

Applying **(DH)** to estimate the coefficients $\Phi_{\xi,\rho\varsigma}(u)$, and the fact that

$$\|v\|_{L^2(K,L)} \leq L^{1/2}(L-K)^{1/2}\|\nabla v\|_{L^2} \quad \text{for all } v \in \mathcal{U}, \tag{7.9}$$

we obtain

$$\begin{aligned} -\sum_{\xi\in\mathbb{Z}_+} \nabla\beta(\xi)v(\xi) \sum_{\rho,\varsigma\in\mathcal{R}} \varsigma\Phi_{\xi,\rho\varsigma}(u)D_\rho v(\xi) \\ \geq -\sum_{\xi\in\mathbb{Z}_+} \nabla\beta(\xi)v(\xi) \sum_{\rho,\varsigma\in\mathcal{R}} \varsigma V_{\rho\varsigma}(0)D_\rho v(\xi) \\ - C_2'K^{-\alpha}\|\nabla\beta\|_{L^\infty}\|v\|_{L^2(K,L)}\|\nabla v\|_{L^2} \end{aligned}$$

$$\geq -\sum_{\xi\in\mathbb{Z}_+} \nabla\beta(\xi)v(\xi) \sum_{\rho,\varsigma\in\mathcal{R}} \varsigma V_{\rho\varsigma}(0) D_\rho v(\xi) - C_2'\delta_1 K^{-\alpha} L^{1/2}(L-K)^{1/2}\|\nabla v\|_{L^2}^2,$$

where $C_2' \lesssim M^{(3,1)}$. Combining the last estimate with (7.8), and again applying (7.9) to the term $\|v\|_{L^2(K,L)}$ in (7.8), we obtain

$$\begin{aligned}\langle \delta^2\mathcal{E}^{\mathrm{a}}(u)v, (1-\beta)v\rangle \geq \sum_{\xi\in\mathbb{Z}_+}(1-\beta(\xi)) \sum_{\rho,\varsigma\in\mathcal{R}} \Phi_{\xi,\rho\varsigma}(u) D_\rho v(\xi) D_\varsigma v(\xi) \\ - \sum_{\xi\in\mathbb{Z}_+} \nabla\beta(\xi)v(\xi) \sum_{\rho,\varsigma\in\mathcal{R}} \varsigma V_{\rho\varsigma}(0) D_\rho v(\xi) \\ - C_3'\epsilon_1'\|\nabla v\|_{L^2}^2,\end{aligned} \tag{7.10}$$

where $C_3' \lesssim C_1' + C_2'$ and

$$\begin{aligned}\epsilon_1' &:= \max(\delta_1 K^{-\alpha} L^{1/2}(L-K)^{1/2}, \delta_1+\delta_2, \delta_2 L^{1/2}(L-K)^{1/2}) \\ &\lesssim \max(\delta_1 K^{-\alpha}, \delta_2) L^{1/2}(L-K)^{1/2} = \epsilon_1.\end{aligned}$$

Similarly, we observe that, if $x \in (\xi, \xi+1)$, then $\nabla I_1[\beta v](x) = D_1[\beta v](\xi)$, and hence

$$\begin{aligned}\nabla I_1[\beta v](x) = \beta\nabla v(x) + \nabla\beta(\xi)v(\xi) + \nabla\beta(\xi) D_1 v(\xi) \\ + O(\delta_2)\cdot(v(\xi) + D_1 v(\xi)).\end{aligned}$$

We continue to argue similarly as in the proof of (7.10), and also use the fact that $\partial_{\mathsf{F}}^2 W(\mathsf{F}) = \sum_{\rho,\varsigma} \rho\varsigma V_{\rho\varsigma}(\mathsf{F}\cdot\mathcal{R})$, to obtain

$$\begin{aligned}\langle \delta^2\mathcal{E}^{\mathrm{c}}(u)v, I_1(\beta v)\rangle \geq \int_{\mathbb{R}_+} I_1\beta \cdot \partial_{\mathsf{F}}^2 W(\nabla u)|\nabla v|^2 \,\mathrm{d}x \\ + \sum_{\xi\in\mathbb{Z}_+} \nabla\beta(\xi)v(\xi) \sum_{\rho,\varsigma} \varsigma\rho V_{\rho\varsigma}(0) D_1 v(\xi) \\ - C_3'\epsilon_1'\|\nabla v\|_{L^2}^2.\end{aligned} \tag{7.11}$$

Combining (7.10) and (7.11) yields the stated result. □

The stability of $\delta^2\mathcal{E}^{\mathrm{bqce}}(u)$, in terms of the approximation parameters, is established in Theorem 7.4. We will see in Section 8 that the second error term, ϵ_1, can be made arbitrarily small by choosing β appropriately and increasing K and $L-K$. It remains to investigate the first error term, $\langle Sv, v\rangle$, occurring in Lemma 7.5.

To motivate the next result it is instructive to think of $\langle Sv, v\rangle$ as being formally of the same structure as

$$\langle \hat{S}v, v\rangle = \int \nabla\beta \cdot v \cdot \nabla^2 v \,\mathrm{d}x.$$

Integrating by parts gives

$$\begin{aligned}\langle \hat{S}v, v\rangle &= -\int \nabla^2\beta \cdot v \cdot \nabla v \,\mathrm{d}x - \int \nabla\beta \cdot |\nabla v|^2 \,\mathrm{d}x \\ &\gtrsim -\|\nabla^2\beta\|_{L^\infty} L^{1/2}(L-K)^{1/2}\|\nabla v\|_{L^2}^2 - \|\nabla\beta\|_{L^\infty}\|\nabla v\|_{L^2}^2,\end{aligned}$$

which is of a similar form to ϵ_1 and is also controllable. We now extend this argument to $\langle Sv, v\rangle$.

Lemma 7.6. Let S be defined by (7.7). Then, for all $v \in \mathcal{U}$,

$$\big|\langle Sv, v\rangle\big| \lesssim M^{(2,0)}\big(\|\nabla^2\beta\|_{L^\infty} L^{1/2}(L-K)^{1/2} + \|\nabla\beta\|_{L^\infty}\big)\|\nabla v\|_{L^2}^2.$$

Proof. We write $S = \sum_{\rho,\varsigma\in\mathcal{R}} \sigma V_{\rho\varsigma}(0) S_\rho$, where

$$\langle S_\rho v, v\rangle = \sum_{\xi\geq K} \nabla\beta(\xi) v(\xi)\big[\rho D_1 v(\xi) - D_\rho v(\xi)\big].$$

Now suppose, without loss of generality, that $\rho > 0$. Then

$$\big[\rho D_1 v(\xi) - D_\rho v(\xi)\big] = \sum_{j=1}^{\rho-1} \big[D_1 v(\xi) - D_1 v(\xi+j)\big],$$

and hence $S_\rho = \sum_{j=1}^{\rho-1} S_{\rho,j}$, where

$$\langle D_{\rho,j} v, v\rangle = \sum_{\xi\geq K} \nabla\beta(\xi) v(\xi)\big[D_1 v(\xi) - D_1 v(\xi+j)\big].$$

Summation by parts gives

$$\begin{aligned}\langle S_{\rho,j} v, v\rangle &= \sum_{\xi\geq K} \big[\nabla\beta(\xi)v(\xi) - \nabla\beta(\xi-j)v(\xi-j)\big] D_1 v(\xi) \\ &= \sum_{\xi\geq K} \big[\nabla\beta(\xi) - \nabla\beta(\xi-j)\big] v(\xi) D_1 v(\xi) \\ &\quad + \sum_{\xi\geq K} \nabla\beta(\xi-j)\big[v(\xi) - v(\xi-j)\big] D_1 v(\xi).\end{aligned}$$

Using the same arguments as in the proof of Lemma 7.5, it is now easy to show that

$$\big|\langle S_{\rho,j} v, v\rangle\big| \lesssim |\rho|\big(\|\nabla^2\beta\|_{L^\infty} L^{1/2}(L-K)^{1/2} + \|\nabla\beta\|_{L^\infty}\big)\|\nabla v\|_{L^2}^2.$$

Inserting this result into the definition of S_ρ and then S concludes the proof. □

Combining Lemma 7.5 and Lemma 7.6 yields the following stability result.

Theorem 7.7. Let $u \in \mathcal{U}$ satisfy **(DH)** and the stability condition (3.19), $K - r_{\rm cut} \geq r_0$. Then

$$\langle \delta \mathcal{F}^{\rm bqcf}(u)v, v \rangle \geq \big(c_0 - C\epsilon^{\rm bqcf}\big) \|\nabla v\|_{L^2}^2,$$

where

$$\epsilon^{\rm bqcf} = \max(\epsilon_1, \|\nabla \beta\|_{L^\infty}),$$

ϵ_1 is defined in Lemma 7.5, and $C \lesssim \max(M^{(2,2)}, M^{(3,1)})$. If $\beta = \beta^*$, then

$$\epsilon^{\rm bqcf} \lesssim \max\big\{(L-K)^{-1}, (L-K)^{-1/2} L^{1/2} K^{-\alpha}, (L-K)^{-3/2} L^{1/2}\big\}.$$

Further remarks

(1) By exploiting symmetries one can improve the estimate of Lemma 7.6, but not the prefactor in the consistency estimate. For stability, and with a smoother blending function, we only need $L - K \gg K^{1/5}$: see Li *et al.* (2012) for more details.

(2) The first proof of stability of the original QCF method, restricted to 1D, was in a discrete $W^{1,\infty}$-type norm (Dobson *et al.* 2010*b*). However, the proof suggested a smaller stability region than the numerical experiments. In the same work, the authors proved that QCF is never uniformly stable in $W^{1,p}$ for any $p < \infty$. Dobson *et al.* (2012) proved a sharp stability result for the QCF method in a discrete H^2-norm, still restricted to 1D, exploiting an interesting spectral equivalence with a QNL-type operator. To date, it is unknown whether the original QCF method is stable in 2D/3D; however, we note that some recent progress for a planar interface has been made by Lu and Ming (2012).

(3) A first proof of stability of the B-QCF method, valid in up to three dimensions, was given in an H^2-type norm by Lu and Ming (2013). This proof uses the machinery of pseudo-difference operators and requires that β is smooth at a macroscopic scale. In our framework, this would require a blending width of order $O(N)$ and thus no improvement in the order of the computational cost as compared to a purely atomistic computation. Li *et al.* (2012) showed that, in fact, the B-QCF method is positive definite in 2D provided that the blending width is much larger than $(\log N)^{1/5} K^{1/5}$ and an associated B-QCE operator is stable. (We expect that in the corresponding 3D result the log-factor is dropped.)

Finally, we remark that it still has to be demonstrated that an error analysis of the B-QCF (or any other a/c coupling) method in an H^2-like setting can incorporate crystal defects. Since the associated elastic fields have singularities in the continuum limit, which appears to prevent H^2-regularity, we see no path towards achieving this. (The QCF analysis of Lu and Ming (2012) and the BQCF analysis of Lu and Ming (2013) only admits smooth elastic solutions.)

7.4. Stability of QNL-type methods

Let $\mathcal{E}^{\rm qnl}$ be of the form (4.12) and assume that it satisfies the three key technical conditions **(F)**, **(L)**, and **(S)**.

Our strategy in the proof of stability of the B-QCE method was to split the test function into two components, and hence the Hessian into a purely atomistic and a purely continuum contribution. Although QNL-type methods do not have a 'built-in' blending, we can nevertheless apply the splitting technique to separate out the interface and continuum from the stability of the atomistic region (*i.e.*, the defect core). We call the following result the *conditional QNL stability theorem.*

Theorem 7.8. Let $u \in \mathcal{U}$ satisfy the strong stability condition (3.19) and suppose that there exists $\gamma^{\rm qnl} \in \mathbb{R}$ such that

$$\big\langle \delta^2 \mathcal{E}^{\rm qnl}(0)v, v\big\rangle \geq \gamma^{\rm qnl} \|\nabla v\|_{L^2}^2 \quad \text{for all } v \in \mathcal{U}_0. \tag{7.12}$$

Then

$$\big\langle \delta^2 \mathcal{E}^{\rm qnl}(u)v, v\big\rangle \geq \big(\min(c_0, \gamma^{\rm qnl}) - CK^{-\min(1,\alpha)}\big)\|\nabla v\|_{L^2}^2 \quad \text{for all } v \in \mathcal{U}_0,$$

where $C \lesssim M^{(2,0)} + C_{\mathbf{DH}} M^{(3,0)}$.

Proof. The idea behind the result is to artificially insert the blending function β^* into the QNL method in the fully atomistic region, with blending width $O(K)$. Then the result follows by closely mimicking the proof of Theorem 7.4. The details of the argument are given in Appendix A.3. □

As a matter of fact, Theorem 7.8 applies to any a/c coupling, including the B-QCE and B-QCF method. However, the natural occurrence of the blending function in those methods allowed for a more natural decomposition of the atomistic and continuum contributions.

Theorem 7.8 reduces the question of stability of a QNL-type method to stability at homogeneous deformations. We will consider two explicit examples.

The reflection method

The reflection method was proposed by Ortner *et al.* (2013) as a 'universally stable' method. Indeed, for this method we are able to provide a simple and general stability result.

Proposition 7.9. Let $\mathcal{E}^{\rm rfl}$ be the energy defined in (4.16). Then

$$\langle \delta^2 \mathcal{E}^{\rm rfl}(0)v, v\rangle \geq \gamma^{\rm a}(0)\|\nabla v\|_{L^2}^2 \quad \text{for all } v \in \mathcal{U}_0.$$

Proof. From the definition of $\mathcal{E}^{\rm rfl}$, we obtain

$$\langle \delta^2 \mathcal{E}^{\rm rfl}(0)v, v\rangle = \langle \delta^2 \mathcal{E}^{*}(0)v, v\rangle + \partial_{\mathsf{F}}^2 W(0)\|\nabla v\|_{L^2(L,\infty)}^2.$$

Since $\mathcal{E}^*$ depends only on $v(\xi)$, $\xi \le L$, and since we know from Lemma 4.1 that $\mathcal{E}^*$ can be understood as a periodic version of $\mathcal{E}^{\rm a}$, it is reasonable to conjecture that

$$\langle \delta^2 \mathcal{E}^*(0) v, v \rangle \ge \gamma^{\rm a}(0) \|\nabla v\|^2_{L^2(0,L)}. \tag{7.13}$$

If we can prove this, then we obtain the stated result.

To prove (7.13), we first write out $\langle \delta^2 \mathcal{E}^*(0) v, v \rangle$, using Lemma 4.1,

$$\langle \delta^2 \mathcal{E}^*(0) v, v \rangle = \frac{1}{2} \sum_{\rho,\varsigma \in \mathcal{R}} V_{\rho\varsigma} \sum_{\xi=-L+1}^{L} D_\rho v^*(\xi) D_\varsigma v^*(\xi).$$

Using $2L$-periodicity of v^*, we can equivalently write this as

$$\langle \delta^2 \mathcal{E}^*(0) v, v \rangle = \frac{1}{2m} \sum_{\rho,\varsigma \in \mathcal{R}} V_{\rho\varsigma} \sum_{\xi=-mL+1}^{mL} D_\rho v^*(\xi) D_\varsigma v^*(\xi) =: \langle H_m v^*, v^* \rangle,$$

for any $m \in \mathbb{N}$.

Extending the definition 'symbolically' to all displacements $w \in \mathcal{U}_0$ with $w(\xi) = 0$ for $|\xi| \ge mL - r_{\rm cut}$, we obtain

$$\langle H_m w, w \rangle \ge \frac{1}{m} \gamma^{\rm a}(0) \|\nabla w\|^2_{L^2}.$$

Now define v_m by

$$v_m(\xi) := \begin{cases} v^*(\xi), & |\xi| < mL - r_{\rm cut}, \\ 0, & |\xi| \ge mL - r_{\rm cut}. \end{cases}$$

Then

$$\begin{aligned} \langle H_m v^*, v^* \rangle &= \langle H_m v_m, v_m \rangle + O(m^{-1}) \\ &\ge \frac{1}{m} \gamma^{\rm a}(0) \|\nabla v_m\|^2_{L^2} + O(m^{-1}) \\ &= \frac{1}{m} \gamma^{\rm a}(0) \|\nabla v^*\|^2_{L^2(-mL,mL)} + O(m^{-1}). \end{aligned}$$

Since $\|\nabla v^*\|^2_{L^2(-mL,mL)} = 2m \|\nabla v\|^2_{L^2(0,L)}$, we obtain

$$\langle H_m v^*, v^* \rangle \ge \gamma^{\rm a}(0) \|\nabla v\|^2_{L^2(0,L)} + O(m^{-1}),$$

and letting $m \to \infty$ yields (7.13). □

Stability of the 'classical' QNL method

In Section 7.9 we have seen that the reflection method is 'universally stable'. That is, up to controllable errors, $\delta^2 \mathcal{E}^{\rm rfl}$ is positive if and only if $\delta^2 \mathcal{E}^{\rm a}$ is positive. For other QNL-type methods, this is not the case but depends crucially on the set-up of the problem.

First, we consider the original second-neighbour QNL method defined by (4.14), which reduces to (2.41) in the case of second-neighbour pair interactions.

Proposition 7.10. In the case of second-neighbour two-body interactions, we have that

$$\big\langle \delta^2\mathcal{E}^{\rm qnl}(0)v, v\big\rangle \geq \gamma^{\rm a}(0)\|\nabla v\|_{L^2}^2 \quad \text{for all } v \in \mathcal{U}_0, \tag{7.14}$$

where $\mathcal{E}^{\rm qnl}$ is the energy functional defined in (2.41).

Proof. To discuss this case, we again adopt the notation introduced in Section 2 and also define $\phi_j'' \equiv \phi_j''(0)$ and $\partial_{\rm F}^2 W \equiv \partial_{\rm F}^2 W(0)$. In Section 2.6 we have already shown that if $\phi_2'' \leq 0$, then

$$\langle \delta^2\mathcal{E}^{\rm qnl}(0)v, v\rangle \geq \partial_{\rm F}^2 W \|v'\|_{\ell^2}^2 \geq \gamma^{\rm a}(0)\|v'\|_{\ell^2}^2.$$

Using a completely analogous calculation, we can show that if $\phi_2'' \geq 0$, then the QNL Hessian can be written in the form

$$\begin{aligned}\langle \delta^2\mathcal{E}^{\rm qnl}(0)v, v\rangle &= \langle \delta^2\mathcal{E}^{\rm a}(0)v, v\rangle + \phi_2'' \sum_{\xi=K+1}^{\infty} |v_\xi''|^2 \\ &\geq \langle \delta^2\mathcal{E}^{\rm a}(0)v, v\rangle \geq \gamma^{\rm a}(0)\|v'\|_{\ell^2}^2,\end{aligned}$$

and we again obtain the stated result. □

Stabilizing QNL-type methods

We have seen in Proposition 7.10 that, for second-neighbour pair interactions, the original QNL method is stable provided that the atomistic model is stable. Unfortunately, for many-body interactions, this cannot be guaranteed. An explicit example can be constructed of an interaction potential for which $\gamma^{\rm a}(0) > 0$, but $\delta^2\mathcal{E}^{\rm qnl}(0)$ is indefinite (Ortner *et al.*, 2013). (Since the construction of this example is not very instructive, we do not give the details here.)

It turns out, however, that, at least in 1D, all QNL-type coupling schemes can be *stabilized*. We only give a brief outline of the argument and refer to Ortner *et al.* (2013) for further details. It is relatively straightforward to see that, for *any* QNL-type a/c coupling, the Hessian can be written in the form

$$\begin{aligned}\big\langle \delta^2\mathcal{E}^{\rm qnl}(0)v, v\big\rangle = &\sum_{\xi=0}^{\infty} c_0(\xi)|D_1 v(\xi)|^2 \\ &+ \sum_{j=1}^{2r_{\rm cut}-1}\sum_{\xi=0}^{\infty} c_j(\xi)\big|D_1 v(\xi+j) - D_1 v(\xi)\big|^2.\end{aligned}$$

For the reflection scheme $\mathcal{E}^{\rm qnl} = \mathcal{E}^{\rm rfl}$, we denote the coefficients by $c_j \equiv c_j^{\rm rfl}$, whereas for a general QNL scheme we just denote them by c_j, as above.

Next, one observes that, if force-consistency **(F)** is satisfied, then $c_0(\xi) \equiv \partial_{\mathsf{F}}^2 W(0)$ for all ξ. Thus, we obtain that

$$\begin{aligned}\big\langle \delta^2\mathcal{E}^{\rm qnl}(0)v, v\big\rangle - \big\langle \delta^2\mathcal{E}^{\rm rfl}(0)v, v\big\rangle \\ = \sum_{j=1}^{2r_{\rm cut}-1}\sum_{\xi=1}^{\infty} \big(c_j(\xi) - c_j^{\rm rfl}(\xi)\big)\big|D_1 v(\xi+j) - D_1 v(\xi)\big|^2.\end{aligned}$$

Since both the QNL energy and the reflection energy reduce to the atomistic model in the atomistic region and to the Cauchy–Born model in the continuum region, it follows that $c_j(\xi) = c_j^{\rm rfl}(\xi)$ except possibly in a small region surrounding the interface $\xi \in \{K, \dots, L\}$. To be precise, it is fairly straightforward to deduce that there exists a constant $C_1 \geq 0$ that depends only on the coefficients $c_j(\xi) - c_j^{\rm rfl}(\xi)$, such that

$$\big\langle \delta^2\mathcal{E}^{\rm qnl}(0)v, v\big\rangle - \big\langle \delta^2\mathcal{E}^{\rm rfl}(0)v, v\big\rangle \geq -C_1 \sum_{\xi=K-r_{\rm cut}+1}^{L-1} |v_\xi''|^2,$$

where we recall that $v_\xi'' = D_1 v(\xi) - D_1 v(\xi-1)$.

Let us now define

$$\mathcal{E}^{\rm stab}(u) := \mathcal{E}^{\rm qnl}(u) + C_1 \sum_{\xi=K-r_{\rm cut}+1}^{L-1} |v_\xi''|^2.$$

Then we obtain that $\mathcal{E}^{\rm stab}$ obviously satisfies the force-consistency **(F)** and locality **(L)** conditions. The scaling condition **(S)** follows from the fact that C_1 is essentially a sum over the coefficients $c_j(\xi) - c_j^{\rm rfl}(\xi)$. In addition to these conditions, we now also obtain that

$$\big\langle \delta^2\mathcal{E}^{\rm stab}(0)v, v\big\rangle \geq \big\langle \delta^2\mathcal{E}^{\rm rfl}(0)v, v\big\rangle \quad \text{for all } v \in \mathcal{U}_0.$$

Since $\mathcal{E}^{\rm rfl}$ is 'universally stable', it follows that $\mathcal{E}^{\rm stab}$ is stable as well. That is, $\mathcal{E}^{\rm stab}$ satisfies all the conditions of the conditional stability Theorem 7.8.

A similarly general construction in 2D/3D is open, but it is already clear from the initial results presented in Ortner *et al.* (2013) that stabilization cannot in general be as straightforward as in the 1D case.

8. *A priori* error estimates and computational cost

We are now ready to put into practice the strategy outlined in Section 4.7. Based on the stability analysis in Section 7 we now have strong reasons to expect that

$$\big\|\nabla u^{\rm a} - \nabla u_h^{\rm ac}\big\|_{L^2} \lesssim \tfrac{1}{c_0}\big(\|\eta_{\rm int}^{\rm ac}\|_{\mathcal{U}_h^*} + \|\eta_{\rm ext}\|_{\mathcal{U}_h^*}\big),$$

with suitable upper bounds on the two consistency components, derived in Sections 5 and 6. We shall now *optimize* the approximation parameters in

such a way that these upper bounds tend to zero as we increase the number of degrees of freedom. For sufficiently small consistency errors, we can then apply an inverse function theorem to make the error estimate fully rigorous.

8.1. Optimizing the finite element grid

The finite mesh size h is the first approximation parameter that we will optimize. In this section, we use a classical technique to optimize the mesh grading.

The two terms occurring in the coarsening and consistency analysis that depend on $\mathcal{T}_h$ are the best approximation and the coarsening error terms

$$\|h\nabla^2\tilde{u}\|_{L^2(L,N)} + \|h\nabla^2\tilde{u}\|^2_{L^4(L,N)}.$$

It is easy to see that, for L sufficiently large, the best approximation error $\|h\nabla^2\tilde{u}\|_{L^2(L,N)}$ is the dominant contribution. Thus, we optimize this term only. A discussion of optimizing a/c methods for the superconvergent error component, $\|h\nabla^2\tilde{u}\|^2_{L^4(L,N)}$, is given in Section 8.6.

Suppose that $u \in \mathcal{U}$ satisfies **(DH)** and $L > r_0$. Then

$$\|h\nabla^2\tilde{u}\|_{L^2(L,N)} \lesssim \|hx^{-\alpha-1}\|_{L^2(L,N)}.$$

We wish to choose h to minimize this quantity, subject to fixing the number of degrees of freedom, $N_{\mathcal{T}_h} - 1$, which is given by

$$N_{\mathcal{T}_h} = \sum_{j=1}^{N_{\mathcal{T}_h}} 1 = \sum_{j=1}^{N_{\mathcal{T}_h}} h_j \frac{1}{h_j} = \int_0^1 \frac{1}{h}\,\mathrm{d}x.$$

We ignore the discreteness of the mesh size function and solve

$$\min \|hx^{-\alpha-1}\|^2_{L^2(L,N)} \quad \text{subject to } \int_L^N \frac{1}{h}\,\mathrm{d}x = \text{const}.$$

The solution to this variational problem satisfies

$$h(x) = \lambda x^{\frac{2}{3}(\alpha+1)} \quad \text{for } x \in (L,N),$$

for some constant $\lambda > 0$. This gives us an optimal scaling of the mesh size function.

We now impose the condition $h(L) \approx 1$, which yields

$$h(x) \approx \left(\frac{x}{L}\right)^{\frac{2}{3}(\alpha+1)} =: \tilde{h}(x) \quad \text{for } x \in (L,N). \tag{8.1}$$

If $\alpha' := \frac{2}{3}(\alpha+1)$, then $\alpha' > 1$, and hence this choice of h yields

$$\int_L^N \frac{1}{h}\,\mathrm{d}x \approx \frac{L^{\alpha'}(N^{1-\alpha'} - L^{1-\alpha'})}{1-\alpha'} \approx \frac{L}{\alpha'-1}. \tag{8.2}$$

Thus, the choice (8.1) gives a comparable number of degrees of freedom in the continuum region to that in the atomistic and interface regions. The resulting best approximation error bound can be estimated by

$$\|hx^{-\alpha-1}\|_{L^2(L,N)} \approx \frac{L^{\frac{1}{2}-(\alpha+1)}}{(\alpha'-1)^{1/2}} \approx L^{-\frac{1}{2}-\alpha}. \tag{8.3}$$

We can now also determine an optimal balance between the choices for L, N and $\mathcal{T}_h$. To balance the interpolation error with the far-field error, we should choose N such that

$$L^{-1/2-\alpha} \approx N^{1/2-\alpha}, \quad \text{that is,} \quad N \approx L^{\frac{\alpha+1/2}{\alpha-1/2}}.$$

We now turn this formal motivation into an explicit construction of a finite element mesh.

Algorithm T.

(1) Set $N := \lceil L^{\frac{\alpha+1/2}{\alpha-1/2}} \rceil$.
(2) Set $\mathcal{N}_h := \{0, \dots, L\}$.
(3) While $n := \max \mathcal{N}_h < N$
Set $\mathcal{N}_h := \mathcal{N}_h \cup \{\min(N, n + \lfloor \tilde{h}(n) \rfloor)\}$.

Meshes constructed via Algorithm T satisfy qualitatively the same properties as predicted by the formal computations (8.2) and (8.3).

Lemma 8.1. Let $u \in \mathcal{U}$ satisfy **(DH)** and let N and $\mathcal{T}_h$ be constructed by Algorithm T. Then, for L sufficiently large, $N_{\mathcal{T}_h} \le C_1 L$,

$$\|h\nabla^2 \tilde{u}\|_{L^2(L,N)} + N^{1/2-\alpha} \le C_2 N_{\mathcal{T}_h}^{-1/2-\alpha}, \quad \text{and} \tag{8.4}$$

$$\|h\nabla^2 \tilde{u}\|^2_{L^4(L,N)} \le C_3 N_{\mathcal{T}_h}^{-1/2-2\alpha}, \tag{8.5}$$

where C_1 depends on α and C_2, C_3 depend on α and on $C_{\mathbf{DH}}$.

Proof. The proof is given in Appendix A.4. □

Cost estimate for the external potential

We now turn the external consistency error estimate into an estimate in terms of $N_{\mathcal{T}_h}$ as well. Let f satisfy **(DH)** and suppose that $\mathcal{T}_h$ and N are constructed using Algorithm T. Since $h(x) \le x/2$ (see Lemma A.3), a straightforward computation yields

$$\begin{aligned}\|\eta_{\text{ext}}\|_{\mathcal{U}_h^*} &\lesssim \|h^2 \nabla f\|_{L^2(L,\infty)} + \frac{C_1}{\log L} \|h^2 \omega \nabla^2 f\|_{L^2(L,\infty)} \\ &\lesssim L^{-\alpha-3/2} + \frac{L^{-\alpha-3/2} \log^2 N}{\log L}.\end{aligned}$$

We insert $N \lesssim L^{\frac{2}{3}(\alpha+1)}$ to obtain the following result. In particular, we can conclude that the external consistency error is dominated by the best approximation error.

Proposition 8.2. Let f satisfy **(DH)** and let $\mathcal{T}_h, N$ be chosen by Algorithm T. Then

$$\|\eta_{\rm ext}\|_{\mathcal{U}_h^*} \leq CL^{-\alpha-3/2}\log L,$$

where C depends on α and on $C_{\mathbf{DH}}$.

Cost estimates for the Cauchy–Born error

Although not part of the coarsening error estimates, we still briefly derive corresponding estimates for the Cauchy–Born modelling error, since this is another generic component used in estimating the consistency error of all a/c couplings.

The only approximation parameter available to control the Cauchy–Born modelling error is the size of the atomistic region (recall that in Algorithm T we fixed N in terms of L). A straightforward calculation yields the following result, which we will later use to conveniently estimate the corresponding terms in the consistency error estimates.

Proposition 8.3. Let $u \in \mathcal{U}$ satisfy **(DH)** and let $L' \geq r_0$. Then

$$\|\nabla^2 \tilde{u}\|^2_{L^4(L',\infty)} + \|\nabla^3 \tilde{u}\|_{L^2(L',\infty)} \leq C(L')^{-\alpha-3/2}, \tag{8.6}$$

where C depends on α and on $C_{\mathbf{DH}}$.

Proof. The result follows from a straightforward computation. □

We notice, in particular, that if $L' \gtrsim L \gtrsim N_{\mathcal{T}_h}$ (in practice we will need to choose $K \gtrsim L$), then the Cauchy–Born modelling error is dominated by the best approximation error.

8.2. Error estimate for QNL-type methods

Fix a strongly stable atomistic solution $u^{\rm a} \in \mathcal{U}$ satisfying the decay hypothesis **(DH)**. We wish to approximate this equilibrium using a QNL-type approximation

$$u_h^{\rm qnl} \in \arg\min\left\{\mathcal{E}^{\rm qnl}(u_h) - \langle f, u_h\rangle_h \,\middle|\, u_h \in \mathcal{U}_h\right\}, \tag{8.7}$$

where $\mathcal{E}^{\rm qnl}$ is of the form (4.12). We now derive a quasi-optimal balance of the approximation parameters K, N and h. In the case of the QNL method, this will follow directly from Section 8.1.

Given an atomistic core size K, we define L as determined by the particular QNL method that we employ. (In practice, $L - K \leq Cr_{\rm cut} \lesssim 1$; we

state this in Theorem 8.4 as an assumption.) Next, we construct N and $\mathcal{T}_h$ using Algorithm T. Thus, we obtain

$$N_{\mathcal{T}_h} \lesssim L \lesssim K.$$

We can now apply Lemma 8.1, Lemma 8.3, and the decay hypothesis **(DH)**, to deduce that the QNL consistency error derived in Theorem 6.13 can be bounded above by

$$\begin{aligned}\big\|\eta_{\rm int}^{\rm qnl}\big\|_{\mathcal{U}_h^*} &\lesssim \|\nabla^2\tilde{u}^{\rm a}\|_{L^2([K-r_{\rm cut},L])} + \|h\nabla^2\tilde{u}^{\rm a}\|^2_{L^{2p}(L,\infty)} \\ &\quad + \|\nabla^3\tilde{u}^{\rm a}\|_{L^p(L,\infty)} + N^{1/2-\alpha} \\ &\lesssim K^{-\alpha-1} + N_{\mathcal{T}_h}^{-1/2-2\alpha} + L^{-\alpha-3/2} + L^{-1/2-\alpha} \\ &\lesssim N_{\mathcal{T}_h}^{-1/2-\alpha} \lesssim K^{-1/2-\alpha}. \end{aligned} \tag{8.8}$$

This means that, by choosing K sufficiently large, we can make the consistency error arbitrarily small. This motivates the following theorem.

Theorem 8.4. Let $u^{\rm a} \in \mathcal{U}$ be a strongly stable atomistic solution satisfying **(DH)**. Consider the QNL problem (8.7) with quasi-optimal choice of $N, \mathcal{T}_h$ constructed by Algorithm T. Suppose, moreover, that $\mathcal{E}^{\rm qnl}$ is stable in the reference state (7.12), and that $L - K$ remains bounded as $K \to \infty$. (For example, this is always satisfied for $\mathcal{E}^{\rm qnl} = \mathcal{E}^{\rm rfl}$.)

Then there exists K_0 such that, for all $K \geq K_0$, (8.7) has a locally unique, strongly stable solution $u_h^{\rm qnl}$ which satisfies

$$\|\nabla u^{\rm a} - \nabla u_h^{\rm qnl}\|_{L^2} \lesssim N_{\mathcal{T}_h}^{-1/2-\alpha}.$$

Proof. We will use the quantitative inverse function theorem, Lemma B.1, with

$$\mathcal{G}_h(u_h) := \delta\mathcal{E}^{\rm qnl}(u_h) - \langle f, \cdot\rangle_h,$$

with $\bar{u}_h = \Pi_h u^{\rm a}$.

We first remark that the scaling condition **(S)** implies a Lipschitz bound for $\delta^2\mathcal{E}^{\rm qnl}$,

$$\big\|\delta^2\mathcal{E}^{\rm qnl}(u) - \delta^2\mathcal{E}^{\rm qnl}(v)\big\|_{\mathcal{L}(\mathcal{U},\mathcal{U}^*)} \leq M\|\nabla u - \nabla v\|_{L^\infty} \quad \text{for all } u, v \in \mathcal{U}, \tag{8.9}$$

where $M \lesssim M^{(3,0)}$. The proof of (8.9) is analogous to the proof of (3.11) and is therefore omitted. Since $\|\cdot\|_{L^\infty} \lesssim \|\cdot\|_{L^2}$, we can also replace the L^∞-norm on the right-hand side with the L^2-norm. This establishes condition (B.1) in Lemma B.1.

The residual estimate (8.8) and the external residual estimate of Proposition 8.2 give

$$\|\mathcal{G}_h(\Pi_h u^{\rm a})\|_{\mathcal{U}_h^*} \lesssim K^{-1/2-\alpha},$$

which establishes the second condition (B.2) in Lemma B.1.

From Theorem 7.8 we obtain that

$$\langle \delta^2 \mathcal{E}^{\mathrm{qnl}}(u^{\mathrm{a}}) v_h, v_h \rangle \geq \big(\min(c_0, \gamma^{\mathrm{qnl}}) - CK^{-\min(1,\alpha)} \big) \|\nabla v_h\|_{L^2}^2.$$

Let $\gamma := \frac{1}{2}\min(c_0, \gamma^{\mathrm{qnl}})$. Applying the Lipschitz bound (8.9) and the best approximation error estimate (8.4), we obtain

$$\langle \delta^2 \mathcal{E}^{\mathrm{qnl}}(\Pi_h u^{\mathrm{a}}) v_h, v_h \rangle \geq \big(2\gamma - CK^{-\min(1,\alpha)} - CK^{-1/2-\alpha} \big) \|\nabla v_h\|_{L^2}^2.$$

Hence, for K sufficiently large, we obtain that

$$\langle \delta \mathcal{G}_h(\Pi_h u^{\mathrm{a}}) v_h, v_h \rangle \geq \gamma \|\nabla v_h\|_{L^2}^2 \quad \text{for all } v_h \in \mathcal{U}_h,$$

which establishes the third condition (B.3) in Lemma B.1.

To check the final condition (B.4), we observe that

$$\frac{2M\eta}{\gamma^2} \lesssim \frac{2MK^{-1/2-\alpha}}{\gamma^2},$$

and hence, for sufficiently large K, (B.4) is satisfied as well.

Thus, we deduce the existence of u_h^{qnl} satisfying $\mathcal{G}_h(u_h^{\mathrm{qnl}}) = 0$. The stability estimate (B.6) guarantees that u_h^{qnl} is in fact a strongly stable solution to (8.7). The error estimate (B.5) implies

$$\|\nabla u_h^{\mathrm{qnl}} - \nabla \Pi_h u^{\mathrm{a}}\|_{L^2} \lesssim K^{-1/2-\alpha} \approx N_{\mathcal{T}_h}^{-1/2-\alpha}.$$

Applying the best approximation error estimate

$$\|\nabla \Pi_h u^{\mathrm{a}} - \nabla u^{\mathrm{a}}\|_{L^2} \lesssim N_{\mathcal{T}_h}^{-1/2-\alpha},$$

which follows from (8.4), we finally obtain the stated error bound. □

Remark 8.5. **(1)** Theorem 8.4 provides a rigorous convergence result for the reflection method (4.15) and for stabilized QNL-type methods (see Section 7.4). For more general QNL-type methods it depends on the details of the potential and the macroscopic strain, whether the stability assumption (7.12) holds. We have provided some examples and counterexamples in Section 7.8.

(2) The convergence rate $N_{\mathcal{T}_h}^{-1/2-\alpha}$ is, in some sense, optimal since it is the rate of the best approximation error. Indeed, it can be checked that the remaining consistency error terms decay at a higher order than the best approximation error. We comment further on the issue of optimal convergence rates in Section 9.1.

8.3. Error estimate for B-QCE

We follow the same strategy as in Section 8.2. Let $u^{\mathrm{a}} \in \mathcal{U}$ be a strongly stable atomistic solution, which we aim to approximate using the B-QCE method,

$$u_h^{\mathrm{bqce}} \in \arg\min \big\{ \mathcal{E}^{\mathrm{bqce}}(u_h) - \langle f, u_h \rangle_h \,\big|\, u_h \in \mathcal{U}_h \big\}. \tag{8.10}$$

Before we state the error estimate, we again turn the consistency estimate of Theorem 6.8 into an estimate in terms of $N_{\mathcal{T}_h}$. Let $K < L$ be given and $N, \mathcal{T}_h$ constructed by Algorithm T, and let $\beta = \beta^*$ defined in (6.12). Then, applying **(DH)**, (8.5) and (8.6) to (6.16), we obtain

$$\begin{aligned} \big\|\eta_{\rm int}^{\rm bqce}\big\|_{\mathcal{U}_h^*} &\lesssim (L-K)^{-3/2} + (L-K)^{-1}\|\nabla^2 \tilde{u}^{\rm a}\|_{L^2(K,L)} \\ &\quad + \|\nabla^3 \tilde{u}\|_{L^2(K,\infty)} + \|h\nabla^2 \tilde{u}\|_{L^4(K,\infty)}^2 + N^{1/2-\alpha} \\ &\lesssim (L-K)^{-3/2} + (L-K)^{-1/2}K^{-\alpha-1} + K^{-\alpha-3/2} + L^{-1/2-\alpha}. \end{aligned} \tag{8.11}$$

It remains to determine the (quasi-)optimal ratio between L and K. We think of L as fixed (and determining the number of degrees of freedom), and aim to optimize the choice of K. We consider three regimes.

(1) If $c_1 K \le L - K \le c_2 K$ for some $c_1, c_2 > 0$, then we also obtain $L - K \approx K \approx L$, and hence

$$\big\|\eta_{\rm int}^{\rm bqce}\big\|_{\mathcal{U}_h^*} \lesssim L^{-3/2} + L^{-3/2-\alpha} + L^{-\alpha-1/2} \approx L^{-\min(3/2,\alpha+1/2)}.$$

(2) If $(L-K)/K \to \infty$ as $K \to \infty$, then the upper bound in (8.11) is bounded below by $L^{-\min(3/2,\alpha+1/2)}$. That is, we cannot obtain an improved convergence rate over the earlier choice, but require more degrees of freedom.

(3) If $(L-K)/K \to 0$ as $K \to \infty$, then we clearly obtain a reduced convergence rate, but the number of degrees of freedom only improves by a constant factor.

In practice, in the B-QCE method we first choose the size of the atomistic region K and then define $L = 2K$. Thus, we obtain $N_{\mathcal{T}_h} \approx L \approx K \approx (L-K)$ and

$$\big\|\eta_{\rm int}^{\rm bqce}\big\|_{\mathcal{U}_h^*} \lesssim N_{\mathcal{T}_h}^{-\min(3/2,\alpha+1/2)} \approx K^{-\min(3/2,\alpha+1/2)}. \tag{8.12}$$

Again, we observe that by choosing K sufficiently large we can make the consistency error arbitrarily small.

According to the discussion above, this choice is asymptotically quasi-optimal, but it may be possible to improve on it quantitatively, as well as in the pre-asymptotic regime.

Theorem 8.6. Let $u^{\rm a} \in \mathcal{U}$ be a strongly stable atomistic solution satisfying **(DH)**. Consider the B-QCE method (8.10) with quasi-optimal choice of approximation parameters $L, N, \mathcal{T}_h, \beta$ for given K, as described above.

Then there exists K_0 such that, for all $K \ge K_0$, (8.10) has a locally unique, strongly stable solution $u_h^{\rm bqce}$, which satisfies

$$\|\nabla u^{\rm a} - \nabla u_h^{\rm bqce}\|_{L^2} \lesssim N_{\mathcal{T}_h}^{-\min(3/2,1/2+\alpha)}.$$

Proof. The proof is analogous to the proof of Theorem 8.4. The Lipschitz bound for $\delta^2\mathcal{E}^{\mathrm{bqce}}$ is again easy to establish. The consistency estimate in terms of K is given in (8.12). Finally, combining Theorem 7.4 with the Lipschitz bound for $\delta^2\mathcal{E}^{\mathrm{bqce}}$ ensures stability,

$$\langle \delta^2\mathcal{E}^{\mathrm{bqce}}(\Pi_h u^{\mathrm{a}})v_h, v_h\rangle \geq \tfrac{1}{2}c_0\|\nabla v_h\|_{L^2}^2,$$

provided that K is sufficiently large. (With our choice of K, L, $\beta = \beta^*$, the stability error is bounded by $\epsilon^{\mathrm{bqce}} \lesssim K^{-\min(1,\alpha)}$.) □

Remark 8.7. The B-QCE method has a reduced convergence rate $N_{\mathcal{T}_h}^{-3/2}$ for $\alpha > 1$ (fast decaying elastic field), but it has the optimal convergence rate $N_{\mathcal{T}_h}^{-1/2-\alpha}$ for $\alpha \in (1/2, 1]$ (slowly decaying elastic field). In the latter case it would be sufficient to choose $L - K \approx K^{(1+2\alpha)/3} \ll K$ to obtain the optimal rate.

8.4. Error estimate for B-QCF

In the B-QCF method, we approximate a strongly stable atomistic equilibrium u^{a} by the solution to

$$\langle \mathcal{F}^{\mathrm{bqcf}}(u_h^{\mathrm{bqcf}}), v_h\rangle = \langle f, v_h\rangle_h \quad \text{for all } v_h \in \mathcal{U}_h, \tag{8.13}$$

where $\mathcal{F}^{\mathrm{bqcf}}$ is given by (4.22). We will again use the blending function $\beta = \beta^*$ defined in (6.12) and, given K and L, define N and $\mathcal{T}_h$ via Algorithm T.

In the consistency error estimate given in Theorem 6.16 the blending function occurs again, but this time as a prefactor. We slightly rewrite (6.25) as

$$\begin{aligned}\|\eta_{\mathrm{int}}^{\mathrm{bqcf}}\|_{\mathcal{U}_h^*} \lesssim \big(1 + L^{1/p}(L-K)^{-1/p}\big) \\ \cdot \big(\|\nabla^3\tilde{u}^{\mathrm{a}}\|_{L^2(K-r_{\mathrm{cut}},\infty)} + \|\nabla^2\tilde{u}^{\mathrm{a}}\|_{L^4(K-2r_{\mathrm{cut}},\infty)}^2 \\ + \|h\nabla^2\tilde{u}^{\mathrm{a}}\|_{L^4(L,N)}^2 + N^{1/2-\alpha}\big).\end{aligned}$$

Applying Lemma 8.1 and Lemma 8.3 to (6.25), and assuming that $K - 2r_{\mathrm{cut}} \gtrsim K$, we obtain

$$\|\eta_{\mathrm{int}}^{\mathrm{bqcf}}\|_{\mathcal{U}_h^*} \lesssim \big(1 + L^{1/p}(L-K)^{-1/p}\big) \cdot \big(K^{-\alpha-3/2} + N_{\mathcal{T}_h}^{-1/2-\alpha}\big). \tag{8.14}$$

We remark that choosing $\beta = \beta^*$ was not necessary, but that $\hat{\beta}$ could have been replaced by any Lipschitz function.

Before we state the B-QCF convergence result, we recall from Section 2.8 that we must optimize β not only for consistency but also for stability:

$$\langle \delta\mathcal{F}^{\mathrm{bqcf}}(u^{\mathrm{a}})v, v\rangle \geq (c_0 - C\epsilon^{\mathrm{bqcf}})\|\nabla v\|_{L^2}^2,$$

where

$$\epsilon^{\mathrm{bqcf}} \lesssim \max\big\{(L-K)^{-1}, (L-K)^{-1/2}L^{1/2}K^{-\alpha}, (L-K)^{-3/2}L^{1/2}\big\}. \tag{8.15}$$

Table 8.1. Summary of *a priori* error estimates in terms of computational cost.

a/c method	$\|\nabla u^{\rm a} - \nabla u_h^{\rm ac}\|_{L^2} \lesssim$	Reference
ATM (Section 3.4)	$N^{-\alpha+1/2}$	Theorem 3.14
B-QCE (Section 4.4)	$N_{\mathcal{T}_h}^{-\min(3/2,\alpha+1/2)}$	Theorem 8.6
QNL (Section 4.5)	$N_{\mathcal{T}_h}^{-\alpha-1/2}$	Theorem 8.4
B-QCF (Section 4.6)	$N_{\mathcal{T}_h}^{-\alpha-1/2}$	Theorem 8.8

We now observe that by choosing $L - K \approx K \approx L \approx N_{\mathcal{T}_h}$, (8.14) and (8.15) become

$$\|\eta_{\rm int}^{\rm bqcf}\|_{\mathcal{U}_h^*} \lesssim K^{-\alpha-3/2} + N_{\mathcal{T}_h}^{-1/2-\alpha} \approx N_{\mathcal{T}_h}^{-1/2-\alpha} \approx K^{-1/2-\alpha}, \quad \text{and} \tag{8.16}$$

$$\epsilon^{\rm bqcf} \lesssim K^{-\min(1,\alpha)}. \tag{8.17}$$

In particular, the consistency error is of the same order of magnitude as the best approximation error and the stability error tends to zero as $K \to \infty$.

Thus, as in the B-QCE method, we first choose K, then define $L = 2K$ and then construct $N, \mathcal{T}_h$ using Algorithm T, to obtain a quasi-optimal implementation of the B-QCF method. This yields the following result.

Theorem 8.8. Let $u^{\rm a} \in \mathcal{U}$ be a strongly stable atomistic solution satisfying **(DH)**. Consider the B-QCF method (8.13) with quasi-optimal choice of approximation parameters $L, N, \mathcal{T}_h, \beta$ for given K, as described above.

Then there exists K_0 such that, for all $K \geq K_0$, (8.13) has a locally unique, strongly stable solution $u_h^{\rm bqcf}$, which satisfies

$$\|\nabla u^{\rm a} - \nabla u_h^{\rm bqcf}\|_{L^2} \lesssim N_{\mathcal{T}_h}^{-1/2-\alpha}.$$

Proof. The proof is analogous to the proof of Theorems 8.4 and 8.6. The Lipschitz bound for $\delta\mathcal{F}^{\rm bqcf}$ is again easy to establish, employing Lemma 6.16. The consistency estimate in terms of K is given in (8.16) and the stability error in terms of K is given in (8.17). □

8.5. Summary of a priori error estimates

For the reader's convenience we summarize all *a priori* error estimates, in terms of computational cost in Table 8.1. We see in particular from this table that the coarsening error dominates both in the QNL and B-QCF methods. In Section 9.1 (optimal a/c couplings) we discuss how to improve upon these rates. Recall also from **(DH)** that $\alpha > 1/2$.

8.6. Remark on superconvergence

In the analyses of the QCF and B-QCF methods by Dobson *et al.* (2010*b*), Makridakis *et al.* (2011) and Lu and Ming (2013), it is shown that the error is of a higher order than for energy-based a/c couplings. The reason we have not observed this here is because the consistency errors are dominated by the best approximation error.

Alternatively we could consider the superconvergent error $\nabla \Pi_h u^{\mathrm{a}} - \nabla u_h^{\mathrm{bqcf}}$, for which we might expect a better rate of convergence. Carrying out the analysis for this error leads to the same rates of convergence as the 'optimal rates' discussed in Section 9.1.

8.7. Numerical tests

We perform a selection of numerical tests to confirm the convergence rates we predicted in the preceding sections.

The model

We choose a one-dimensional variant (3.7) of the *embedded atom method* (EAM) (Daw and Baskes 1984), which is a popular atomistic model for solids. In this model ((3.7) for macroscopic stretch $\mathsf{A} = 1$), the site potential is given by

$$V(\boldsymbol{g}) = \frac{1}{2} \sum_{\rho \in \mathcal{R}} \phi\big(|\rho + g_\rho|\big) + \psi\bigg(\sum_{\rho \in \mathcal{R}} \eta\big(|\rho + g_\rho|\big) \bigg),$$

where ϕ is a pair potential, η an electron density function and ψ an embedding energy (typically convex). Mimicking popular variants of EAM, we define

$$\begin{aligned} \phi(r) &= 2\mathrm{e}^{-2a(|r|-1)} - 4\mathrm{e}^{-a(|r|-1)}, \\ \eta(r) &= \mathrm{e}^{-b|r|}, \\ \psi(t) &= c\big((t-t_0)^2 + (t-t_0)^4\big), \end{aligned}$$

where a, b, c, t_0 are parameters of the model. Throughout our computational experiments we choose

$$r_{\mathrm{cut}} = 2, \quad a = 3, \quad b = 3, \quad c = 5 \quad \text{and} \quad t_0 = \sum_{\rho \in \mathcal{R}} \mathrm{e}^{-0.95b|\rho|}.$$

Nonlinear solver

Let $\mathcal{F}^{\mathrm{ac}} : \mathcal{U}_h \to \mathcal{U}_h^*$ denote the force-operator associated with an a/c coupling. To compute the solution of the variational problem

$$\langle \mathcal{F}^{\mathrm{ac}}(u_h^{\mathrm{ac}}), v_h \rangle = \langle f, v_h \rangle_h \quad \text{for all } v_h \in \mathcal{U}_h,$$

we use a preconditioned steepest descent method with fixed step size s. Given an iterate $u_h^{[\ell]}$ we compute

$$\int_0^N \big(\nabla u_h^{[\ell+1]} - \nabla u_h^{[\ell]}\big) \cdot \nabla v_h \,\mathrm{d}x = -s\big\{\langle \mathcal{F}^{\mathrm{ac}}(u_h^{[\ell]}), v_h\rangle - \langle f, v_h\rangle_h\big\}$$

for all $v_h \in \mathcal{U}_h$. The step size s is chosen by trial end error to ensure stability of the iteration. As a starting guess, we choose $\Pi_h u^{\mathrm{a}}$, where u^{a} is a prescribed exact solution (see next paragraph). The iteration is terminated when the ℓ^∞-norm of the residual falls below the tolerance 10^{-8}.

Finally, we remark that in the case of the B-QCF method the iteration is not a steepest descent method (since there is no associated energy), but that it is nevertheless convergent due to the fact that $\delta\mathcal{F}^{\mathrm{bqcf}}$ is positive definite in a neighbourhood of the B-QCF solution.

More sophisticated and more efficient nonlinear solvers should of course be employed for 2D/3D problems.

Convergence rates

We fix an exact solution

$$u^{\mathrm{a}}(\xi) := \tfrac{1}{10}(1+\xi^2)^{-\alpha/2}\xi,$$

and compute the external forces $f(\xi)$ to be equal to the internal forces under the displacement u^{a}. The parameter α is a prescribed decay exponent. One may readily check that this solution and the associated external forces satisfy the decay hypothesis **(DH)**.

We then solve the atomistic method (ATM) with far-field boundary condition (3.21), the QCE method (4.6), the B-QCE method (8.10), the B-QCF method (8.13) and the reflection method (QNL(REFL)) (8.7) with $\mathcal{E}^{\mathrm{qnl}} = \mathcal{E}^{\mathrm{rfl}}$, and compute the error in the energy norm.

The results for $\alpha = 1.5$ (rapid decay) are shown in Figure 8.1 and the results for $\alpha = 0.8$ (slow decay) are shown in Figure 8.2. We observe precisely the rates predicted in the preceding sections.

Moreover, we note that, in the case $\alpha = 1.5$, the B-QCE scheme is indeed less efficient than the B-QCF and QNL schemes. However, since the convergence of *all* schemes (including the naive ATM scheme) is fairly fast, this may not be of great significance.

By contrast, in the case $\alpha = 0.8$ where a/c couplings yield much more significant computational savings, the best approximation error dominates the coupling error in the B-QCE scheme and hence the computational cost of B-QCE, B-QCF and QNL are essentially equivalent. For a similar reason, the error in the QCE method is initially close to the best approximation error and only stagnates once the elastic field is well resolved.

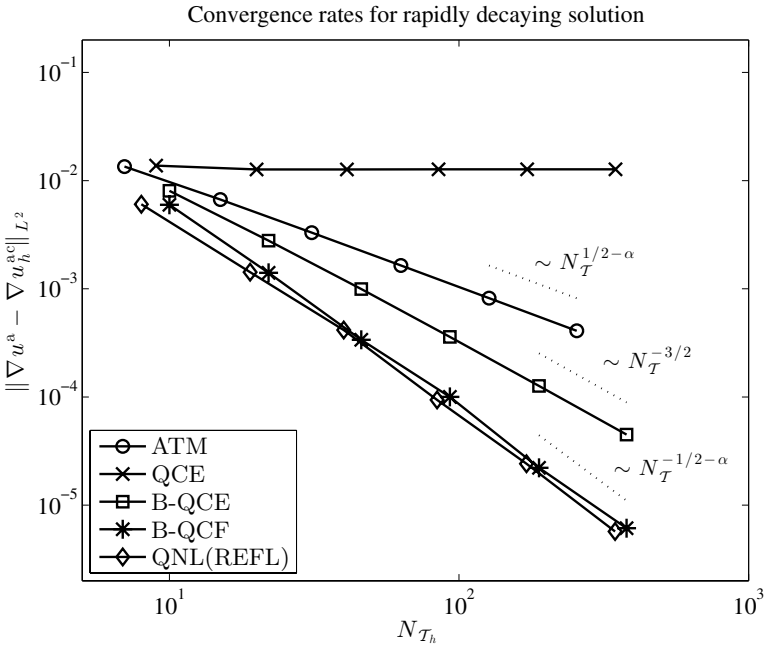

Figure 8.1. Convergence rates of various a/c couplings for a rapidly decaying atomistic solution ($\alpha = 1.5$).

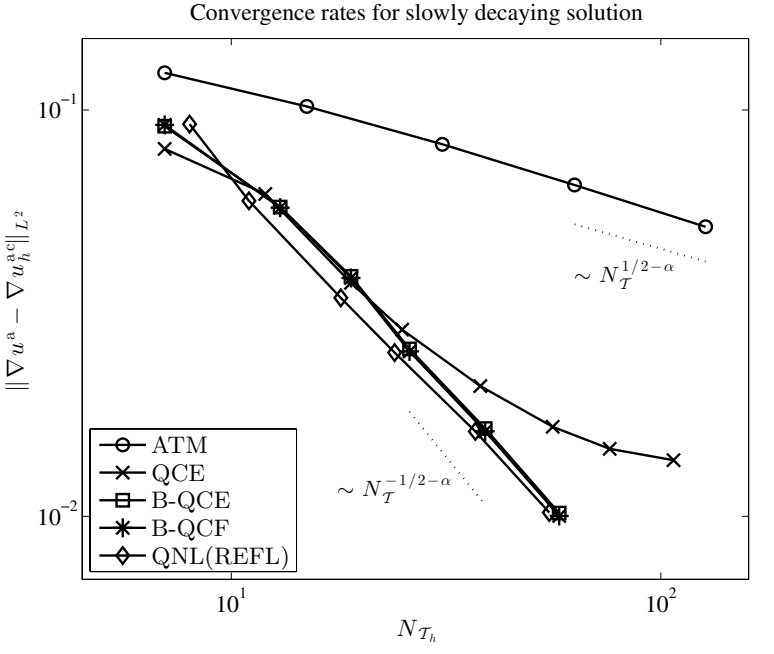

Figure 8.2. Convergence rates of various a/c couplings for a slowly decaying atomistic solution ($\alpha = 0.8$).

9. Extensions and open problems

In this article we have presented a numerical analysis of the fundamental a/c coupling methods. To conclude, we will briefly comment on several further important topics that we skipped or only touched upon, as well as open problems that motivate further research.

9.1. 'Optimal' a/c coupling

Suppose, for a moment, that we need not discretize the continuum region, but can solve the Cauchy–Born model at negligible computational cost. In this case, we may ignore both the far-field and the coarsening errors, and would obtain, using the notation and concepts from Section 8, the following error estimates for the B-QCE, QNL and B-QCF methods (we drop the subscripts h since we have not discretized the continuum model):

$$\begin{aligned}
\big\|\nabla u^{\mathrm{a}} - \nabla u^{\mathrm{bqce}}\big\|_{L^2} &\lesssim \|\nabla^2\beta\|_{L^2} + \|\nabla\beta\nabla^2\tilde{u}^a\|_{L^2} + \eta^{\mathrm{cb}},\\
\big\|\nabla u^{\mathrm{a}} - \nabla u^{\mathrm{qnl}}\big\|_{L^2} &\lesssim \|\nabla^2\tilde{u}^{\mathrm{a}}\|_{L^2(K-r_{\mathrm{cut}},L)} + \eta^{\mathrm{cb}},\\
\big\|\nabla u^{\mathrm{a}} - \nabla u^{\mathrm{bqcf}}\big\|_{L^2} &\lesssim \eta^{\mathrm{cb}},
\end{aligned}$$

where $\eta^{\mathrm{cb}} := \|\nabla^3\tilde{u}^a\|_{L^2(K-r_{\mathrm{cut}},\infty)} + \|\nabla^2\tilde{u}^a\|^2_{L^4(K-r_{\mathrm{cut}},\infty)}$, and we assumed that in the B-QCF method β, K, L are chosen such that the prefactor in the estimate is of order $O(1)$.

In these estimates, we again clearly observe the improvements in interface contribution to the error that the QNL and B-QCF methods represent. Applying the decay hypothesis **(DH)** to converting the estimates into estimates in terms of the number of degrees of freedom in the atomistic and interface region (which we have just assumed is now proportional to computational cost), we obtain for $\alpha > 1/2$ that

$$\begin{aligned}
\big\|\nabla u^{\mathrm{a}} - \nabla u^{\mathrm{bqce}}\big\|_{L^2} &\lesssim K^{-3/2},\\
\big\|\nabla u^{\mathrm{a}} - \nabla u^{\mathrm{qnl}}\big\|_{L^2} &\lesssim K^{-\alpha-1},\\
\big\|\nabla u^{\mathrm{a}} - \nabla u^{\mathrm{bqcf}}\big\|_{L^2} &\lesssim K^{-\alpha-3/2},
\end{aligned} \tag{9.1}$$

where we assumed that $\beta = \beta^*$ and $L - K \approx K$ in the B-QCE and B-QCF methods, and that $L - K = O(1)$ in the QNL method.

These estimates are natural limits that cannot be improved upon by changing the type of continuum model discretization. Moreover, we note that a recent result of Dobson (2011) implies that the estimate for the QNL method is optimal, that is, there exists no QNL-type scheme, coupling an atomistic to the Cauchy–Born model, that has an accuracy higher than first-order in the interface region.

We note two interesting challenges. First, it would be highly desirable to construct practical a/c schemes that achieve the optimal rates stated above. Second, by admitting more general (higher-order) continuum models, it may be possible to construct a/c schemes that can in fact improve upon the rates in (9.1).

9.2. Stability

As is the case with all approximation schemes, the two central pillars of the *a priori* error analysis of a/c couplings are *consistency* and *stability*. The stability of a/c couplings in 2D/3D is an entirely open question. We are aware of only three results in this direction, all of which are unsatisfactory in our view. Ortner and Shapeev (2013) obtain stability results in a 2D pair interaction setting by assuming that nearest-neighbour interactions dominate, which would break down for large deformations. Lu and Ming (2013) prove stability for the B-QCF Jacobian operator as a map from H^2 to L^2, but achieve this only for an impractical $O(N)$ blending width. Moreover, it is not clear how to incorporate crystal defects into their analysis. Finally, Li *et al.* (2012) prove positivity of the B-QCF Jacobian operator in 2D, but only under the assumption that the B-QCE Hessian is positive definite.

The approach to split test functions, which we employed in Section 7, is unlikely to generalize to 2D/3D. It was only possible to employ this in 1D because we could split the displacement *gradients* instead of the displacements themselves.

The result of Ortner and Shapeev (2013) would be generalizable to any of the a/c couplings we considered as well as to 3D, but this would not be satisfactory as it cannot be readily generalized to many-body interactions, and there is even less hope of extending it in such a way that stability of a/c couplings can be proved up to bifurcation points.

An entirely new approach may be required to obtain a satisfactory understanding of the stability of a/c couplings in 2D/3D.

9.3. Mesh and model adaptivity

We have presented an *a priori* error analysis approach to designing a/c couplings with a balance of approximation parameters that is quasi-optimal in the asymptotic regime. However, for many real defects, there is a significant pre-asymptotic regime; see, for example, Luskin *et al.* (2013). For practical computations, it is therefore desirable to develop quantitative *a posteriori* error estimates and corresponding mesh and model adaptation schemes.

Adaptive methods to determine the region needing atomistic accuracy and to select an efficient mesh in the continuum region have been considered (Miller and Tadmor 2003) and goal-oriented approaches have been studied by Prudhomme, Bauman and Oden (2006) and Arndt and Luskin

(2007, 2008*a*, 2008*b*). An adaptive algorithm that is conceptually similar to the framework of the present article has been developed by Ortner and Wang (2013).

Another key open question in this context is a rigorous criterion for the prediction of defect nucleation in the continuum region. For example, in a nano-indentation experiment (Miller and Rodney 2008), an indenter is pushed into a crystal surface in a quasi-static loading scenario. At some critical load, a dislocation dipole forms under the indenter, but the precise location of the nucleation is unknown, and in fact, the atomistic solution up to that point is sufficiently regular to employ the Cauchy–Born approximation. Predicting the correct nucleation load and nucleation region requires augmentation of the Cauchy–Born model with a suitable atomistic stability criterion.

9.4. Electronic structure

Classical interatomic potentials of the form employed in the present article are normally obtained by postulating a functional form, which is usually guided by physical intuition, with free parameters that are subsequently fitted to experimental data or simulations obtained from a more accurate model, such as density functional theory (DFT). Consequently, these models cannot account for all possible configurations and indeed are likely to be inaccurate in defect cores (unless, of course, the model has been fitted to the specific defect under consideration).

It is therefore of considerable interest to materials science research to extend the construction and analysis of a/c couplings (or possibly other kinds of multiscale schemes) to DFT models, or other more accurate quantum mechanics based models. Some recent work in this direction can be found in Gavini, Bhattacharya and Ortiz (2007) and Garcia-Cervera, Lu and E (2007). A closely related alternative approach is the DFT/linear elasticity coupling developed, for example, by Woodward and Rao (2002) and by Trinkle (2008) (see also Section 9.6 for other examples of a/c couplings employing linear elasticity as the continuum model).

As far as we are aware, there exists no systematic error analysis of these types of a/c couplings, with the exception of a highly simplified model by Langwallner *et al.* (2013). However, see Blanc *et al.* (2002) or E and Lu (2013) for analyses of the Cauchy–Born approximation of some DFT models, which might provide a starting point for the analysis of a/c couplings.

9.5. Finite temperature equilibrium and dynamic quasicontinuum methods

The computation of finite temperature equilibrium properties is usually done within the framework of statistical physics. The goal is then to compute the canonical average of observables (such as thermal expansion) that

only depend on the rep-atoms. To this end, it is enough to know the free energy associated with the rep-atoms, which is obtained by integrating the canonical Gibbs measure over all of the constrained atoms (Tadmor *et al.* 2013, Blanc, Le Bris, Legoll and Patz 2010). However, this free energy, termed the coarse-grained free energy in what follows, is a high-dimensional integral (since the number of constrained atoms is large), and it must therefore be approximated for computation.

To approximate the coarse-grained free energy, two asymptotic regimes have been considered in the literature. Dupuy, Tadmor, Miller and Phillips (2005) used a local harmonic approximation, which corresponds to a low temperature regime, and the Cauchy–Born rule to derive an approximate coarse-grained free energy of the form

$$\mathcal{E}^{\mathrm{c}}(u_h,\, \theta) = \int_0^N W(\nabla u_h,\, \theta)\, \mathrm{d}x, \tag{9.2}$$

where $W(\mathsf{F},\, \theta)$ is a Cauchy–Born elastic free energy density. The hot-QC energy of Tadmor *et al.* (2013) then uses a QCE coupling of the atomistic model with this coarse-grained free energy,

$$\mathcal{E}^{\mathrm{qce}}(u_h,\, \theta) = \sum_{\xi=0}^{K} \Phi_\xi^{\mathrm{a}}(u_h) + \int_{K+1/2}^{N} W(\nabla u_h,\, \theta)\, \mathrm{d}x, \tag{9.3}$$

to compute the canonical average of observables that depend only on the atomistic region.

Another possibility is to consider the thermodynamic limit when the number of constrained atoms goes to infinity, while the temperature remains fixed and is not necessarily small. This regime has been investigated in the one-dimensional case and in some two-dimensional cases in Blanc *et al.* (2010) and Blanc and Legoll (2013). These studies provide insight into the accuracy of the harmonic approximation previously mentioned.

We conclude this section by noting that many interesting phenomena actually involve dynamical effects. This goes beyond the equilibrium setting described above. For instance, quasi-static fracture and plastic deformation generally evolve by a sequence of rare events in which the system oscillates in an energy well for a long time scale before moving to a new energy well.

To handle such problems, one approach is to approximate the exact atomistic dynamics by a non-equilibrium dynamics using the free energy (9.3) in order to reduce the number of degrees of freedom. One possibility is to use a Langevin equation where the potential energy is given by (9.3). However, such direct molecular dynamics applied to a/c energies such as (9.3) still cannot reach the time scales necessary for useful information, which requires the system to visit many states. Thus, acceleration of the time dynamics is needed concurrently with coarse-graining in space. An example

of such a scheme is the hyper-QC method Kim *et al.* (2013), which has been developed to utilize the hyperdynamics method of Voter (1997) to achieve long-time dynamics with hot-QC.

9.6. Other types of a/c coupling schemes

The recent article of Miller and Tadmor (2009) reviews and benchmarks a list of at least fourteen different a/c couplings. Most of these schemes have at their core some aspects of the three fundamental a/c coupling concepts considered in the present article: energy-based blending, force-based coupling (and blending) and ghost force removal (QNL-type ideas). However, they are presented in a primarily algorithmic format and it would be interesting to distinguish the various approximate models from nonlinear solver and implementation issues to provide a classification more suitable to a numerical analysis of these methods.

It is likely that there are other fundamentally different and competitive approaches to a/c coupling that we have not considered in the present paper. As potential competitors we mention the field-based a/c coupling developed by Iyer and Gavini (2011), the approach of Anitescu *et al.* (2009), which is based on an optimization framework, the stress-based a/c coupling of Makridakis *et al.* (2011) or the method of Olson, Bochev, Luskin and Shapeev (2013), which minimizes the difference between the atomistic and continuum solutions in an overlap region. The latter has been shown to be stable (and positive definite), although no practical extension to 2D/3D has yet been formulated.

We briefly describe below a small selection of alternative a/c coupling methods. Some of these methods are formulated as finite temperature equilibrium or dynamics methods; the static methods can potentially be extended to finite temperature equilibrium and dynamics by the ideas described in Section 9.5.

The coupled atomistic and discrete dislocation method (CADD) couples an atomistic region with a region modelled by dislocations that interact through their linear elastic fields (Shilkrot, Miller and Curtin 2004), thereby allowing the simulation of atomistic systems with a large number of dislocations. Recent extensions have further coupled the discrete dislocation region with an even larger region modelled by continuum crystal plasticity (Wallin, Curtin, Ristinmaa and Needleman 2008).

The bridging scale method (BSM) decomposes the atomistic displacement into a coarse-grid displacement and a fine-grid displacement by projection (Liu *et al.* 2006*b*, Tang, Hou and Liu 2006). In the 'continuum' region, the fine-grid displacement is modelled rather than computed, thus giving a closed coarse-grained model, and in the 'atomistic region' the fine-grid displacement is computed, giving fully atomistic resolution.

The coarse-grained molecular dynamics (CGMD) method uses a coarse-grained Hamiltonian (Rudd and Broughton 2005, Rudd and Broughton 2000) defined for continuous, piecewise linear displacements with respect to a coarse mesh. The coarse-grained Hamiltonian is given by an approximation of the canonical average of the molecular Hamiltonian constrained to the space of atomistic displacements with mean square projection onto a given continuous, piecewise linear displacement.

If linear elasticity is used as the continuum model, then boundary integral methods can be employed instead of finite element methods to compute the elastic fields. The use of fast solution methods for the boundary integral and approximations of the boundary integral can give efficient methods (Haq, Movchan and Rodin 2007, Li 2009). These methods are in spirit close to the predecessors of a/c coupling such as the method of Sinclair (1971).

Peridynamics seeks to model atomistic systems with defects by a nonlocal continuum theory (Du, Gunzburger, Lehoucq and Zhou 2013, Silling and Lehoucq 2010). As a continuum theory it must be discretized for numerical implementation, thus leading to a nonlocal particle model in regions where the mesh is refined to length scales less than the 'horizon', which plays the role of a cut-off radius in a nonlocal atomistic model. To reach larger length scales (Seleson, Beneddine and Prudhomme 2013), the mesh must be coarsened beyond the length scale of the horizon, which leads to local approximations when quadrature points are added to the interior of elements (this can be seen by adapting the derivation in Section 4.3 for a nonlocal atomistic model to a nonlocal peridynamic continuum model). The mathematical framework and results presented in this article for a/c coupling can thus potentially be applied to the analysis of numerical approximations of peridynamics models.

An evaluation within the framework given in this article of the cost of each of the above methods for the computation of defects would enable their relative merits to be assessed. Further discussion of alternative a/c coupling methods can be found in the books by Tadmor and Miller (2011), Liu, Karpov and Park (2006*a*), and E (2011), and in the review article by Curtin and Miller (2003).

9.7. Benchmarks

The accuracy of atomistic-to-continuum coupling methods has generally been studied by comparing to the solution of fully atomistic models (Miller and Tadmor 2009, Van Koten *et al.* 2012). Since these approaches do not always distinguish the many potential sources of error (atomistic core size, blending function, coupling error, continuum modelling error, continuum mesh, far-field error, iterative solution error), they do not provide a definite test of the relative accuracy of the various atomistic-to-continuum coupling

methods. It would be useful to develop a more comprehensive, theory-based approach to benchmarking a/c multiscale methods that can also provide further insight into the optimization of the atomistic core size, blending functions, continuum meshes, and other approximation parameters. Some initial steps in this direction have been taken in Luskin *et al.* (2013) and Li *et al.* (2013), but a more systematic benchmark protocol on a much wider range of model problems is required.

A. Proofs

A.1. Proofs from Section 3

Proof of Proposition 3.1. The proof uses standard arguments for interpolation error estimates.

Let $\hat{w}$ be a quadratic polynomial on $[\xi-2, \xi+1]$ with nodal values $w(\xi)$. Then it is straightforward to see that $\tilde{w}(x) = \hat{w}(x)$ on $[\xi-1, \xi]$.

Using this fact and the stability of the interpolation $v \mapsto \tilde{v}$, we estimate, for any quadratic $\hat{w}$,

$$\begin{aligned}\|\nabla^j(\tilde{v}-\hat{v})\|_{L^p(\xi-1,\xi)} &\lesssim \|\nabla^j(\tilde{v}-\tilde{w})\|_{L^p(\xi-1,\xi)} + \|\nabla^j(\hat{v}-\hat{w})\|_{L^p(\xi-1,\xi)} \\ &\lesssim \|\hat{v}-\hat{w}\|_{W^{1,p}(\xi-2,\xi+1)} + \|\nabla^j(\hat{v}-\hat{w})\|_{L^p(\xi-1,\xi)} \\ &\lesssim \|\hat{v}-\hat{w}\|_{W^{j,p}(\xi-2,\xi+1)}.\end{aligned}$$

One can now readily show that, for suitable choice of $\hat{w}$,

$$\|\hat{v}-\hat{w}\|_{W^{j,p}(\xi-2,\xi+1)} \lesssim \|\nabla^j\hat{v}\|_{L^p(\xi-2,\xi+1)}.$$

This establishes the first result.

The second inequality of the second result can be deduced by an analogous argument, employing a linear $\hat{w}$.

The first inequality of the second result follows from Hölder's inequality and the observation that $\int_{\xi-1}^{\xi} \nabla\tilde{v}(x)\,\mathrm{d}x = \nabla v|_{(\xi-1,\xi)}$. □

Proof of Proposition 3.3. Let $\eta \in \mathbb{Z}_+$ and let $u \in \mathcal{U}$ be defined by $u'_\xi = 1$ for $\xi = \eta$ and $u'_\xi = 0$ otherwise. Since linear combinations of such functions are dense in $\mathcal{U}$, it is sufficient to show that they belong to the closure of $\mathcal{U}_0$. To that end, let $u_n \in \mathcal{U}_0$ be defined by

$$u'_{n,\xi} := \begin{cases} 1, & \xi = \eta, \\ -1/n, & \xi = \eta+1, \dots, \eta+n, \\ 0, & \text{otherwise.} \end{cases}$$

Then it is straightforward to show that $\|\nabla u_n - \nabla u\|_{L^2} = n^{-1/2} \to 0$. □

Lemma A.1. For any $\rho \in \mathbb{Z} \setminus \{0\}$, we have

$$\|D_\rho u\|_{\ell^2} \leq \|\nabla_\rho u\|_{L^2} = |\rho| \|\nabla u\|_{L^2} \quad \text{for all } u \in \mathcal{U}. \tag{A.1}$$

Proof. For each $u \in \mathcal{U}$, we have

$$\begin{aligned}\|D_\rho u\|_{\ell^2}^2 &= \sum_{\xi \in \mathbb{Z}} \big|u(\xi+\rho) - u(\xi)\big|^2 = \sum_{\xi \in \mathbb{Z}} \left| \int_{t=0}^1 \nabla_\rho u(\xi + t\rho)\,\mathrm{d}t \right|^2 \\ &\leq \sum_{\xi \in \mathbb{Z}} \int_{t=0}^1 |\nabla_\rho u(\xi+t\rho)|^2\,\mathrm{d}t = \|\nabla_\rho u\|_{L^2}^2.\end{aligned}$$

The last equality is due to a simple counting argument. □

Proof of Proposition 3.7 and Lemma 3.9. In this proof, it is convenient to revert to displacements of $\mathbb{Z}$, rather than $\mathbb{Z}_+$. To account for this, we obtain a factor $\frac{1}{2}$ in front of the energy functional. The ℓ^p norms are now defined on all of $\mathbb{Z}$ and the L^p norms on all of $\mathbb{R}$.

We prove the continuity of $\mathcal{E}^{\mathrm{a}}$ together with the Fréchet differentiability. We begin by proving that (3.12) and (3.10) are well-defined expressions, and at the same time prove the bounds (3.11). For second and higher variations, we apply the generalized Cauchy–Schwarz inequality and (A.1) to obtain

$$\begin{aligned}\big|\langle \delta^j \mathcal{E}^{\mathrm{a}}(u)\boldsymbol{v}\rangle\big| &\leq \frac{1}{2} \sum_{\boldsymbol{\rho} \in \mathcal{R}^j} \frac{m(\boldsymbol{\rho})}{\prod_{i=1}^j |\rho_i|} \sum_{\xi \in \mathbb{Z}} \prod_{i=1}^j |D_{\rho_i} v_i(\xi)| \\ &\leq \frac{1}{2} \sum_{\boldsymbol{\rho} \in \mathcal{R}^j} \frac{m(\boldsymbol{\rho})}{\prod_{i=1}^j |\rho_i|} \prod_{i=1}^j \|D_{\rho_i} v_i\|_{\ell^{p_i}} \\ &\leq \frac{1}{2} \sum_{\boldsymbol{\rho} \in \mathcal{R}^j} \frac{m(\boldsymbol{\rho})}{\prod_{i=1}^j |\rho_i|} \prod_{i=1}^j \|\nabla_{\rho_i} v_i\|_{L^{p_i}} \leq \frac{1}{2} M^{(j)} \prod_{i=1}^j \|\nabla v_i\|_{L^{p_i}}.\end{aligned}$$

Thus we have shown (3.11). Moreover, if we choose $p_i \geq 2$, then we have $\|\nabla v_i\|_{L^{p_i}} \leq \|\nabla v_i\|_{L^2}$, and hence it follows that (3.10) is indeed well-defined for any $\boldsymbol{v} \in \mathcal{U}^j$.

To show that (3.12) is also well-defined, we simply note that

$$\Phi^{\mathrm{a}}_{\xi,\rho}(u) - \Phi^{\mathrm{a}}_{\xi,\rho}(0) = \langle \delta \Phi^{\mathrm{a}}_{\xi,\rho}(\theta u), u\rangle = \sum_{\varsigma \in \mathcal{R}} \Phi^{\mathrm{a}}_{\xi,\rho\varsigma}(\theta u) D_\varsigma u(\xi),$$

where $\theta \in (0,1)$, and apply the above argument (for the case $j = 2$) again.

To prove continuity of $\mathcal{E}^{\mathrm{a}}$, we define the modified potential

$$\Psi_\xi(u) := \Phi^{\mathrm{a}}_\xi(u) - \langle \delta \Phi^{\mathrm{a}}_\xi(0), u\rangle = \Phi^{\mathrm{a}}_\xi(u) - \sum_{\rho \in \mathcal{R}} \Phi^{\mathrm{a}}_{\xi,\rho}(0) D_\rho u(\xi).$$

Since $\sum_{\xi\in\mathbb{Z}} D_\rho u(\xi) = 0$ for all $u \in \mathcal{U}_0$, we have

$$\mathcal{E}^{\mathrm{a}}(u) = \frac{1}{2}\sum_{\xi\in\mathbb{Z}^d} \Psi_\xi(u) \quad \text{for all } u \in \mathcal{U}_0. \tag{A.2}$$

We will show that this definition of the energy is in fact well-formed for all $u \in \mathcal{U}$, as well as continuous and k times differentiable with variations given by (3.12) and (3.10). Since the new form agrees with the formal definition on $\mathcal{U}_0$, the result then follows.

To prove that (A.2) is well-defined, we expand

$$\Psi_\xi(u) = \Psi_\xi(0) + \sum_{\rho\in\mathcal{R}} \Psi_{\xi,\rho}(0) D_\rho u(\xi) + \sum_{\rho,\varsigma\in\mathcal{R}} \Psi_{\xi,\rho\varsigma}(\theta u) D_\rho u(\xi) D_\varsigma u(\xi),$$

where $\theta \in (0,1)$. Since $\Psi_\xi(0) = \Psi_{\xi,\rho}(0) = 0$, it is now easy to show, using the fact that $Du(\xi) \in \ell^2$, that $(\Psi_\xi(u))_{\xi\in\mathbb{Z}} \in \ell^1$ for all $u \in \mathcal{U}$.

To prove differentiability, we first note that, since $V \in C^k$,

$$\begin{aligned}\Psi_\xi(u+h) = \Psi_\xi(u) + \langle \delta\Psi_\xi(u), h\rangle + \cdots + \tfrac{1}{k!}\langle \delta^k \Psi_\xi(u)(h,\dots,h)\rangle \\ + o(\|\nabla h\|^k_{L^2(\xi - r_{\mathrm{cut}}, \xi + r_{\mathrm{cut}})}).\end{aligned}$$

The bounds (3.11) show that the sum over $\xi \in \mathbb{Z}$ is well-defined, and one can readily deduce that $\mathcal{E}^{\mathrm{a}}$ is k times Fréchet-differentiable. □

A.2. Proofs from Section 5 (coarsening)

Proof of Lemma 5.2. For each $T \in \mathcal{T}_h$, since ∇v_h is constant in T, we have

$$\begin{aligned}&\int_T \big(\partial_{\mathsf{F}} W(\nabla \Pi_h u) - \partial_{\mathsf{F}} W(\nabla \tilde{u})\big) \nabla v_h \,\mathrm{d}x \\ &\quad = \int_T \big(\partial_{\mathsf{F}} W(\nabla I_h u) - \partial_{\mathsf{F}} W(\nabla \tilde{u})\big)\,\mathrm{d}x \cdot \nabla v_h|_T \\ &\qquad + \int_T \big(\partial_{\mathsf{F}} W(\nabla \Pi_h u) - \partial_{\mathsf{F}} W(\nabla I_h u)\big)\,\mathrm{d}x \cdot \nabla v_h|_T. \end{aligned}\tag{A.3}$$

Using (5.2) we obtain

$$|\partial_{\mathsf{F}} W(\nabla \Pi_h u) - \partial_{\mathsf{F}} W(\nabla I_h u)| \le M^{(2,0)} |\nabla \Pi_h u - \nabla I_h u| \lesssim N^{-\alpha}.$$

Moreover, using the fact that $\int_T \nabla I_h u \,\mathrm{d}x = \int_T \nabla \tilde{u}\,\mathrm{d}x$, and the interpolation error estimate for $I_h u$ from Lemma 5.1, we have

$$\begin{aligned}\left|\int_T \big(\partial_{\mathsf{F}} W(\nabla I_h u) - \partial_{\mathsf{F}} W(\nabla \tilde{u})\big)\,\mathrm{d}x\right| &\le \left|\int_T \partial_{\mathsf{F}} W'(\nabla I_h u)(\nabla I_h u - \nabla \tilde{u})\,\mathrm{d}x\right| \\ &\quad + M^{(2,0)} \int_T |\nabla I_h u - \nabla \tilde{u}|^2 \,\mathrm{d}x \\ &\lesssim \|\nabla I_h u - \nabla \tilde{u}\|^2_{L^2(T)} \lesssim \|h \nabla^2 \tilde{u}\|^2_{L^2(T)}.\end{aligned}$$

Combining these estimates with (A.3) we obtain

$$\left| \int_T \big(\partial_{\mathsf{F}} W(\nabla \Pi_h u) - \partial_{\mathsf{F}} W(\nabla \tilde{u})\big) \nabla v_h \, \mathrm{d}x \right| \lesssim \big(\|h \nabla^2 \tilde{u}\|^2_{L^4(T)} + h_T^{1/2} N^{-\alpha} \big) \|\nabla v_h\|_{L^2(T)}.$$

Summing over $T \in \mathcal{T}_h$, $T \subset [L, N]$ and again applying Hölder's inequality yields the stated result. □

Lemma A.2. Let $\omega(x) := x \log(x)$ and $L > 1$. Then

$$\|\omega^{-1} v\|_{L^2(L,\infty)} \leq \frac{1}{\log L} \|\nabla v\|_{L^2} \quad \text{for all } v \in \mathcal{U}.$$

Proof. For each $x > K$ we have

$$v(x) = \int_0^x \nabla v(s) \, \mathrm{d}s \leq x^{1/2} \|\nabla v\|_{L^2},$$

hence

$$\|\omega^{-1} v\|_{L^2(L,\infty)} \leq \|\omega^{-1} x^{1/2}\|_{L^2(L,\infty)} \|\nabla v\|_{L^2}.$$

Integrating the constant gives

$$\int_K^\infty \omega^{-2} x \, \mathrm{d}x = \int_L^\infty \frac{1}{x \log^2 x} \, \mathrm{d}x = \frac{1}{\log L}. \qquad \square$$

Proof of Proposition 5.4. We begin by adding and subtracting $\langle I_h f, v_h \rangle_{\mathbb{Z}_+}$:

$$\big| \langle f, v_h \rangle_{\mathbb{Z}_+} - \langle f, v_h \rangle_h \big| \leq \big| \langle f - I_h f, v_h \rangle_{\mathbb{Z}_+} \big| + \big| \langle I_h f, v_h \rangle_{\mathbb{Z}_+} - \langle f, v_h \rangle_h \big|. \quad \text{(A.4)}$$

Using a similar argument as in the proof of Lemma 6.16, we can estimate the second group on the right-hand side of (A.4) by

$$\big| \langle I_h f, v_h \rangle_{\mathbb{Z}_+} - \langle f, v_h \rangle_h \big| \lesssim \|h^2 \nabla \tilde{f}\|_{L^2} \|\nabla v_h\|_{L^2}. \quad \text{(A.5)}$$

The estimate of the first term on the right-hand side of (A.4) requires some care. First, we reduce it to a more conventional continuum object: if $g := \tilde{f} - I_h \tilde{f}$ and $\mathbb{Z}_{L,N} := \{L, \ldots, N\}$, then

$$\begin{aligned} \big| \langle g, v_h \rangle_{Z_+} \big| &= \big| \langle g, v_h \rangle_{\mathbb{Z}_{L,N}} \big| \\ &\leq \left| \langle g, v_h \rangle_{\mathbb{Z}_{L,N}} - \int_L^N g v_h \, \mathrm{d}x \right| + \left| \int_L^N g v_h \, \mathrm{d}x \right|. \end{aligned} \quad \text{(A.6)}$$

To estimate the first group on the right-hand side of (A.6) we note that $\langle g, v_h \rangle_{\mathbb{Z}_{L,N}}$ is a trapezoidal rule approximation to $\int_L^N g v_h \, \mathrm{d}x$ with mesh size $h = 1$, which yields

$$\left| \langle g, v_h \rangle_{\mathbb{Z}_{L,N}} - \int_L^N g v_h \, \mathrm{d}x \right| \lesssim \|\nabla g \nabla v_h\|_{L^1(L,N)} + \|\nabla^2 g v_h\|_{L^1(L,N)}.$$

We write $\nabla^2 g v_h = (\omega \nabla^2 g)(\omega^{-1} v_h)$, and apply the Cauchy–Schwarz and weighted Poincaré inequalities to obtain

$$\begin{aligned}\Big| \langle g, v_h \rangle_{\mathbb{Z}_{L,N}} - \int_L^N g v_h \,\mathrm{d}x \Big| \\ &\lesssim \|\nabla g\|_{L^2(L,N)} \|\nabla v_h\|_{L^2} + \|\omega \nabla^2 g\|_{L^2(L,N)} \|\omega^{-1} v_h\|_{L^2(L,N)} \\ &\lesssim \big(\|\nabla g\|_{L^2(L,N)} + \|\omega^{-1} \nabla^2 g\|_{L^2(L,N)} \big) \|\nabla v_h\|_{L^2}.\end{aligned}$$

Finally, using the fact that $\nabla^2 g = \nabla^2 \tilde{f}$ and $\|\nabla g\|_{L^2} \le \|\nabla \tilde{f}\|_{L^2}$ (since $\nabla I_h \tilde{f}$ is the L^2-projection of $\nabla \tilde{f}$), we obtain

$$\begin{aligned}\Big| \langle g, v_h \rangle_{\mathbb{Z}_{L,N}} - \int_L^N g v_h \,\mathrm{d}x \Big| \\ &\lesssim \Big\{ \|\nabla \tilde{f}\|_{L^2(L,N)} + \frac{1}{\log L} \|\omega^{-1} \nabla^2 \tilde{f}\|_{L^2(L,N)} \Big\} \|\nabla v_h\|_{L^2}.\end{aligned} \tag{A.7}$$

We are left to estimate the second group on the right-hand side of (A.6). Fix an element $T \subset [L, N]$. Then

$$\begin{aligned}\Big| \int_T (\tilde{f} - I_h \tilde{f}) v_h \,\mathrm{d}x \Big| &\le \|h^2 \nabla^2 \tilde{f}\|_{L^2(T)} \|v_h\|_{L^2(T)} \\ &\le \max_T \omega^{-1} \max_T \omega \, \|\omega h^2 \nabla^2 \tilde{f}\|_{L^2(T)} \|\omega^{-1} v_h\|_{L^2(T)}.\end{aligned}$$

One readily checks that, due to the assumption that $h(x) \lesssim \kappa x$, we have

$$\max_T \omega^{-1} \max_T \omega \lesssim \frac{(1+\kappa) \log^2(1+\kappa)}{\log^2(\min_T x)} + (1+\kappa) =: C_\kappa.$$

(Note that for practical meshes we expect that $C_\kappa \eqsim \kappa$.) Summing over $T \in \mathcal{T}_h, T \subset [L, N]$ and applying a Poincaré inequality followed by the weighted Poincaré inequality (Lemma A.2), we arrive at

$$\Big| \int_T (\tilde{f} - I_h \tilde{f}) v_h \,\mathrm{d}x \Big| \lesssim \frac{C_\kappa}{\log L} \|\omega h^2 \nabla^2 \tilde{f}\|_{L^2(L,N)} \|\nabla v_h\|_{L^2}. \tag{A.8}$$

Inserting (A.8) and (A.7) into (A.6) and the resulting estimate as well as (A.5) into (A.4) yields the stated result. □

A.3. Proof of conditional QNL stability

Proof of Theorem 7.8. Let $K' := \lfloor K/2 \rfloor < K$, and let

$$\beta(x) := \begin{cases} 0, & 0 \le x \le K', \\ \hat{\beta}\big(\frac{x-K'}{K-K'}\big), & K' \le x \le K, \\ 1, & K \le x, \end{cases}$$

where $\hat{\beta}$ is the quasi-optimal blending function defined in (6.12). Recall from Section 8.3 that

$$\|\nabla\sqrt{\beta}\|_{L^\infty} + \|\nabla\sqrt{1-\beta}\|_{L^\infty} \lesssim K^{-1}.$$

We can now write

$$\begin{aligned}\left\langle \delta^2\mathcal{E}^{\mathrm{qnl}}(u)v, v\right\rangle &= \sum_{\xi\in\mathbb{Z}_+}\sum_{\rho,\varsigma\in\mathcal{R}} \Phi^{\mathrm{qnl}}_{\xi,\rho\varsigma}(u) D_\rho v(\xi) D_\varsigma v(\xi)\\ &= \sum_{\xi\in\mathbb{Z}_+}\sum_{\rho,\varsigma\in\mathcal{R}} \Phi^{\mathrm{a}}_{\xi,\rho\varsigma}(u)(1-\beta(\xi)) D_\rho v(\xi) D_\varsigma v(\xi)\\ &\quad + \sum_{\xi\in\mathbb{Z}_+}\sum_{\rho,\varsigma\in\mathcal{R}} \Phi^{\mathrm{qnl}}_{\xi,\rho\varsigma}(u)\beta(\xi) D_\rho v(\xi) D_\varsigma v(\xi),\end{aligned}$$

where we also used the fact that, according to our definition of β, the first sum ranges only over those sites where $\Phi^{\mathrm{qnl}}_\xi = \Phi^{\mathrm{a}}_\xi$.

We now define $v^{\mathrm{a}}, v^{\mathrm{c}}$ according to Lemma 7.3 to obtain

$$\langle \delta^2\mathcal{E}^{\mathrm{qnl}}(u)v, v\rangle \geq \langle \delta^2\mathcal{E}^{\mathrm{a}}(u)v^{\mathrm{a}}, v^{\mathrm{a}}\rangle + \langle \delta^2\mathcal{E}^{\mathrm{qnl}}(u)v^{\mathrm{c}}, v^{\mathrm{c}}\rangle - CK^{-1}\|\nabla v\|^2_{L^2}. \quad \text{(A.9)}$$

If K is sufficiently large, then $\delta^2\mathcal{E}^{\mathrm{qnl}}(u)$ can be estimated using the decay hypothesis **(DH)** (see the proof of Theorem 7.4 for a similar argument) by

$$\langle \delta^2\mathcal{E}^{\mathrm{qnl}}(u)v^{\mathrm{c}}, v^{\mathrm{c}}\rangle \geq \langle \delta^2\mathcal{E}^{\mathrm{qnl}}(0)v^{\mathrm{c}}, v^{\mathrm{c}}\rangle - CK^{-\alpha}\|\nabla v^{\mathrm{c}}\|^2_{L^2}. \quad \text{(A.10)}$$

Combining (A.9) and (A.10) and the assumptions of the theorem gives the stated result. □

A.4. Proofs from Section 8 (mesh optimization)

To prove Lemma 8.1 we first establish a crucial auxiliary result.

Lemma A.3. Let $N, \mathcal{T}_h$ be constructed using Algorithm T, then, for L sufficiently large, $h(x) \leq x/2$ for all $x \in [L, N]$.

Proof. For $x \in (\nu_j, \nu_{j+1})$, $j \geq L$, we have

$$\frac{h(x)}{x} \leq \frac{\tilde{h}(\nu_j)}{\nu_j},$$

where $\tilde{h}(x) = (x/L)^{\frac{2}{3}(\alpha+1)}$ was defined in (8.1). It is easy to see that $\tilde{h}(x)/x$ is monotonically increasing, hence it is sufficient to check that $\tilde{h}(N)/N \leq 1/2$.

In Algorithm T we defined $N := \lceil L^{(\alpha+1/2)/(\alpha-1/2)}\rceil \approx L^{(\alpha+1/2)/(\alpha-1/2)}$. An easy calculation shows that, in this case,

$$\frac{\tilde{h}(N)}{N} \approx L^{\left[\frac{\alpha+1/2}{\alpha-1/2}-1\right]\frac{2}{3}(\alpha+1)} L^{-\frac{\alpha+1/2}{\alpha-1/2}} = L^{-1/3}.$$

Thus, choosing L sufficiently large, we obtain $h(x) \le x/2$ for all $x \in [L, N]$. □

Proof of Lemma 8.1. Algorithm T ensures that $h(x) \le \tilde{h}(x)$ for all $x \in [L, N] \setminus \mathcal{N}_h$. From this, it is easy to prove the estimates (8.4) and (8.5) provided we replace $N_{\mathcal{T}_h}$ with L on the right-hand sides.

If we can prove that

$$h(x) \ge c\tilde{h}(x), \tag{A.11}$$

then the formal estimate (8.2) becomes rigorous (*i.e.*, we obtain $N_{\mathcal{T}_h} \le C_1 L$) and we also obtain (8.4) and (8.5) as stated.

Let $\alpha' = \frac{2}{3}(\alpha + 1)$ and let $x \in (L, N)$ belong to an element (ν_j, ν_{j+1}). Then

$$\begin{aligned} h(x) &= \tilde{h}(x)\frac{h(x)}{\tilde{h}(x)} = \tilde{h}(x)\frac{\tilde{h}(\nu_j)}{\tilde{h}(x)} \ge \tilde{h}(x)\frac{\tilde{h}(\nu_j)}{\tilde{h}(\nu_{j+1})} \\ &= \tilde{h}(x)\left(\frac{\nu_j}{\nu_{j+1}}\right)^{\alpha'} = \tilde{h}(x)\left(\frac{\nu_{j+1} - \tilde{h}(\nu_j)}{\nu_{j+1}}\right)^{\alpha'} = \tilde{h}(x)\left(1 - \frac{\tilde{h}(\nu_j)}{\nu_{j+1}}\right)^{\alpha'}. \end{aligned}$$

From Lemma A.3 we know that, for L sufficiently large, $\tilde{h}(\nu_{j+1}) \le \frac{1}{2}\nu_{j+1}$, and hence

$$1 - \frac{\tilde{h}(\nu_j)}{\nu_{j+1}} \ge 1 - \frac{\tilde{h}(\nu_{j+1})}{\nu_{j+1}} \ge 1 - \frac{1}{2} = \frac{1}{2}.$$

Thus, we obtain

$$h(x) \ge \tilde{h}(x)\left(\frac{1}{2}\right)^{\alpha'}.$$

This concludes the proof of (A.11) and hence of the lemma. □

B. Inverse function theorem

All rigorous error estimates that we derive in the main text use the following quantitative version of the inverse function theorem.

Lemma B.1. Let $\mathcal{U}_h$ be a subspace of $\mathcal{U}$, equipped with $\|\nabla \cdot\|_{L^2}$, and let $\mathcal{G}_h \in C^1(\mathcal{U}_h, \mathcal{U}_h^*)$ with Lipschitz-continuous derivative $\delta\mathcal{G}_h$:

$$\|\delta\mathcal{G}_h(u_h) - \delta\mathcal{G}_h(v_h)\|_{\mathcal{L}} \le M\|\nabla u_h - \nabla v_h\|_{L^2} \quad \text{for all } u_h, v_h \in \mathcal{U}_h, \tag{B.1}$$

where $\|\cdot\|_{\mathcal{L}}$ denotes the $\mathcal{L}(\mathcal{U}_h, \mathcal{U}_h^*)$-operator norm.

Let $\bar{u}_h \in \mathcal{U}_h$ satisfy

$$\|\mathcal{G}_h(\bar{u}_h)\|_{\mathcal{U}_h^*} \le \eta, \tag{B.2}$$

$$\langle \delta\mathcal{G}_h(\bar{u}_h)v_h, v_h\rangle \ge \gamma\|\nabla v_h\|_{L^2}^2 \quad \text{for all } v_h \in \mathcal{U}_h, \tag{B.3}$$

such that L, η, γ satisfy the relation

$$\frac{2M\eta}{\gamma^2} < 1. \tag{B.4}$$

Then there exists a (locally unique) $u_h \in \mathcal{U}_h$ such that $\mathcal{G}_h(u_h) = 0$,

$$\|\nabla u_h - \nabla \bar{u}_h\|_{L^2} \leq 2\frac{\eta}{\gamma}, \quad \text{and} \tag{B.5}$$

$$\langle \delta \mathcal{G}_h(u_h) v_h, v_h \rangle \geq \left(1 - \frac{2M\eta}{\gamma^2}\right) \gamma \|\nabla v_h\|_{L^2}^2 \quad \text{for all } v_h \in \mathcal{U}_h. \tag{B.6}$$

Proof. The result is a simplified and specialized version of Lemma 2.2 of Ortner (2011), but similar statements can be obtained from most proofs of the inverse function theorem. □

C. List of symbols

$\langle \cdot, \cdot \rangle_h$ Coarse-grained inner product, page 433
α Decay/regularity parameter, page 429
β Blending function, page 436
β^* Quasi-optimal blending function, page 454
$\hat{\beta}$ Quasi-optimal blending function on the reference interval $[0, 1]$, page 454
$\chi_{\xi,\rho}$ Weighted characteristic function of a bond, required for bond-density formula, page 447
$\mathcal{E}^*$ Atomistic contribution to the reflection energy functional, page 439
$\mathcal{E}^{\mathrm{a}}$ Atomistic energy functional, page 424
$\mathcal{E}^{\mathrm{bqce}}$ Blended quasicontinuum (B-QCE) energy functional, page 436
$\mathcal{E}^{\mathrm{c}}$ Cauchy–Born continuum energy functional, page 435
$\mathcal{E}^{\mathrm{qce}}$ Quasicontinuum (QCE) energy functional, page 434
$\mathcal{E}^{\mathrm{qnl}}$ QNL energy functional, page 437
$\mathcal{E}^{\mathrm{rfl}}$ Energy functional of the reflection method, page 439
Φ_ξ^{a} Atomistic site energy functional, page 424
Φ_ξ^{c} Cauchy–Born site energy functional, page 434
Φ_ξ^{i} QNL interface site energy functional, page 437
η_{ext} Consistency error for approximating external forces, page 442
$\eta_{\mathrm{int}}^{\mathrm{ac}}$ Consistency error for approximating internal forces, page 442
$\mathcal{F}^{\mathrm{bqcf}}$ Blended force-based quasicontinuum (B-QCF) operator, page 442
$\mathcal{F}_\zeta^{\mathrm{ac}}$ Force operator, *e.g.*, $\mathcal{F}_\zeta^{\mathrm{qnl}}$, page 437
$\gamma^{\mathrm{a}}(\mathsf{F})$ Stability constant for the homogeneous lattice $\mathsf{A}\mathbb{Z}$, page 464
γ^{qnl} QNL stability constant for the reference state, page 472

Acknowledgements

The work of ML was supported in part by the PIRE grant OISE-0967140, DOE Award DE-SC0002085, and AFOSR Award FA9550-12-1-0187. ML is also grateful for the opportunity to present this work at the University of Heidelberg as the Werner Romberg Guest Professor.

CO was supported by EPSRC grant EP/H003096 'Analysis of Atomistic-to-Continuum Coupling Methods'.

ML and CO would also like to acknowledge the support of the Institute for Pure & Applied Mathematics and the suggestions and advice of Andrew Binder, Matthew Dobson, Frederic Legoll, Xingjie Helen Li, Derek Olson, which helped us to eradicate several mistakes and unclear passages.

REFERENCES[1]

N. C. Admal and E. B. Tadmor (2010), 'A unified interpretation of stress in molecular systems', *J. Elasticity* **100**, 63–143.

M. Anitescu, D. Negrut, P. Zapol and A. El-Azab (2009), 'A note on the regularity of reduced models obtained by nonlocal quasi-continuum-like approaches', *Math. Program. Ser. A* **118**, 207–236.

M. Arndt and M. Luskin (2007), 'Goal-oriented atomistic-continuum adaptivity for the quasicontinuum approximation', *Internat. J. Multiscale Comput. Engng* **5**, 407–415.

M. Arndt and M. Luskin (2008*a*), 'Error estimation and atomistic-continuum adaptivity for the quasicontinuum approximation of a Frenkel–Kontorova model', *SIAM J. Multiscale Model. Simul.* **7**, 147–170.

M. Arndt and M. Luskin (2008*b*), 'Goal-oriented adaptive mesh refinement for the quasicontinuum approximation of a Frenkel–Kontorova model', *Comput. Methods Appl. Mech. Engng* **197**, 4298–4306.

D. N. Arnold and R. S. Falk (1989), 'A uniformly accurate finite element method for the Reissner–Mindlin plate', *SIAM J. Numer. Anal.* **26**, 1276–1290.

S. Badia, P. Bochev, R. Lehoucq, M. L. Parks, J. Fish, M. Nuggehally and M. Gunzburger (2007), 'A force-based blending model for atomistic-to-continuum coupling', *Internat. J. Multiscale Comput. Engng* **5**, 387–406.

S. Badia, M. Parks, P. Bochev, M. Gunzburger and R. Lehoucq (2008), 'On atomistic-to-continuum coupling by blending', *Multiscale Model. Simul.* **7**, 381–406.

M. I. Baskes, C. F. Melius and W. D. Wilson (1981), Solubility and diffusivity of hydrogen and helium at dislocations and in the stress-field near a crack tip. In *Hydrogen Effects in Metals* (I. M. Bernstein and A. W. Thompson, eds), TMS-AIME, pp. 67–75.

[1] The URLs cited in this work were correct at the time of going to press, but the publisher and the authors make no undertaking that the citations remain live or are accurate or appropriate.

P. T. Bauman, H. Ben Dhia, N. Elkhodja, J. T. Oden and S. Prudhomme (2008), 'On the application of the Arlequin method to the coupling of particle and continuum models', *Comput. Mech.* **42**, 511–530.

T. Belytschko and S. P. Xiao (2003), 'Coupling methods for continuum model with molecular model', *Internat. J. Multiscale Comput. Engng* **1**, 115–126.

X. Blanc and F. Legoll (2013), 'A numerical strategy for coarse-graining two-dimensional atomistic models at finite temperature: The membrane case', *Comput. Mater. Sci.* **66**, 84–95.

X. Blanc, C. Le Bris and F. Legoll (2005), 'Analysis of a prototypical multiscale method coupling atomistic and continuum mechanics', *M2AN: Math. Model. Numer. Anal.* **39**, 797–826.

X. Blanc, C. Le Bris and P.-L. Lions (2002), 'From molecular models to continuum mechanics', *Arch. Ration. Mech. Anal.* **164**, 341–381.

X. Blanc, C. Le Bris, F. Legoll and C. Patz (2010), 'Finite-temperature coarse-graining of one-dimensional models: Mathematical analysis and computational approaches', *J. Nonlinear Sci.* **20**, 241–275.

M. Born and K. Huang (1954), *Dynamical Theory of Crystal Lattices*, Oxford University Press.

A.-L. Cauchy (1882), De la pression ou tension dans un système de points matériels. In *Oeuvres complétes d'Augustin Cauchy*, Vol. 2^e Sèrie, tome VIII, Gauthier-Villars, pp. 253–277. First published in 1828.

W. A. Curtin and R. M. Miller (2003), 'Atomistic/continuum coupling in computational materials science', *Model. Simul. Mater. Sci.* **11**, R33–R68.

M. S. Daw and M. I. Baskes (1984), 'Embedded-atom method: Derivation and application to impurities, surfaces, and other defects in metals', *Phys. Rev. B* **20**, 6443–6453.

M. Dobson (2011), There is no pointwise consistent quasicontinuum energy. arXiv:1109.1897

M. Dobson and M. Luskin (2008*a*), 'Analysis of a force-based quasicontinuum approximation', *Math. Model. Numer. Anal.* **42**, 113–139.

M. Dobson and M. Luskin (2008*b*), 'Iterative solution of the quasicontinuum equilibrium equations with continuation', *J. Sci. Comput.* **37**, 19–41.

M. Dobson and M. Luskin (2009*a*), 'An analysis of the effect of ghost force oscillation on quasicontinuum error', *Math. Model. Numer. Anal.* **43**, 591–604.

M. Dobson and M. Luskin (2009*b*), 'An optimal order error analysis of the one-dimensional quasicontinuum approximation', *SIAM. J. Numer. Anal.* **47**, 2455–2475.

M. Dobson, M. Luskin and C. Ortner (2010*a*), 'Accuracy of quasicontinuum approximations near instabilities', *J. Mech. Phys. Solids* **58**, 1741–1757.

M. Dobson, M. Luskin and C. Ortner (2010*b*), 'Stability, instability, and error of the force-based quasicontinuum approximation', *Arch. Ration. Mech. Anal.* **197**, 179–202.

M. Dobson, M. Luskin and C. Ortner (2011), 'Iterative methods for the force-based quasicontinuum approximation: Analysis of a 1D model problem', *Comput. Methods Appl. Mech. Engng* **200**, 2697–2709.

M. Dobson, C. Ortner and A. V. Shapeev (2012), 'The spectrum of the force-based quasicontinuum operator for a homogeneous periodic chain', *Multiscale Model. Simul.* **10**, 744–765.

Q. Du, M. Gunzburger, R. Lehoucq and K. Zhou (2013), 'Analysis of the volume-constrained peridynamic Navier equation of linear elasticity', *J. Elasticity*, to appear.

L. M. Dupuy, E. B. Tadmor, R. E. Miller and R. Phillips (2005), 'Finite temperature quasicontinuum: Molecular dynamics without all the atoms', *Phys. Rev. Lett.* **95**, 060202.

W. E (2011), *Principles of Multiscale Modeling*, Cambridge University Press.

W. E and J. Lu (2013), 'The Kohn–Sham equation for deformed crystals', *Mem. Amer. Math. Soc.* **221**, to appear.

W. E and P. Ming (2007), 'Cauchy–Born rule and the stability of crystalline solids: Static problems', *Arch. Ration. Mech. Anal.* **183**, 241–297.

W. E, J. Lu and J. Z. Yang (2006), 'Uniform accuracy of the quasicontinuum method', *Phys. Rev. B* **74**, 214115.

B. Eidel and A. Stukowski (2009), 'A variational formulation of the quasicontinuum method based on energy sampling in clusters', *J. Mech. Phys. Solids* **57**, 87–108.

H. Fischmeister, H. Exner, M.-H. Poech, S. Kohlhoff, P. Gumbsch, S. Schmauder, L. S. Sigi and R. Spiegler (1989), 'Modelling fracture processes in metals and composite materials', *Z. Metallkde.* **80**, 839–846.

G. Friesecke and F. Theil (2002), 'Validity and failure of the the Cauchy–Born hypothesis in a two-dimensional mass-spring lattice', *J. Nonlin. Sci.* **12**, 445–478.

C. J. Garcia-Cervera, J. Lu and W. E (2007), 'A sub-linear scaling algorithm for computing the electronic structure of materials', *Commun. Math. Sci.* **5**, 999–1026.

V. Gavini, K. Bhattacharya and M. Ortiz (2007), 'Quasi-continuum orbital-free density-functional theory: A route to multi-million atom non-periodic DFT calculation', *J. Mech. Phys. Solids* **55**, 697–718.

M. Gunzburger and Y. Z. Zhang (2010), 'A quadrature-rule type approximation to the quasi-continuum method', *Multiscale Model. Simul.* **8**, 571–590.

S. Haq, A. B. Movchan and G. J. Rodin (2007), 'Lattice Green's functions in nonlinear analysis of defects', *J. Appl. Mech.* **74**, 686–690.

R. Hardy (1982), 'Formulas for determining local properties in molecular dynamics simulations: Shock waves', *J. Chem. Phys.* **76**, 622–628.

T. Hudson and C. Ortner (2012), 'On the stability of Bravais lattices and their Cauchy–Born approximations', *M2AN: Math. Model. Numer. Anal.* **46**, 81–110.

M. Iyer and V. Gavini (2011), 'A field theoretical approach to the quasi-continuum method', *J. Mech. Phys. Solids* **59**, 1506–1535.

H. Kanzaki (1957), 'Point defects in face-centred cubic lattice I: Distortion around defects', *J. Phys. Chem. Solids* **2**, 24–36.

W. K. Kim, M. Luskin, D. Perez, E. B. Tadmor and A. F. Voter (2012), Hyper-QC: An accelerated finite-temperature quasicontinuum method using hyper-dynamics. Submitted.

J. Knap and M. Ortiz (2001), 'An analysis of the quasicontinuum method', *J. Mech. Phys. Solids* **49**, 1899–1923.

S. Kohlhoff, P. Gumbsch and H. F. Fischmeister (1991), 'Crack propagation in b.c.c. crystals studied with a combined finite-element and atomistic model', *Phil. Mag. A* **64**, 851–878.

B. Langwallner, C. Ortner and E. Süli (2013), 'Atomistic-to-continuum coupling approximation of a one-dimensional toy model for density functional theory', *Multiscale Model. Simul.* **11**, 59–91.

X. Li (2009), 'Efficient boundary condition for molecular statics models of solids', *Phys. Rev. B* **80**, 104112.

X. H. Li and M. Luskin (2013), 'Lattice stability for atomistic chains modeled by local approximations of the embedded atom method', *Comput. Mater. Sci.* **66**, 96–103.

X. H. Li, M. Luskin and C. Ortner (2012), 'Positive-definiteness of the blended force-based quasicontinuum method', *SIAM J. Multiscale Model. Simul.* **10**, 1023–1045.

X. H. Li, M. Luskin, C. Ortner and A. Shapeev (2013), Theory-based benchmarking of the blended force-based quasicontinuum method. Manuscript.

X. H. Li, M. Luskin, C. Ortner, A. Shapeev and B. Vankoten (2013). Manuscript.

P. Lin (2003), 'Theoretical and numerical analysis for the quasi-continuum approximation of a material particle model', *Math. Comp.* **72**, 657–675.

P. Lin (2007), 'Convergence analysis of a quasi-continuum approximation for a two-dimensional material without defects', *SIAM J. Numer. Anal.* **45**, 313–332.

W. K. Liu, E. G. Karpov and H. S. Park (2006*a*), *Nano Mechanics and Materials: Theory, Multiscale Methods and Applications*, Wiley.

W. K. Liu, H. Park, D. Qian, E. G. Karpov, H. Kadowaki and G. J. Wagner (2006*b*), 'Bridging scale methods for nanomechanics and materials', *Comput. Methods Appl. Mech. Engng* **195**, 1407–1421.

J. Lu and P. Ming (2012), Stability of a force-based hybrid method in three dimensions with sharp interface. arXiv:1212.3643

J. Lu and P. Ming (2013), 'Convergence of a force-based hybrid method in three dimensions', *Commun. Pure Appl. Math.* **66**, 83–108.

M. Luskin and C. Ortner (2009), 'An analysis of node-based cluster summation rules in the quasicontinuum method', *SIAM J. Numer. Anal.* **47**, 3070–3086.

M. Luskin and C. Ortner (2012), Linear stationary iterative methods for the force-based quasicontinuum approximation. In *Numerical Analysis and Multiscale Computations* (B. Engquist, O. Runborg and R. Tsai, eds), Vol. 82 of *Lecture Notes in Computer Science and Engineering*, Springer, pp. 331–368.

M. Luskin, C. Ortner and B. Van Koten (2013), 'Formulation and optimization of the energy-based blended quasicontinuum method', *Comput. Methods Appl. Mech. Engng* **253**, 160–168.

C. Makridakis and E. Süli (2013), 'Finite element analysis of Cauchy–Born approximations to atomistic models', *Arch. Ration. Mech. Anal.* **207**, 813–843.

C. Makridakis, D. Mitsoudis and P. Rosakis (2012), On atomistic-to-continuum couplings without ghost forces in three dimensions. arXiv:1211.7158

C. Makridakis, C. Ortner and E. Süli (2011), '*A priori* error analysis of two force-based atomistic/continuum models of a periodic chain', *Numer. Math.* **119**, 83–121.

R. Miller and D. Rodney (2008), 'On the nonlocal nature of dislocation nucleation during nanoindentation', *J. Mech. Phys. Solids* **56**, 1203–1223.

R. Miller and E. Tadmor (2003), 'The quasicontinuum method: Overview, applications and current directions', *J. Computer-Aided Mater. Design* **9**, 203–239.

R. Miller and E. Tadmor (2009), 'A unified framework and performance benchmark of fourteen multiscale atomistic/continuum coupling methods', *Model. Simul. Mater. Sci. Engng* **17**, 053001.

P. Ming and J. Z. Yang (2009), 'Analysis of a one-dimensional nonlocal quasicontinuum method', *Multiscale Model. Simul.* **7**, 1838–1875.

M. Mullins and M. Dokainish (1982), 'Simulation of the (0 0 1) plane crack in α-iron employing a new boundary scheme', *Phil. Mag. A* **46**, 771–787.

D. Olson, P. Bochev, M. Luskin and A. Shapeev (2013), An optimization-based atomistic-to-continuum coupling method. Manuscript.

C. Ortner (2011), '*A priori* and *a posteriori* analysis of the quasinonlocal quasicontinuum method in 1D', *Math. Comp.* **80**, 1265–1285.

C. Ortner (2012), 'The role of the patch test in 2D atomistic-to-continuum coupling methods', *ESAIM: Math. Model. Numer. Anal.* **46**, 1275–1319.

C. Ortner and A. Shapeev (2012), Interpolants of lattice functions for the analysis of atomistic/continuum multiscale methods. arXiv:1204.3705

C. Ortner and A. V. Shapeev (2013), 'Analysis of an energy-based atomistic/continuum coupling approximation of a vacancy in the 2D triangular lattice', *Math. Comp.*, to appear.

C. Ortner and E. Süli (2008), 'Analysis of a quasicontinuum method in one dimension', *M2AN: Math. Model. Numer. Anal.* **42**, 57–91.

C. Ortner and F. Theil (2013), 'Justification of the Cauchy–Born approximation of elastodynamics', *Arch. Ration. Mech. Anal.* **207**, 1025–1073.

C. Ortner and H. Wang (2013), '*A posteriori* error control for a quasicontinuum approximation of a periodic chain', *Math. Model. Methods Appl. Sci.*, to appear.

C. Ortner and L. Zhang (2012), Construction and sharp consistency estimates for atomistic/continuum coupling methods with general interfaces: A 2D model problem, *SIAM J. Numer. Anal.* **50**, 2940–2965.

C. Ortner, A. Shapeev and L. Zhang (2013), Manuscript.

M. L. Parks, P. B. Bochev and R. B. Lehoucq (2008), 'Connecting atomistic-to-continuum coupling and domain decomposition', *Multiscale Model. Simul.* **7**, 362–380.

S. Prudhomme, P. T. Bauman and J. T. Oden (2006), 'Error control for molecular statics problems', *Internat. J. Multiscale Comput. Engng* **4**, 647–662.

S. Prudhomme, H. Ben Dhia, P. T. Bauman, N. Elkhodja and J. T. Oden (2008), 'Computational analysis of modeling error for the coupling of particle and continuum models by the Arlequin method', *Comput. Methods Appl. Mech. Engng* **197**, 3399–3409.

R. Rudd and J. Broughton (2000), 'Concurrent coupling of length scales in solid state systems', *Physica Status Solidi B* **217**, 251–291.

R. E. Rudd and J. Q. Broughton (2005), 'Coarse-grained molecular dynamics: Nonlinear finite elements and finite temperature', *Phys. Rev. B* **72**, 144104.

P. Seleson, S. Beneddine and S. Prudhomme (2013), 'A force-based coupling scheme for peridynamics and classical elasticity', *Comput. Mater. Sci.* **66**, 34–49.

P. Seleson and M. Gunzburger (2010), 'Bridging methods for atomistic-to-continuum coupling and their implementation', *Commun. Comput. Phys.* **7**, 831–876.

A. V. Shapeev (2011), 'Consistent energy-based atomistic/continuum coupling for two-body potentials in one and two dimensions', *Multiscale Model. Simul.* **9**, 905–932.

V. B. Shenoy, R. Miller, E. B. Tadmor, D. Rodney, R. Phillips and M. Ortiz (1999), 'An adaptive finite element approach to atomic-scale mechanics: The quasicontinuum method', *J. Mech. Phys. Solids* **47**, 611–642.

L. E. Shilkrot, R. E. Miller and W. A. Curtin (2004), 'Multiscale plasticity modeling: Coupled atomistics and discrete dislocation mechanics', *J. Mech. Phys. Solids* **52**, 755–787.

T. Shimokawa, J. J. Mortensen, J. Schiøtz and K. W. Jacobsen (2004), 'Matching conditions in the quasicontinuum method: Removal of the error introduced at the interface between the coarse-grained and fully atomistic region', *Phys. Rev. B* **69**, 214104.

S. Silling and R. Lehoucq (2010), Peridynamic theory of solid mechanics. In *Advances in Applied Mechanics* (H. Aref and E. van der Giessen, eds), Vol. 44 of *Advances in Applied Mechanics*, Elsevier, pp. 73–168.

J. E. Sinclair (1971), 'Improved atomistic model of a bcc dislocation core', *J. Appl. Phys.* **42**, 5231.

E. B. Tadmor and R. E. Miller (2011), *Modeling Materials: Continuum, Atomistic and Multiscale Techniques*, Cambridge University Press.

E. B. Tadmor, F. Legoll, W. K. Kim, L. M. Dupuy and R. E. Miller (2013), 'Finite-temperature quasicontinuum', *Appl. Mech. Rev.*, to appear.

E. B. Tadmor, M. Ortiz and R. Phillips (1996), 'Quasicontinuum analysis of defects in solids', *Philosophical Magazine A* **73**, 1529–1563.

S. Tang, T. Y. Hou and W. K. Liu (2006), 'A mathematical framework of the bridging scale method', *Internat. J. Numer. Methods Engng* **65**, 1688–1713.

D. R. Trinkle (2008), 'Lattice Green function for extended defect calculations: Computation and error estimation with long-range forces', *Phys. Rev. B* **78**, 014110.

B. Van Koten and M. Luskin (2011), 'Analysis of energy-based blended quasicontinuum approximations', *SIAM J. Numer. Anal.* **49**, 2182–2209.

B. Van Koten and C. Ortner (2012), Symmetries of 2-lattices and second order accuracy of the Cauchy–Born model. arXiv:1203.5854

B. Van Koten, X. H. Li, M. Luskin and C. Ortner (2012), A computational and theoretical investigation of the accuracy of quasicontinuum methods. In *Numerical Analysis of Multiscale Problems* (I. Graham, T. Hou, O. Lakkis and R. Scheichl, eds), Vol. 83 of *Lecture Notes in Computer Science and Engineering*, Springer, pp. 67–96.

A. F. Voter (1997), 'Hyperdynamics: Accelerated molecular dynamics of infrequent events', *Phys. Rev. Lett.* **78**, 3908–3911.

D. Wallace (1998), *Thermodynamics of Crystals*, Dover.

M. Wallin, W. Curtin, M. Ristinmaa and A. Needleman (2008), 'Multi-scale plasticity modeling: Coupled discrete dislocation and continuum crystal plasticity', *J. Mech. Phys. Solids* **56**, 3167–3180.

C. Woodward and S. Rao (2002), 'Flexible *ab initio* boundary conditions: Simulating isolated dislocations in bcc Mo and Ta', *Phys. Rev. Lett.* **88**, 216402.

S. P. Xiao and T. Belytschko (2004), 'A bridging domain method for coupling continua with molecular dynamics', *Comput. Methods Appl. Mech. Engng* **193**, 1645–1669.